

Physiologically Based Pharmacokinetic Modeling of Quinidine to Establish a CYP3A4, P-gp and CYP2D6 Drug-Drug-Gene Interaction Network

Supplement S1 - Model Information and Evaluation

Denise Feick¹, Simeon Rüdesheim^{1,2}, Fatima Zahra Marok¹, Dominik Selzer¹, Helena Leonie Hanae Loer¹, Donato Teutonico³, Sebastian Frechen⁴, Maaike van der Lee⁵, Dirk Jan A. R. Moes⁵, Jesse J. Swen⁵, Matthias Schwab^{2,6,7}, and Thorsten Lehr¹

¹Clinical Pharmacy, Saarland University, Saarbrücken, Germany

²Dr. Margarete Fischer-Bosch-Institute of Clinical Pharmacology, Stuttgart, Germany

³Translational Medicine & Early Development, Sanofi-Aventis R&D, Chilly-Mazarin, France

⁴Bayer AG, Pharmaceuticals, Research & Development, Systems Pharmacology & Medicine, Leverkusen, Germany

⁵Department of Clinical Pharmacy & Toxicology, Leiden University Medical Center, Leiden, The Netherlands

⁶Departments of Clinical Pharmacology, Pharmacy and Biochemistry, University of Tübingen, Tübingen, Germany

⁷Cluster of Excellence iFIT (EXC2180) "Image-guided and Functionally Instructed Tumor Therapies", University of Tübingen, Tübingen, Germany

Funding:

This work is part of the Horizon 2020 INSPIRATION (Qualified Open Systems Pharmacology Modeling Network of Drug-Drug-Gene-Interactions) project. The INSPIRATION project (FKZ 031L0241) is supported by the German Federal Ministry of Education and Research under the framework of ERACoSysMed. Matthias Schwab was supported in parts by the Robert Bosch Stiftung Stuttgart, Germany, and the Deutsche Forschungsgemeinschaft (DFG) under Germany's Excellence Strategy-EXC 2180-390900677.

Conflict of Interest:

Donato Teutonico is an employee of Sanofi. Donato Teutonico uses Open Systems Pharmacology software, tools, or models in his professional role. Donato Teutonico and Thorsten Lehr are members of the Open Systems Pharmacology Management Team. Sebastian Frechen uses Open Systems Pharmacology software, tools, or models in his professional role. Sebastian Frechen is a member of the Open Systems Pharmacology Sounding Board. All other authors declared no competing interest for this work.

Corresponding Author:

Prof. Dr. Thorsten Lehr, Clinical Pharmacy, Saarland University, Campus C5 3, 66123 Saarbrücken, Germany, Phone: +49 681 302 70255, Email: thorsten.lehr@mx.uni-saarland.de

Contents

S1 PBPK Model Building	2
S1.1 System-Dependent Parameters	2
S1.2 Michaelis-Menten Kinetics	5
S1.3 Quinidine – Clinical studies	6
S1.4 Quinidine – Drug-dependent parameters	8
S2 Quinidine – PBPK Model Evaluation	9
S2.1 Plasma concentration-time profiles (semilogarithmic representation)	9
S2.2 Amount excreted unchanged in urine profiles (semilogarithmic representation)	14
S2.3 Plasma concentration-time profiles (linear representation)	16
S2.4 Amount excreted unchanged in urine profiles (linear representation)	21
S2.5 Predicted compared to observed concentrations	23
S2.6 Mean relative deviation of plasma concentration predictions	24
S2.7 Predicted compared to observed AUC_{last} and C_{max} values	26
S2.8 Geometric mean fold errors of predicted AUC_{last} and C_{max} values	27
S2.9 Geometric mean fold errors of predicted V_d and half-life values	29
S2.10 Sensitivity Analyses	31
S3 DD(G)I Modeling	33
S3.1 Types of Interaction	33
S3.1.1 Competitive inhibition	33
S3.1.2 Non-competitive inhibition	33
S3.1.3 Mechanism-based inactivation	33
S3.1.4 Induction	33
S3.2 Published PBPK DDI models	34
S3.3 DD(G)I – Clinical studies	37
S3.3.1 Quinidine as victim	37
S3.3.2 Quinidine as perpetrator	38
S3.4 Plasma concentration-time profiles (semilogarithmic representation)	39
S3.4.1 Quinidine as victim	39
S3.4.2 Quinidine as perpetrator	41
S3.5 Amount excreted unchanged in urine profiles (semilogarithmic representation)	43
S3.5.1 Quinidine as victim	43
S3.6 Plasma concentration-time profiles (linear representation)	44
S3.6.1 Quinidine as victim	44
S3.6.2 Quinidine as perpetrator	46
S3.7 Amount excreted unchanged in urine profiles (linear representation)	48
S3.7.1 Quinidine as victim	48
S3.8 DDI AUC_{last} and C_{max} ratios	49
S3.8.1 Quinidine as victim	49
S3.8.2 Quinidine as perpetrator	50
S3.9 Geometric mean fold errors of predicted DD(G)I AUC_{last} and C_{max} ratios	51
S3.9.1 Quinidine as victim	51
S3.9.2 Quinidine as perpetrator	52
References	53

S1 PBPK Model Building

S1.1 System-Dependent Parameters

Table S1: Relevant enzymes, transporters and binding proteins

Protein	Relevant model	Highest expression	Reference concentration [$\mu\text{mol/L}$]	
			Mean ^a	GSD
Enzymes				
AADAC	Rifampicin	Liver [1]	1.00 ^b [2]	1.40 ^c
CYP1A2	Fluvoxamine, Mexiletine	Liver [3]	1.80 [4]	1.63 [5]
CYP2B6	Carbamazepine	Liver [1]	1.56 [4]	1.56 [5]
CYP2C8	Carbamazepine	Liver [3]	2.56 [4]	2.05 [5]
CYP2C19	R-/S-Omeprazole	Liver [3]	0.76 [4]	1.80 [5]
CYP2D6	Dextromethorphan, Fluvoxamine, R-/S-Metoprolol, Mexiletine, Paroxetine	Liver [3]	0.40 [4]	2.49 [5]
CYP3A4	Carbamazepine, Dextromethorphan, Dextrorphan, Itraconazole (+ metabolites), R-/S-Omeprazole, Paroxetine, Quinidine, 3-Hydroxyquinidine, R-/S-Verapamil (+ metabolites)	Liver [3]	4.32 [4]	1.18 liver, 1.46 int. [5]
EPHX1	Carbamazepine 10,11-epoxide	Liver [1]	1.00 ^b [2]	1.40 ^c
UGT2B7	Carbamazepine	Kidney [6]	2.78 [7]	1.60 [5]
UGT2B15	Dextrorphan	Liver [1]	2.48 ^d [8, 9]	1.26 [8]
Transporters				
MATE1	Cimetidine	Kidney [10, 11]	0.13 ^e [9, 12]	1.53 [12]
OAT3	Cimetidine	Kidney [13]	0.09 ^e [9, 12]	1.53 [12]
OATP1B1	Rifampicin	Liver [13]	0.07 ^f [14]	1.54 [14]
OCT1	Cimetidine	Liver [15]	0.16 ^f [14, 16]	1.50 [16]
P-gp	Digoxin, Quinidine, Rifampicin, R-/S-Verapamil (+ metabolites)	Duodenum mucosa, Upper jejunum mucosa, Lower jejunum mucosa, Upper ileum mucosa Lower ileum mucosa [13]	1.41 ^g [17]	1.60 [14]
Binding proteins				
ATP1A2	Digoxin	Brain [15]	0.48 ^g [17]	1.40 ^c

AADAC: arylacetamide deacetylase, ATP1A2: ATPase Na^+/K^+ transporting subunit alpha 2, CYP: cytochrome P450, EPHX: epoxide hydrolase, GSD: geometric standard deviation, int: intestine, MATE: multidrug and toxin extrusion protein, OAT: organic anion transporter, OATP: organic anion transporting polypeptide, OCT: organic cation transporter, P-gp: P-glycoprotein, UGT: uridine 5'-diphospho-glucuronosyltransferase. ^a In the tissue of highest expression. ^b If no information was available, the mean reference concentration was set to 1.00 $\mu\text{mol/L}$ and the catalytic rate constant was optimized according to [2]. ^c If no information was available, a moderate variability of 35% CV was assumed (= 1.40 GSD). ^d Calculated from protein per mg microsomal protein \times 40 mg microsomal protein per g liver [9]. ^e Calculated from transporter per mg membrane protein \times 26.2 mg human kidney microsomal protein per g kidney [9]. ^f Calculated from transporter per mg membrane protein \times 37.0 mg membrane protein per g liver [14]. ^g Previously optimized by Hanke et al [17].

Table S2: Expression data of relevant enzymes

	AADAC	CYP1A2	CYP2B6	CYP2C8	CYP2C19	CYP2D6	CYP3A4	EPHX1	UGT2B7	UGT2B15
Properties										
Localization	Intracellular	Intracellular	Intracellular	Intracellular	Intracellular	Intracellular	Intracellular	Intracellular	Intracellular	Intracellular
Half-life liver/intestine [h]^a	36/23	39/23	32/23	23/23	26/23	51/23	36/23 [18, 19]	36/23	36/23	36/23
Relative expression in various organs and tissues [%]										
Data source	RT-PCR [1]	RT-PCR [3]	RT-PCR [1]	RT-PCR [3]	RT-PCR [3, 20]	RT-PCR [3]	RT-PCR [3]	RT-PCR [1]	EST [6]	RT-PCR [1]
Blood Cells	0	0	0	0	0	0	0	1	0	0
Plasma	0	0	0	0	0	0	0	1	0	0
Bone	0	0	0	0	0	0	0	2	0	0
Brain	0	0	0	0	0	1	0	4	8	0
Fat	0	0	0	0	0	0	0	0	0	0
Gonads	0	0	1	1	0	77	0	18	13	0
Heart	0	0	0	0	0	0	0	12	0	0
Kidney	0	0	10	0	0	2	1	15	100	0
Liver Periportal	100	100	100	100	100	100	100	100	23	100
Liver Pericentral	100	100	100	100	100	100	100	100	23	100
Lung	3	0	60	0	0	2	0	14	0	0
Muscle	0	0	0	0	0	0	0	36	0	0
Pancreas	15	0	0	0	0	0	0	10	0	2
Skin	0	0	0	0	0	0	0	0	3	0
Spleen	0	0	0	0	0	0	0	6	0	0
Duodenum mucosa	25	0	7	0	2	9	7	6	4	0
Upper jejunum mucosa	25	0	7	0	1	9	7	6	4	0
Lower jejunum mucosa	25	0	7	0	1	9	7	6	4	0
Upper ileum mucosa	25	0	7	0	1	9	7	6	4	0
Lower ileum mucosa	25	0	7	0	1	9	7	6	4	0
Colon ascendens mucosa	0	0	0	0	0	0	0	4	0	0
Colon transversum mucosa	0	0	0	0	0	0	0	4	0	0
Colon descendens mucosa	0	0	0	0	0	0	0	4	0	0
Colon sigmoid mucosa	0	0	0	0	0	0	0	4	0	0
Stomach non-muc. tissue	8	0	0	0	0	0	0	5	13	3
Small intestine non-muc. tissue	25	0	7	0	1	9	7	6	4	0
Large intestine non-muc. tissue	0	0	0	0	0	0	0	4	0	0

AADAC: arylacetamide deacetylase, CYP: cytochrome P450, EPHX: epoxide hydrolase, EST: expressed sequence tag, non-muc.: non-mucosal, RT-PCR: reverse transcription-polymerase chain reaction measured expression profile, UGT: uridine 5'-diphospho-glucuronosyltransferase. ^a Information from PK-Sim® expression database.

Table S3: Expression data of relevant transporters and binding proteins

	MATE1	OAT3	OATP1B1	OCT1	P-gp	ATP1A2
Properties						
Localization	Cell membrane	Cell membrane	Cell membrane	Cell membrane	Cell membrane	Interstitial
Direction	Efflux	Influx	Influx	Influx	Efflux	n.a.
Half-life liver/intestine [h]^a	n.a./n.a.	n.a./n.a.	36/23	36/23	36/23	36/23
Relative expression in various organs and tissues [%]						
Data source	[10, 11]	RT-PCR [13]	RT-PCR [13]	Array [15]	RT-PCR [13, 17]	Array [15]
Blood Cells	0	0	0	0	0	0
Plasma	0	0	0	0	0	0
Bone	0	0	0	2	2	1
Brain	0	0	0 (blood-brain barrier)	8 (blood-brain barrier)		100
Fat	0	0	0	0	0	0
Gonads	0	0	1	0	2	5
Heart	0	0	0	1	4	32
Kidney	100 (apical)	100 (basolateral)	0	3 (basolateral)	71 (apical)	2
Liver Periportal	0	0	100 (basolateral)	100 (basolateral)	19 (apical)	2
Liver Pericentral	0	0	100 (basolateral)	100 (basolateral)	19 (apical)	2
Lung	0	0	0	1	7	3
Muscle	0	0	0	4	1	70
Pancreas	0	0	0	1	1	1
Skin	0	0	0	1	0	4
Spleen	0	0	0	0	7	1
Duodenum mucosa	0	0	0	2 (apical)	100 (apical)	5
Upper jejunum mucosa	0	0	0	2 (apical)	100 (apical)	5
Lower jejunum mucosa	0	0	0	2 (apical)	100 (apical)	5
Upper ileum mucosa	0	0	0	2 (apical)	100 (apical)	5
Lower ileum mucosa	0	0	0	2 (apical)	100 (apical)	5
Colon ascendens mucosa	0	0	0	0	40 (apical)	8
Colon transversum mucosa	0	0	0	0	40 (apical)	8
Colon descendens mucosa	0	0	0	0	40 (apical)	8
Colon sigmoid mucosa	0	0	0	0	40 (apical)	8
Stomach non-mucosal tissue	0	0	0	1	3	3
Small intestine non-mucosal tissue	0	0	0	2	28	5
Large intestine non-mucosal tissue	0	0	0	3	11	8

Array: microarray expression profile, ATP1A2: ATPase Na⁺/K⁺ transporting subunit alpha 2, MATE: multidrug and toxin extrusion protein, n.a.: not applicable, OAT: organic anion transporter, OATP: organic anion transporting polypeptide, OCT: organic cation transporter, P-gp: P-glycoprotein, RT-PCR: reverse transcription-polymerase chain reaction measured expression profile. ^a Information from PK-Sim® expression database.

S1.2 Michaelis-Menten Kinetics

$$v = \frac{v_{max} * [S]}{K_M + [S]} = \frac{k_{cat} * [E] * [S]}{K_M + [S]} \quad (\text{S1})$$

v = reaction velocity, v_{max} = maximum reaction velocity, $[S]$ = free substrate concentration, K_M = Michaelis-Menten constant, k_{cat} = catalytic or transporter rate constant and $[E]$ = enzyme concentration.

S1.3 Quinidine – Clinical studies

Table S4: Clinical study data used for quinidine model development

Quinidine administration											
Dose salt [mg]	Dose base [mg]	Route	n	Population ^a	Fem. [%]	Age [years]	Weight [kg]	BMI [kg/m ²]	Molecule	Dataset	Reference
260.3 ^b	162.2	s.d. iv 60 min inf	7	European [21]	-	-	-	-	QUI	te	Fremstad 1979 [22]
300 ^b	187.5	s.d. iv 30 min inf	9	American [23]	0	28.6 (22-37)	68.4	-	QUI	te	Darbar 1997 ^c [24]
300 ^b	187.5	s.d. iv 30 min inf	9	American [23]	0	28.6 (22-37)	71.5	-	QUI	te	Darbar 1997 ^d [24]
6/kg ^b	3.74/kg	s.d. iv 25 min inf	1	American [23]	0	32	82	-	QUI	te	Guentert 1979 [25]
6/kg ^b	3.74/kg	s.d. iv 25 min inf	1	American [23]	0	23	70.4	-	QUI	te	Guentert 1979 [25]
6/kg ^b	3.74/kg	s.d. iv 25 min inf	1	American [23]	0	23	72.2	-	QUI	te	Guentert 1979 [25]
6.42/kg ^b	4.00/kg	s.d. iv 20 min inf	12	Asian [26]	0	22.1	66.5	-	QUI	te	Shin 2007 [27]
6.42/kg ^b	4.00/kg	s.d. iv 20 min inf	7	American [23]	0	26.2	69.8	-	QUI	te	Shin 2007 [27]
6.42/kg ^b	4.00/kg	s.d. iv 20 min inf	12	Asian [26]	100	22.7	53.4	-	QUI	te	Shin 2007 [27]
6.42/kg ^b	4.00/kg	s.d. iv 20 min inf	6	American [23]	100	27.7	60.7	-	QUI	te	Shin 2007 [27]
481.4 ^b	300	s.d. iv 15 min inf	1	European [21]	0	27	60	-	QUI, QUB	tr	Ochs 1980 [28]
481.4 ^b	300	s.d. iv 15 min inf	1	European [21]	0	23	80	-	QUI, QUB	tr	Ochs 1980 [28]
520.6 ^b	324.4	s.d. iv 60 min inf	6	European [21]	-	-	-	-	QUI	te	Fremstad 1979 [22]
0.1 ^e	0.08	s.d. po sol	7	Japanese [29]	0	27	-	21.8	QUI, OHQ	tr	Maeda 2011 [30]
1 ^e	0.83	s.d. po sol	7	Japanese [29]	0	27	-	21.8	QUI, OHQ	tr	Maeda 2011 [30]
10 ^e	8.29	s.d. po sol	7	Japanese [29]	0	27	-	21.8	QUI, OHQ	tr	Maeda 2011 [30]
100 ^e	82.87	s.d. po sol	7	Japanese [29]	0	27	-	21.8	QUI, OHQ	tr	Maeda 2011 [30]
100 ^e	82.87	s.d. po tab	9	European [21]	56	25 (21-32)	64 (41-80)	-	QUI	te	Kaukonen 1997 [31]
200 ^e	165.7	s.d. po cap	10	European [21]	0	(21-26)	(62-85)	(19-26)	QUI, OHQ	tr	Andreasen 2007 [32]
200 ^e	165.7	s.d. po tab	6	European [21]	0	-	-	-	QUI, OHQ	te	Damkier 1999 [33]
200 ^e	165.7	s.d. po tab	6	European [21]	0	-	-	-	QUI, OHQ	te	Damkier 1999a [34]
200 ^e	165.7	s.d. po tab	12	European [21]	0	24 (19-37)	75 (65-101)	-	QUI	te	Laganière 1996 [35]
200 ^e	165.7	s.d. po sol	13	American [23]	11	(22-40)	-	-	QUI	te	Mason 1976 [36]
200 ^e	165.7	s.d. po cap	13	American [23]	11	(22-40)	-	-	QUI	te	Mason 1976 [36]
200 ^e	165.7	s.d. po tab	13	American [23]	11	(22-40)	-	-	QUI	te	Mason 1976 [36]
250 ^e	207.2	s.d. po cap	8	European [21]	0	(18-26)	(48-62)	(162.5-180) ^f	QUI	te	Rao 1995 [37]
400 ^e	331.5	s.d. po tab	8	European [21]	0	(22-34)	-	-	QUI	te	Bleske 1990 [38]
400 ^e	331.5	s.d. po tab	8	European [21]	0	(22-29)	(60-94)	-	QUI, OHQ	te	Ching 1991 [39]
400 ^e	331.5	s.d. po tab	6	European [21]	0	(23-34)	-	-	QUI	te	Edwards 1987 [40]
400 ^e	331.5	s.d. po tab	6	American [23]	0	(25-38)	-	-	QUI	te	Hardy 1983 [41]
400 ^e	331.5	s.d. po tab	9	American [23]	0	(21-35)	-	-	QUI	te	Kolb 1984 [42]
400 ^e	331.5	s.d. po tab	7	European [21]	43	28.9 (27-31)	68.4 (57.7-79.5)	-	QUI	te	Ochs 1978 [43]
400 ^e	331.5	s.d. po tab	11	American [23]	0	(20-37)	-	-	-	te	Strum 1977 ^g [44]
600 ^e	497.2	s.d. po tab	9	American [23]	0	28.6 (22-27)	68.4	-	QUI	tr/te	Darbar 1997 ^c [24]
600 ^e	497.2	s.d. po tab	9	American [23]	0	28.6 (22-37)	71.5	-	QUI	te	Darbar 1997 ^d [24]
600 ^e	497.2	s.d. po tab	8	European [21]	0	26.4 (23-37)	67.1 (60-76)	1.74 (1.60-1.83) ^f	QUI	te	Frigo 1977 [45]

BMI: body mass index, calc: calculated, cap: capsule, fem: females, inf: infusion, iv: intravenous, n: number of study participants, OHQ: 3-hydroxyquinidine, po: oral, q.i.d.: four times daily, QUB: quinidine unbound, QUI: quinidine, s.d.: single dose, sol: solution, tab: tablet, te: test dataset, t.i.d.: three times daily, tr: training dataset, -: not available. Values are given as mean (range). Respective doses of quinidine base were calculated and incorporated in simulations. ^a Population used in simulations. ^b Quinidine glucunonate dose. ^c Low-salt diet. ^d High-salt diet. ^e Quinidine sulfate dose. ^f Height of subjects [cm]. ^g Administration of four immediate-release formulations (Treatment A-D).

Table S4: Clinical study data used for quinidine model development (*continued*)

Quinidine administration											
Dose salt [mg]	Dose base [mg]	Route	n	Population ^a	Fem. [%]	Age [years]	Weight [kg]	BMI [kg/m ²]	Molecule	Dataset	Reference
200 ^e	165.7	t.i.d. po tab	5	European [21]	0	(26-33)	73.4 (62-90)		QUI	te	Bolme 1977 [46]
300 ^e	248.6	t.i.d. po tab	5	European [21]	0	(26-33)	73.4 (62-90)	-	QUI	te	Bolme 1977 [46]
400 ^e	331.5	t.i.d. po tab	3	European [21]	0	(26-33)	68 (62-75)	-	QUI	te	Bolme 1977 [46]
400 + 200 ^e	331.5 +165.7	s.d. + q.i.d. po tab	7	European [21]	43	28.9 (27-31)	68.4 (57.7-79.5)	-	QUI	tr	Ochs 1978 [43]

BMI: body mass index, calc: calculated, cap: capsule, fem: females, inf: infusion, iv: intravenous, n: number of study participants, OHQ: 3-hydroxyquinidine, po: oral, q.i.d.: four times daily, QUB: quinidine unbound, QUI: quinidine, s.d.: single dose, sol: solution, tab: tablet, te: test dataset, t.i.d.: three times daily, tr: training dataset, -: not available. Values are given as mean (range). Respective doses of quinidine base were calculated and incorporated in simulations. ^a Population used in simulations. ^b Quinidine glucunonate dose. ^c Low-salt diet. ^d High-salt diet. ^e Quinidine sulfate dose. ^f Height of subjects [cm]. ^g Administration of four immediate-release formulations (Treatment A-D).

S1.4 Quinidine – Drug-dependent parameters

Table S5: Drug-dependent parameters of the quinidine model

Parameter	Quinidine			3-Hydroxyquinidine			Description
	Value or 95% CI ^a	Source	Literature	Value or 95% CI ^a	Source	Literature	
MW [g/mol]	324.42	Lit.	324.42 [47, 48]	340.42	Lit.	340.42 [47, 49]	Molecular weight of quinidine base
pK _a (base 1)	4.02	Lit.	4.02 [50]	4.03	Lit.	4.03 [51]	Acid dissociation constant
pK _a (base 2)	9.05	Lit.	9.05 [47, 48]	8.63	Lit.	8.63 [47, 49]	Acid dissociation constant
pK _a (acid)	13.89	Lit.	13.89 [47, 48]	13.55	Lit.	13.55 [47, 49]	Acid dissociation constant
Solubility (pH 7.0) [g/L]	11.11	Lit.	11.11 (quinidine sulfate) [52]	12.57	Lit.	12.57 [51]	Solubility
Lipophilicity	2.51	Lit.	2.51 (logP) [47, 48]	1.66	Lit.	1.66 (logP) [51]	Lipophilicity
f _{u,p} [%]	21	Lit.	21 ^b [53]	31	Lit.	31 ^b [53]	Fraction unbound plasma
P-gp K _M [$\mu\text{mol/L}$]	0.23	Lit.	0.23 [54]	-	-	-	Michaelis-Menten constant
P-gp k _{cat} [1/min]	0.77 ± 0.08	Opt.	-	-	-	-	Transport rate constant
CYP3A4 (QUI → OHQ) K _M [$\mu\text{mol/L}$]	51.8	Lit.	74.0 × 0.70 ^c [55, 56]	-	-	-	Michaelis-Menten constant
CYP3A4 (QUI → OHQ) k _{cat} [1/min]	2.21 ± 1.02	Opt.	-	-	-	-	Catalytic rate constant
CYP3A4 (QUI → sink) K _M [$\mu\text{mol/L}$]	65.03	Lit.	92.9 × 0.70 ^c [55, 56]	-	-	-	Michaelis-Menten constant
CYP3A4 (QUI → sink) k _{cat} [1/min]	3.84 ± 1.39	Opt.	-	-	-	-	Catalytic rate constant
CYP3A4 CL [1/min]	-	-	-	0.08 ± 0.06	Opt.	-	First-order clearance
CL _{hep} [1/min]	-	-	-	0.45 ± 0.39	Opt.	-	Hepatic metabolic clearance
GFR fraction	1	Asm.	-	1	Asm.	-	Fraction of filtered drug in the urine
EHC continuous fraction	1	Asm.	-	1	Asm.	-	Fraction of bile continually released
P-gp K _i [$\mu\text{mol/L}$]	0.10	Lit.	0.10 [57]	-	-	-	Conc. for 50% inhibition (comp.)
CYP2D6 K _i [$\mu\text{mol/L}$]	0.017	Lit.	0.017 ^d [58]	2.30	Lit.	2.30 [59]	Conc. for 50% inhibition (comp.)
Partition coefficients	Diverse	Calc.	Berezhkovskiy [60]	Diverse	Calc.	Berezhkovskiy [60]	Cell to plasma partition coefficients
Cell. perm. [cm/min]	$7.99 \cdot 10^{-3}$	Calc.	PK-Sim [61]	$8.45 \cdot 10^{-4}$	Calc.	PK-Sim [61]	Permeability into the cellular space
Intest. perm. [cm/min]	$6.47 \cdot 10^{-6} \pm 5.78 \cdot 10^{-7}$	Opt.	2.59 · 10 ⁻⁵ (calc.)	$2.94 \cdot 10^{-6}$	Calc	$2.94 \cdot 10^{-6}$	Transcellular intestinal permeability
Formulation	Weibull ^e	Lit.	[62, 63]	-	-	-	Formulation used in predictions

asm.: assumed, Berezhkovskiy: Berezhkovskiy calculation method, calc.: calculated, cell.: cellular, CI: confidence interval, CL: clearance, comp.: competitive, conc.: concentration, CYP: cytochrome P450, EHC: enterohepatic circulation, GFR: glomerular filtration rate, intest.: intestinal, lit.: literature, OHQ: 3-hydroxyquinidine, opt.: optimized, P-gp: P-glycoprotein, PK-Sim: PK-Sim standard calculation method, QUI: quinidine, -: not implemented/not available. ^a 95% confidence interval calculated for optimized parameters, ^b Calculated with f_{u,p} predictor [53]. ^c Reported K_M values adjusted for fraction unbound in the incubation (f_{u,inc}) = 70% (calculated) [56]. ^d Estimated *in vivo* K_i value reported [58]. ^e Weibull function [64] with a dissolution time of 8.76 min (50% dissolved) and a dissolution shape of 0.42 for immediate release quinidine sulfate formulations (calculated with DDSolver) [62, 63].

S2 Quinidine – PBPK Model Evaluation

S2.1 Plasma concentration-time profiles (semilogarithmic representation)

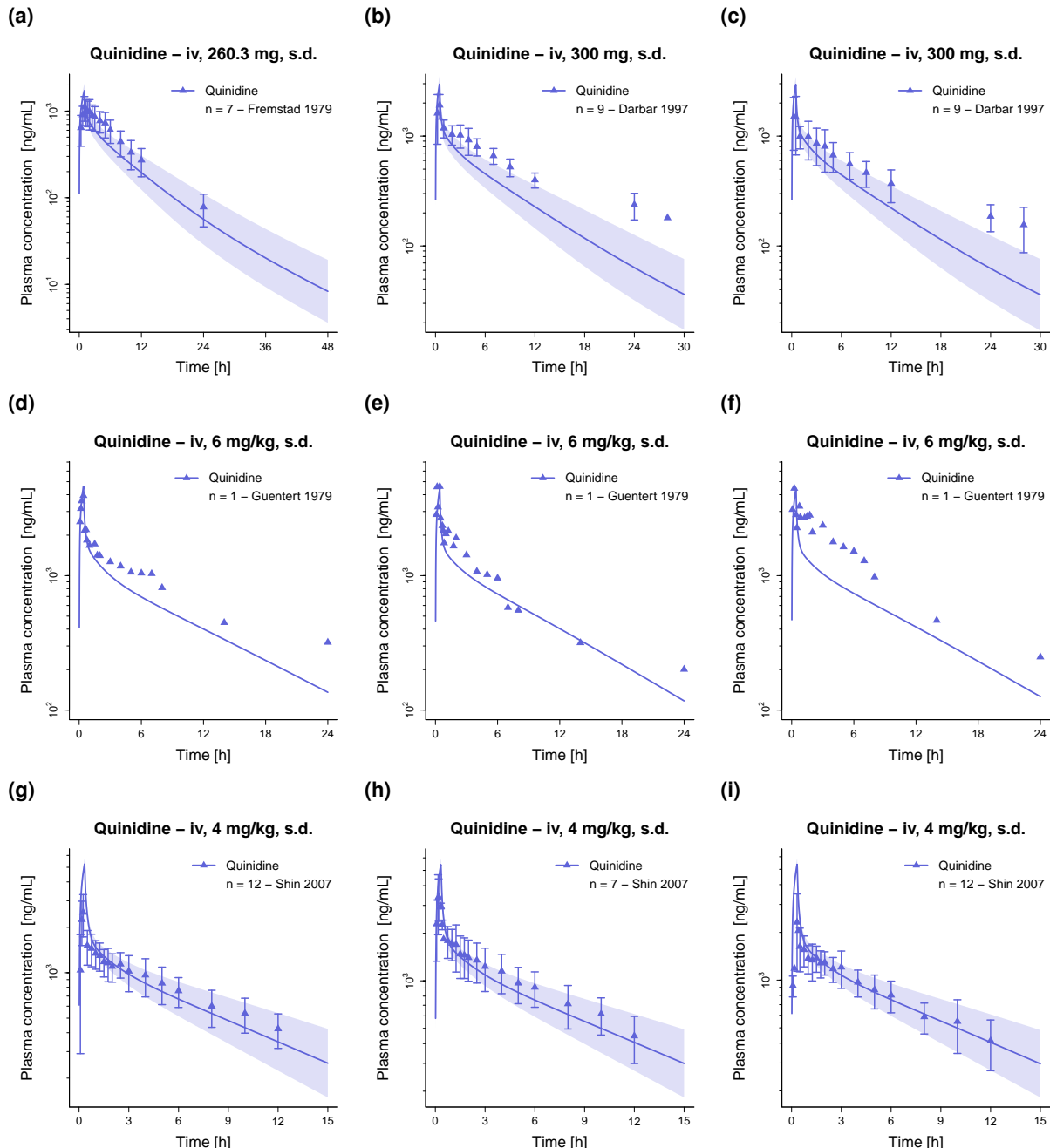


Figure S1: Quinidine plasma concentration-time profiles (semilogarithmic representation). Population predicted geometric means and individual predictions are shown as lines, corresponding geometric standard deviations are shown as shaded areas and observed data are shown as dots (training dataset) and triangles (test dataset) (\pm standard deviation, if reported). Doses indicate quinidine gluconate administration. Respective doses of quinidine base were calculated and incorporated in simulations. iv: intravenous, n: number of study participants, s.d.: single dose.

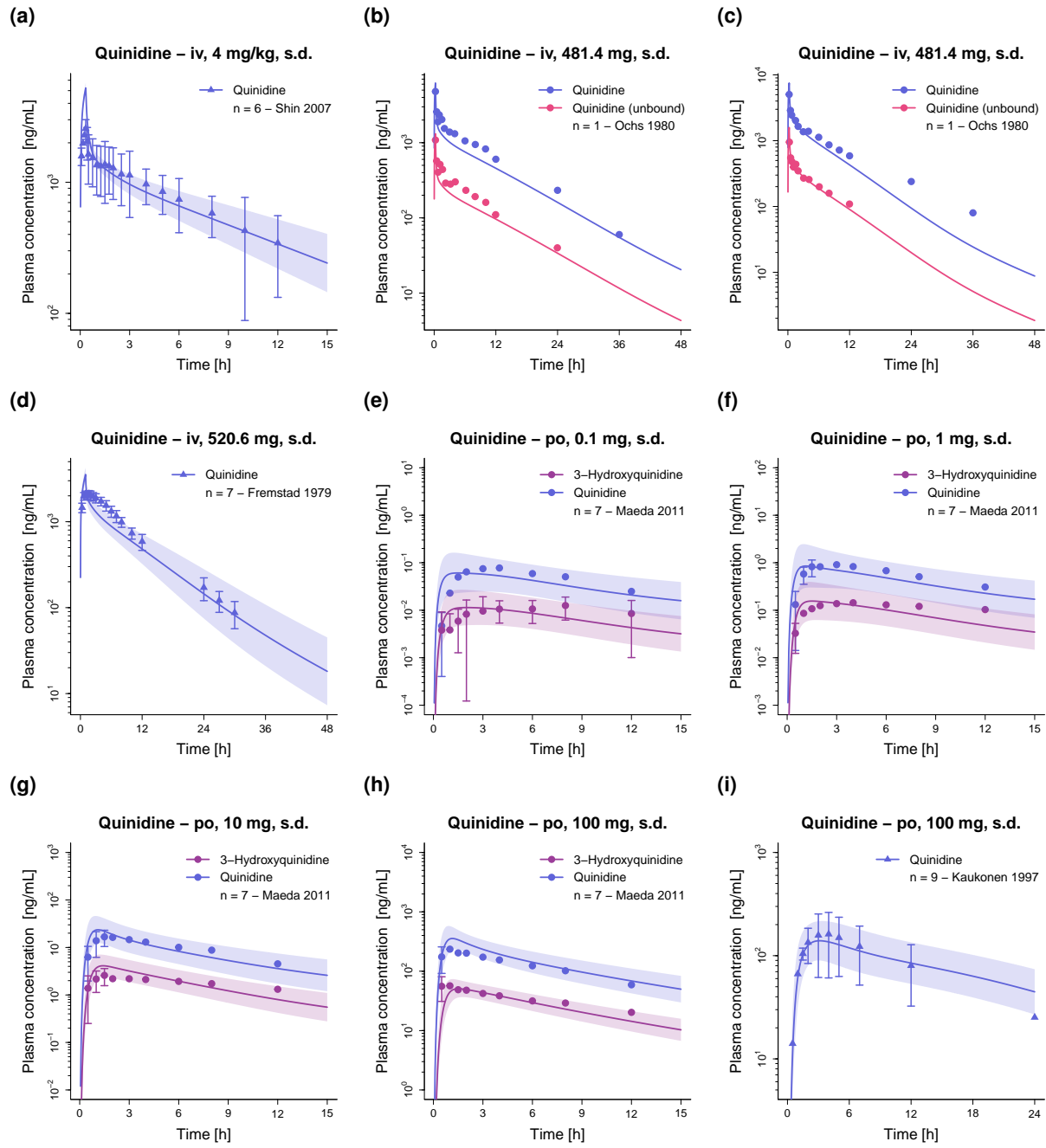


Figure S2: Quinidine plasma concentration-time profiles (semilogarithmic representation). Population predicted geometric means and individual predictions are shown as lines, corresponding geometric standard deviations are shown as shaded areas and observed data are shown as dots (training dataset) and triangles (test dataset) (\pm standard deviation, if reported). Doses indicate (a–d) quinidine gluconate and (e–i) quinidine sulfate administration. Respective doses of quinidine base were calculated and incorporated in simulations. iv: intravenous, n: number of study participants, po: oral, s.d.: single dose.

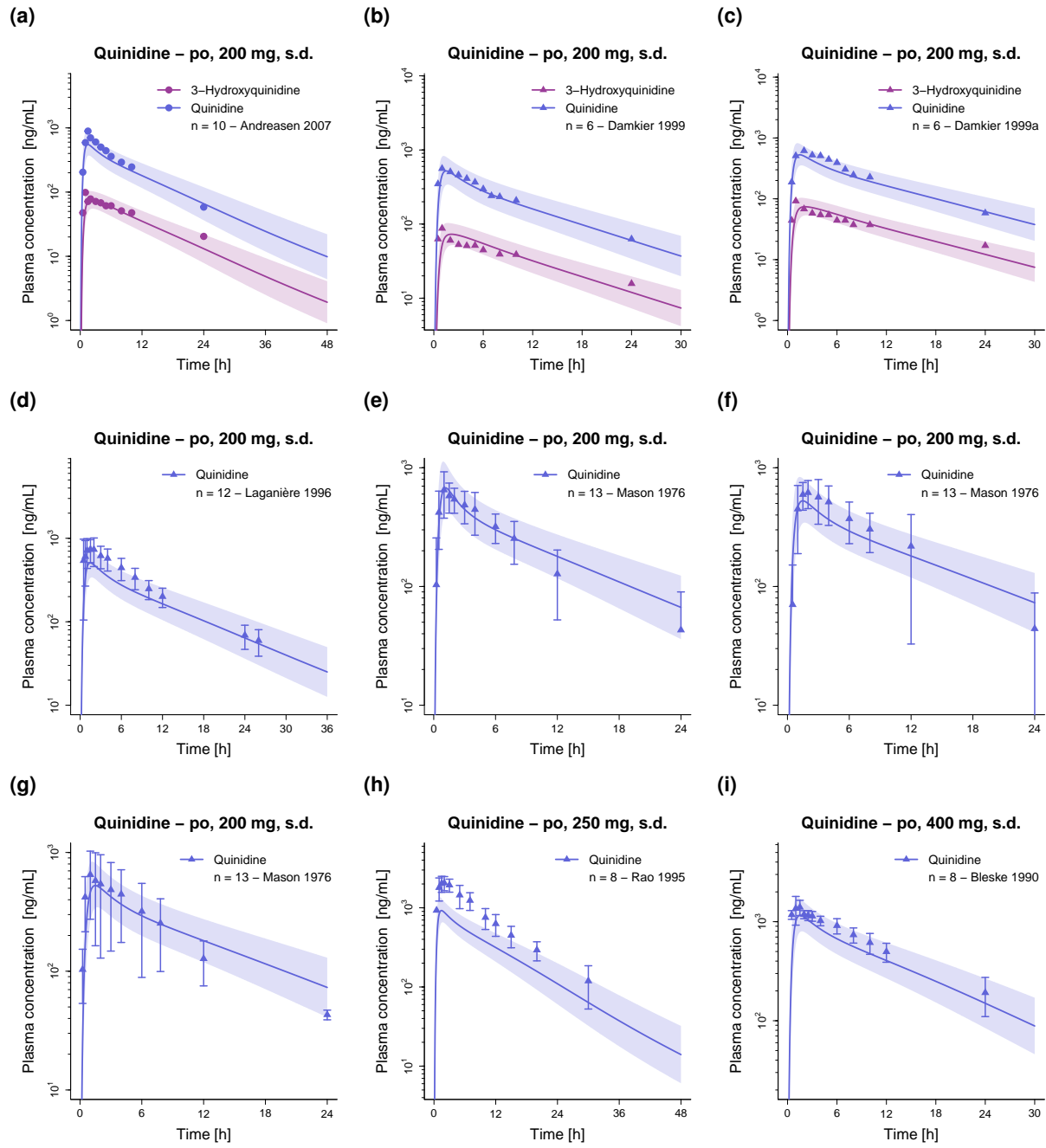


Figure S3: Quinidine plasma concentration-time profiles (semilogarithmic representation). Population predicted geometric means are shown as lines, corresponding geometric standard deviations are shown as shaded areas and observed data are shown as dots (training dataset) and triangles (test dataset) (\pm standard deviation, if reported). Doses indicate quinidine sulfate administration. Respective doses of quinidine base were calculated and incorporated in simulations. n: number of study participants, po: oral, s.d.: single dose.

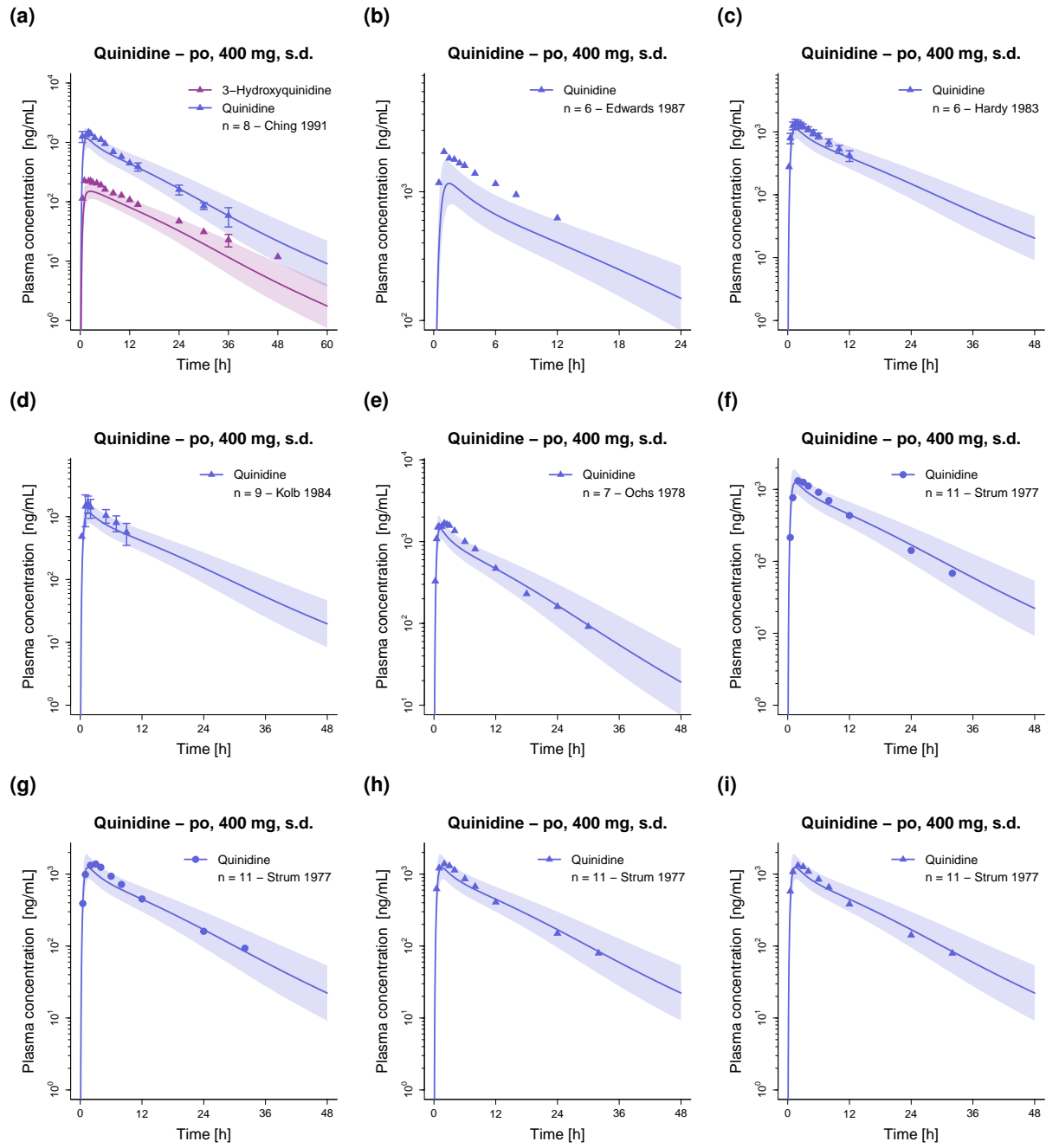


Figure S4: Quinidine plasma concentration-time profiles (semilogarithmic representation). Population predicted geometric means are shown as lines, corresponding geometric standard deviations are shown as shaded areas and observed data are shown as dots (training dataset) and triangles (test dataset) (\pm standard deviation, if reported). Doses indicate quinidine sulfate administration. Respective doses of quinidine base were calculated and incorporated in simulations. n: number of study participants, po: oral, s.d.: single dose.

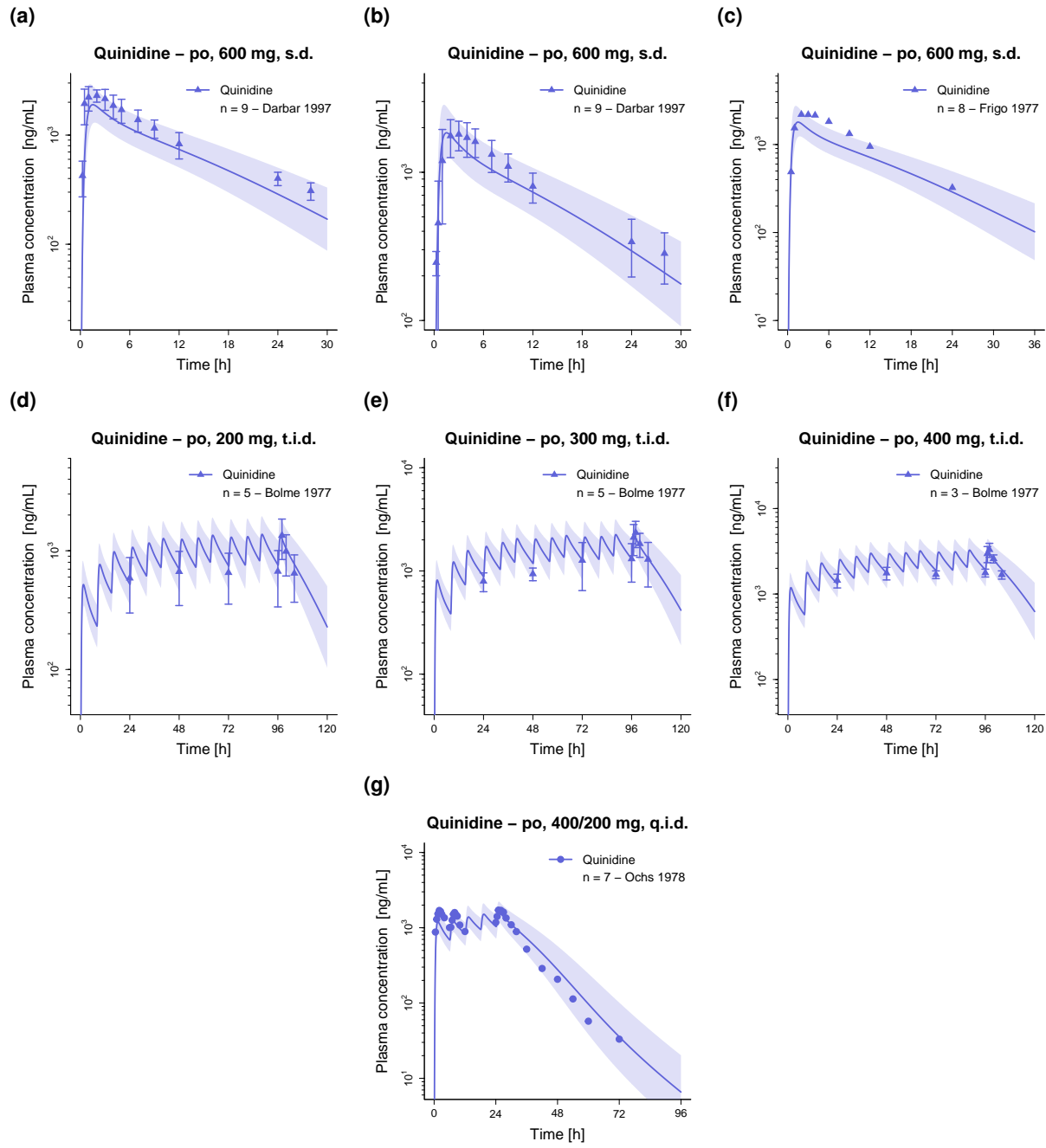


Figure S5: Quinidine plasma concentration-time profiles (semilogarithmic representation). Population predicted geometric means are shown as lines, corresponding geometric standard deviations are shown as shaded areas and observed data are shown as dots (training dataset) and triangles (test dataset) (\pm standard deviation, if reported). Doses indicate quinidine sulfate administration. Respective doses of quinidine base were calculated and incorporated in simulations. n: number of study participants, po: oral, q.i.d.: four times daily, s.d.: single dose, t.i.d.: three times daily.

S2.2 Amount excreted unchanged in urine profiles (semilogarithmic representation)

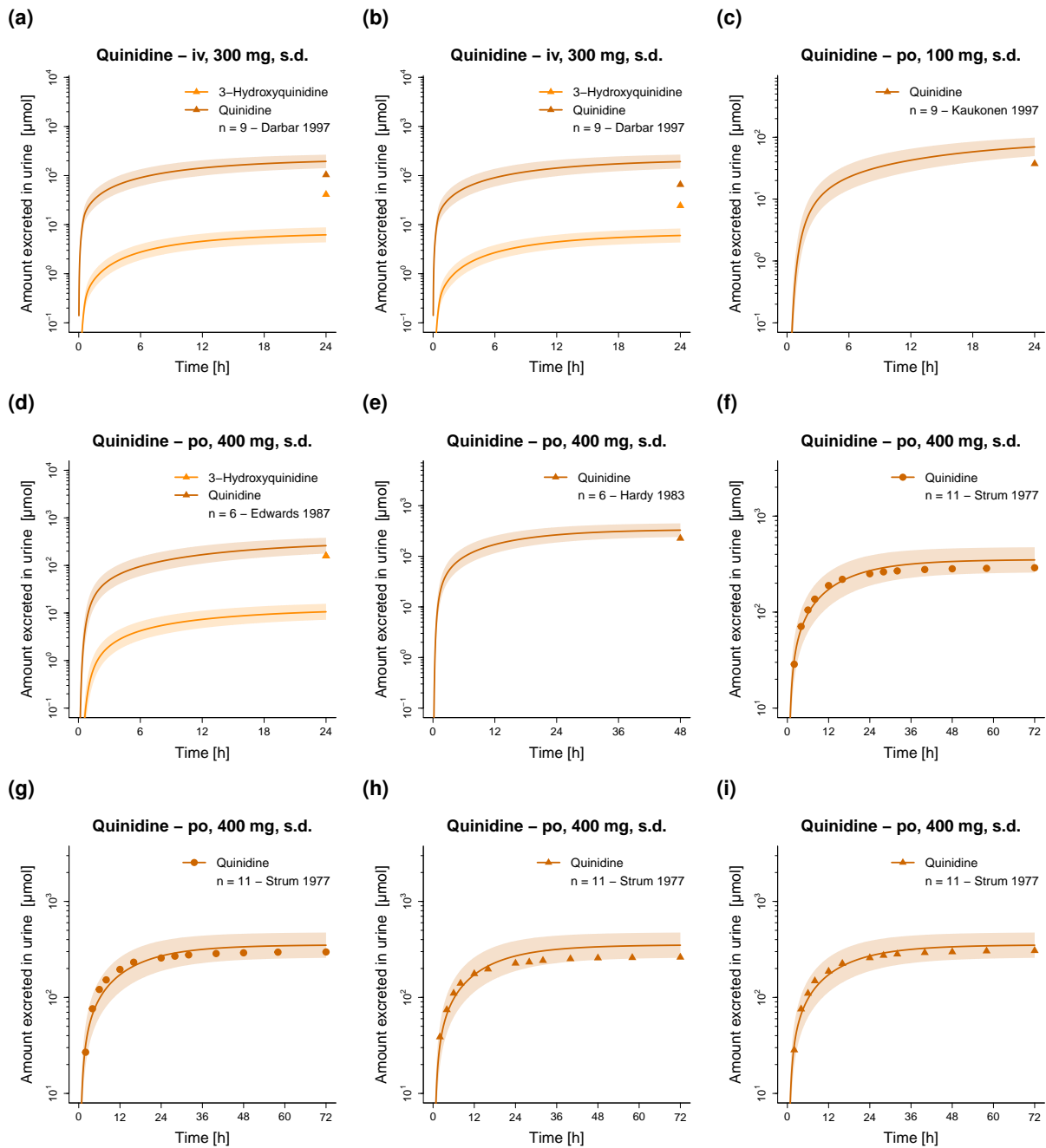


Figure S6: Quinidine amount excreted unchanged in urine profiles (semilogarithmic representation). Population predicted geometric means are shown as lines, corresponding geometric standard deviations are shown as shaded areas and observed data are shown as dots (training dataset) and triangles (test dataset). Doses indicate (a–b) quinidine gluconate and (c–i) quinidine sulfate administration. Respective doses of quinidine base were calculated and incorporated in simulations. iv: intravenous, n: number of study participants, po: oral, s.d.: single dose.

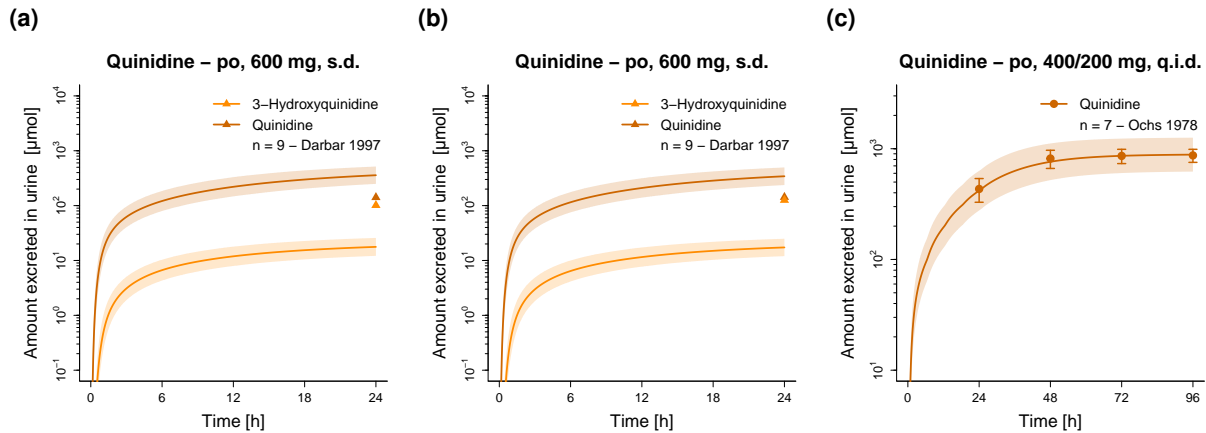


Figure S7: Quinidine amount excreted unchanged in urine profiles (semilogarithmic representation). Population predicted geometric means are shown as lines, corresponding geometric standard deviations are shown as shaded areas and observed data are shown as dots (training dataset) and triangles (test dataset) (\pm standard deviation, if reported). Doses indicate quinidine sulfate administration. Respective doses of quinidine base were calculated and incorporated in simulations. n: number of study participants, po: oral, q.i.d.: four times daily, s.d.: single dose.

S2.3 Plasma concentration-time profiles (linear representation)

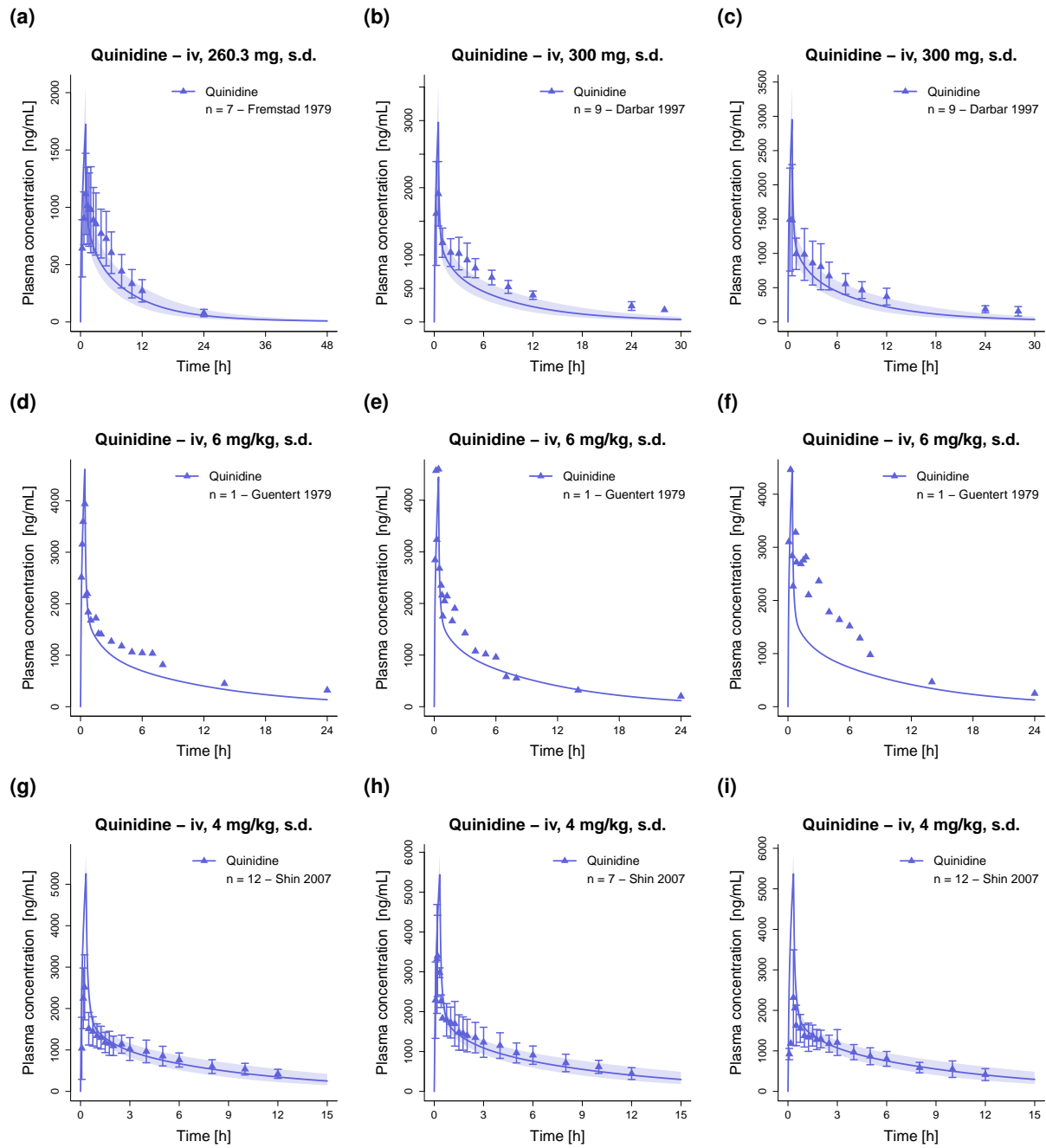


Figure S8: Quinidine plasma concentration-time profiles (linear representation). Population predicted geometric means and individual predictions are shown as lines, corresponding geometric standard deviations are shown as shaded areas and observed data are shown as dots (training dataset) and triangles (test dataset) (\pm standard deviation, if reported). Doses indicate quinidine gluconate administration. Respective doses of quinidine base were calculated and incorporated in simulations. iv: intravenous, n: number of study participants, s.d.: single dose.

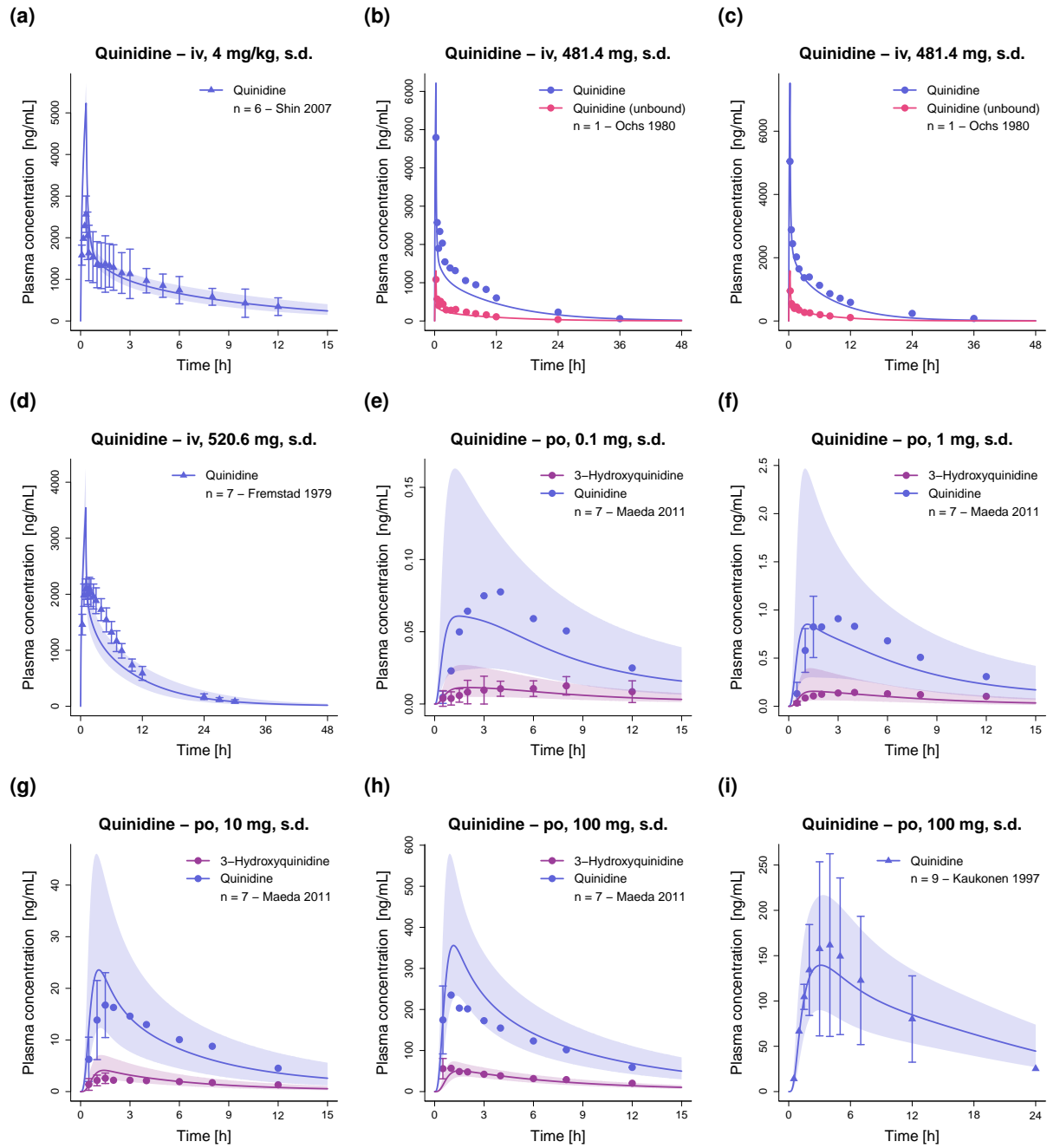


Figure S9: Quinidine plasma concentration-time profiles (linear representation). Population predicted geometric means and individual predictions are shown as lines, corresponding geometric standard deviations are shown as shaded areas and observed data are shown as dots (training dataset) and triangles (test dataset) (\pm standard deviation, if reported). Doses indicate (a–d) quinidine gluconate and (e–i) quinidine sulfate administration. Respective doses of quinidine base were calculated and incorporated in simulations. iv: intravenous, n: number of study participants, po: oral, s.d.: single dose.

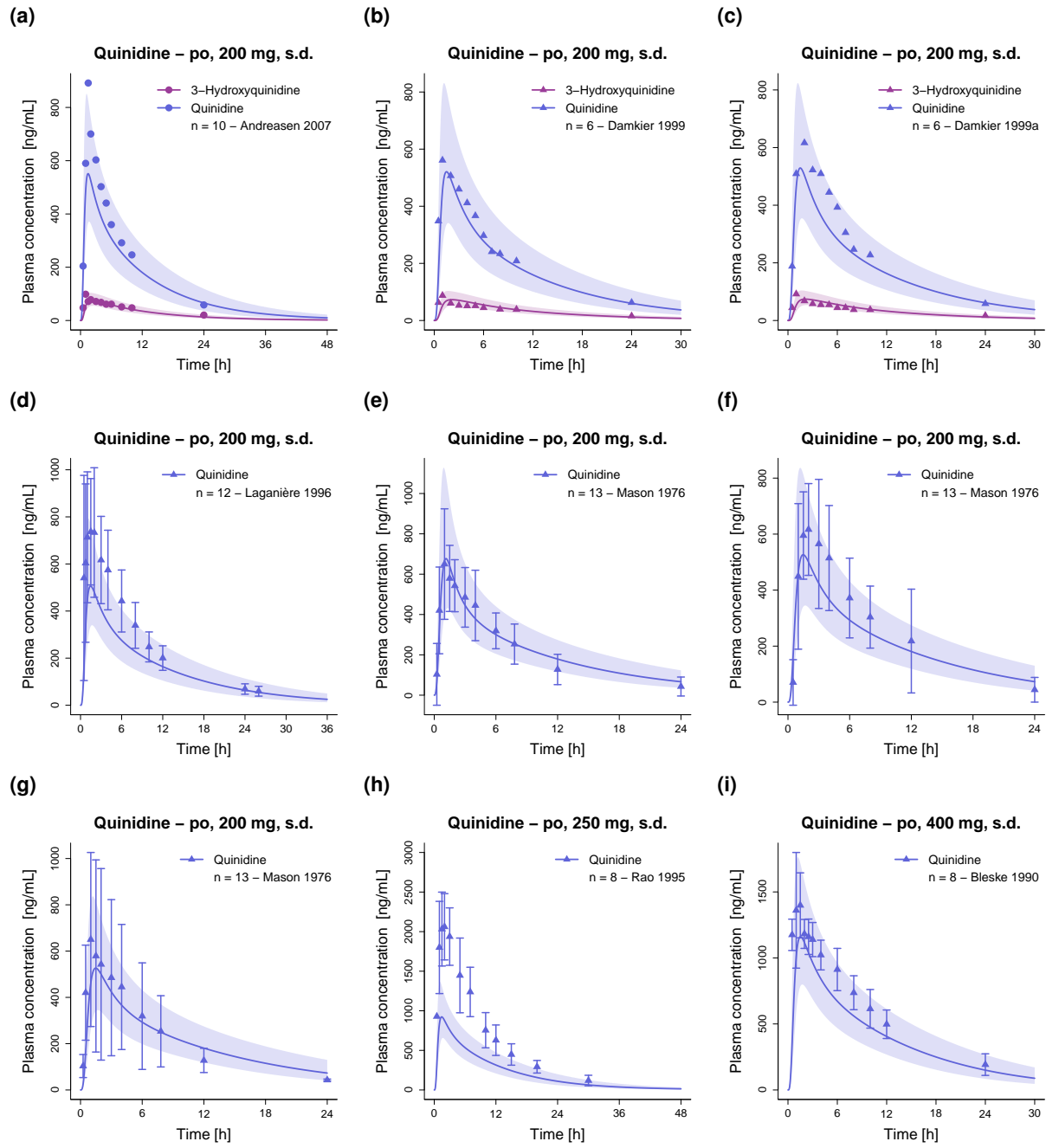


Figure S10: Quinidine plasma concentration-time profiles (linear representation). Population predicted geometric means are shown as lines, corresponding geometric standard deviations are shown as shaded areas and observed data are shown as dots (training dataset) and triangles (test dataset) (\pm standard deviation, if reported). Respective doses of quinidine base were calculated and incorporated in simulations. n: number of study participants, po: oral, s.d.: single dose.

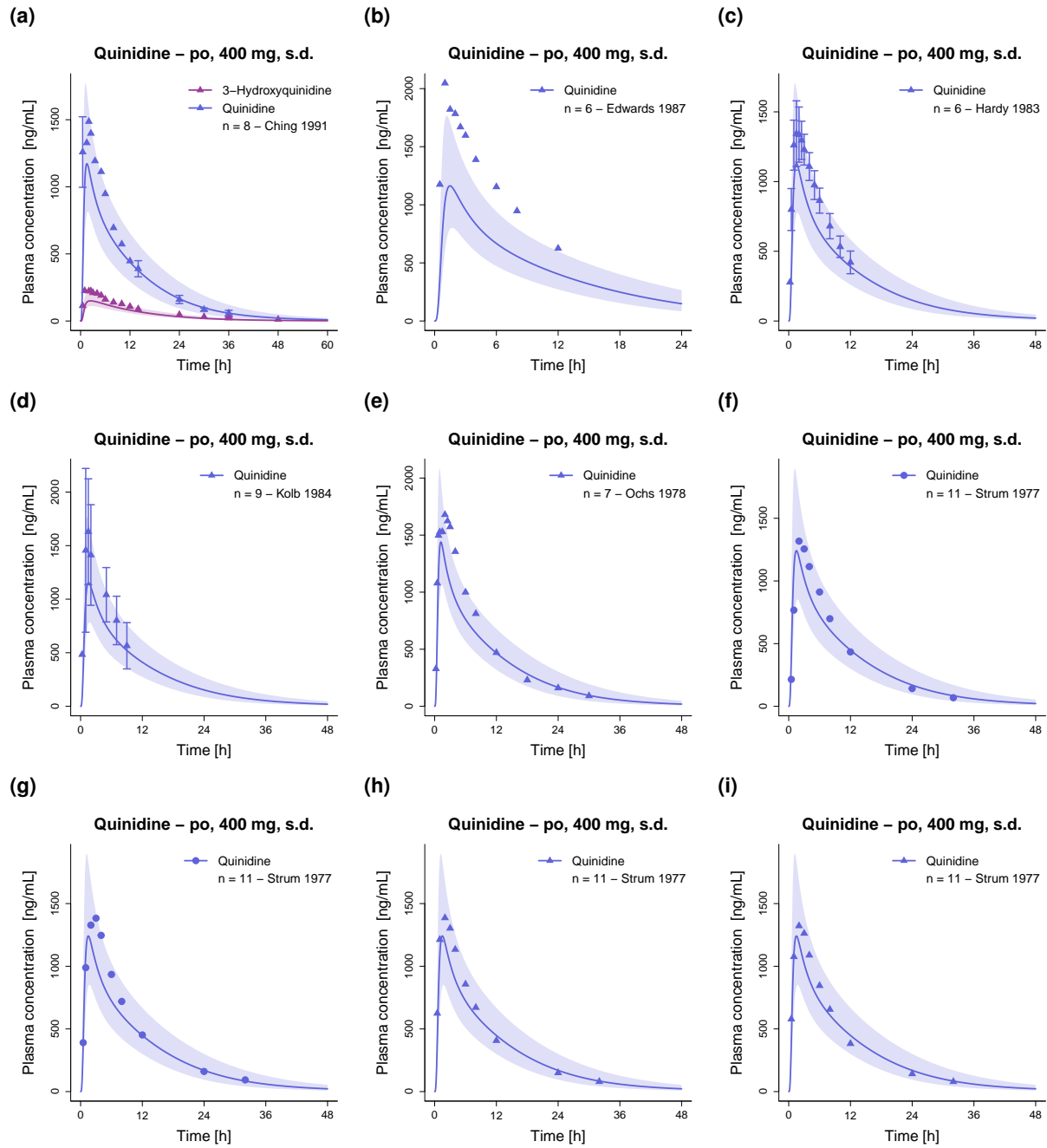


Figure S11: Quinidine plasma concentration-time profiles (linear representation). Population predicted geometric means are shown as lines, corresponding geometric standard deviations are shown as shaded areas and observed data are shown as dots (training dataset) and triangles (test dataset) (\pm standard deviation, if reported). Respective doses of quinidine base were calculated and incorporated in simulations. n: number of study participants, po: oral, s.d.: single dose.

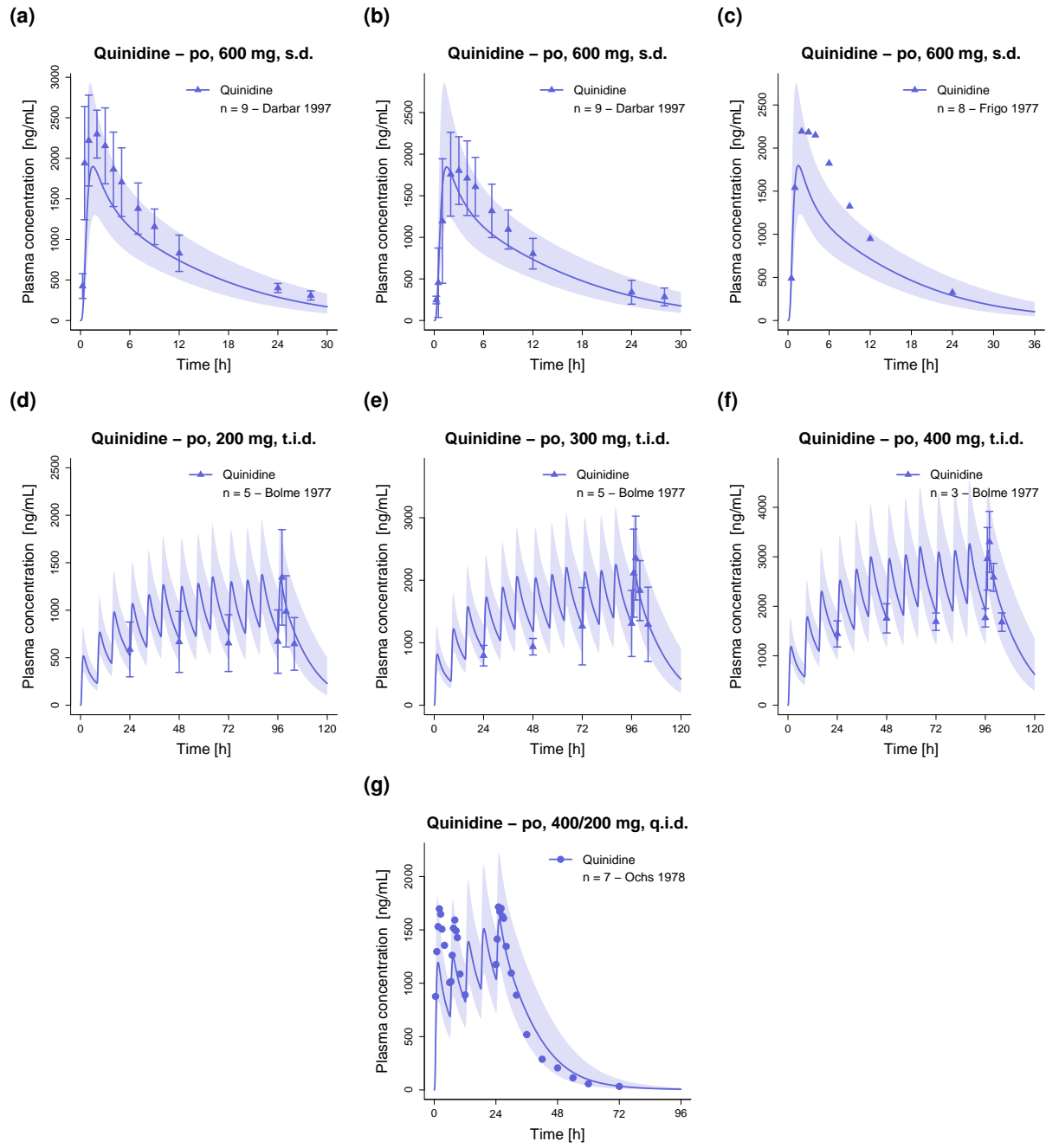


Figure S12: Quinidine plasma concentration-time profiles (linear representation). Population predicted geometric means are shown as lines, corresponding geometric standard deviations are shown as shaded areas and observed data are shown as dots (training dataset) and triangles (test dataset) (\pm standard deviation, if reported). Respective doses of quinidine base were calculated and incorporated in simulations. n: number of study participants, po: oral, q.i.d.: four times daily, s.d.: single dose.

S2.4 Amount excreted unchanged in urine profiles (linear representation)

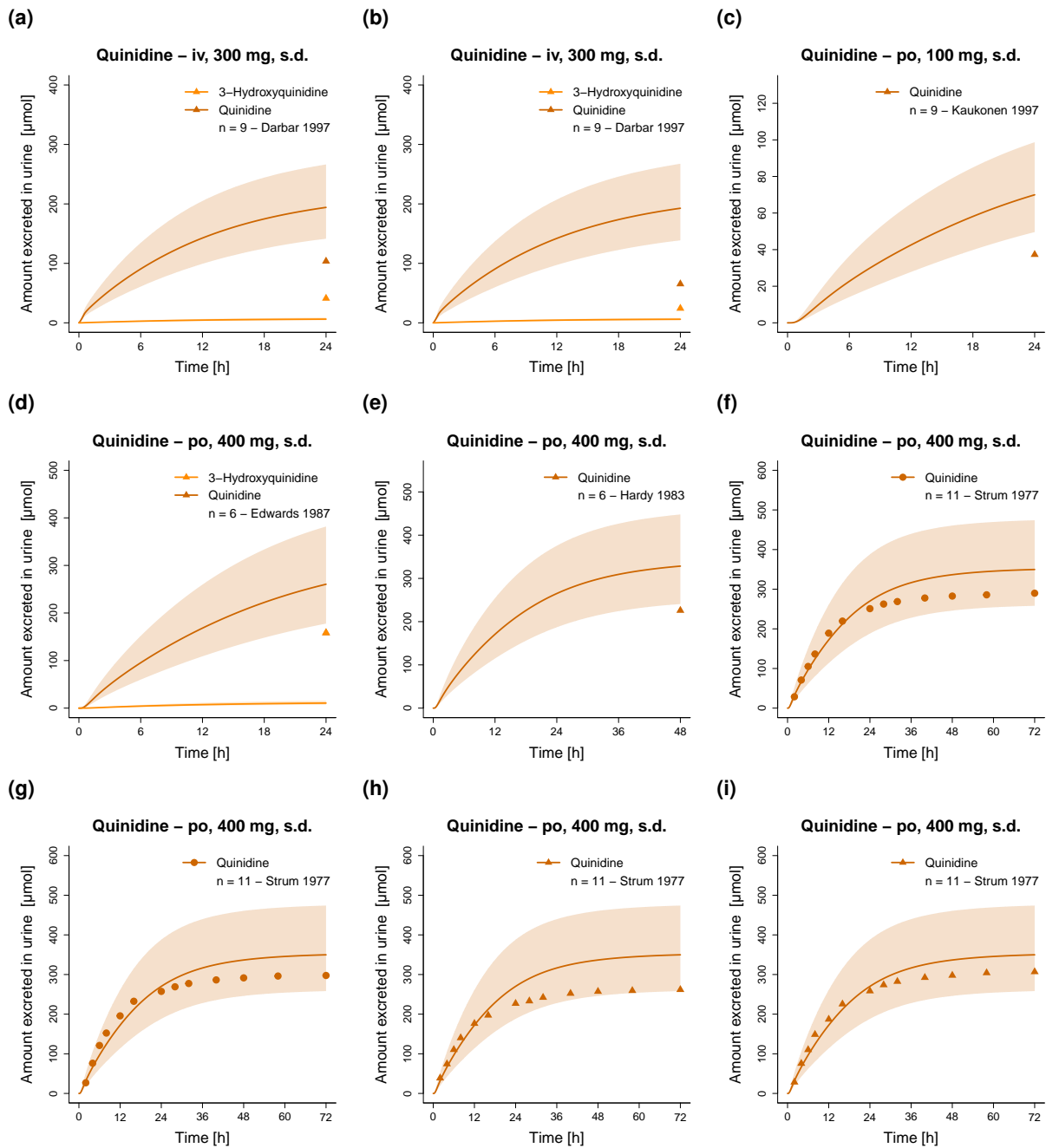


Figure S13: Quinidine amount excreted unchanged in urine profiles (linear representation). Population predicted geometric means are shown as lines, corresponding geometric standard deviations are shown as shaded areas and observed data are shown as dots (training dataset) and triangles (test dataset). Doses indicate (a-b) quinidine gluconate and (c-i) quinidine sulfate administration. Respective doses of quinidine base were calculated and incorporated in simulations. iv: intravenous, n: number of study participants, po: oral, s.d.: single dose.

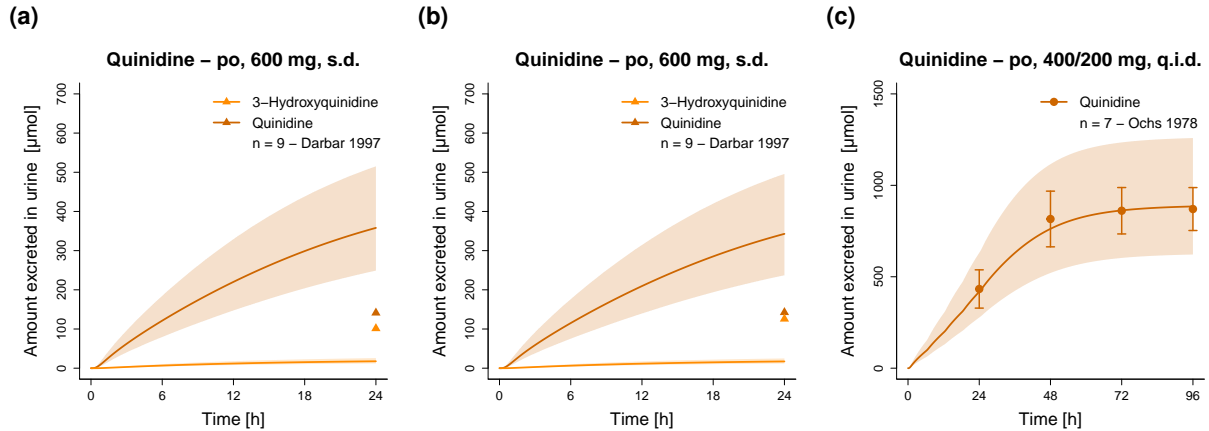


Figure S14: Quinidine amount excreted unchanged in urine profiles (linear representation). Population predicted geometric means are shown as lines, corresponding geometric standard deviations are shown as shaded areas and observed data are shown as dots (training dataset) and triangles (test dataset) (\pm standard deviation, if reported). Doses indicate quinidine sulfate administration. Respective doses of quinidine base were calculated and incorporated in simulations. n: number of study participants, po: oral, q.i.d.: four times daily, s.d.: single dose.

S2.5 Predicted compared to observed concentrations

(a) Plasma concentrations training dataset (b) Plasma concentrations test dataset

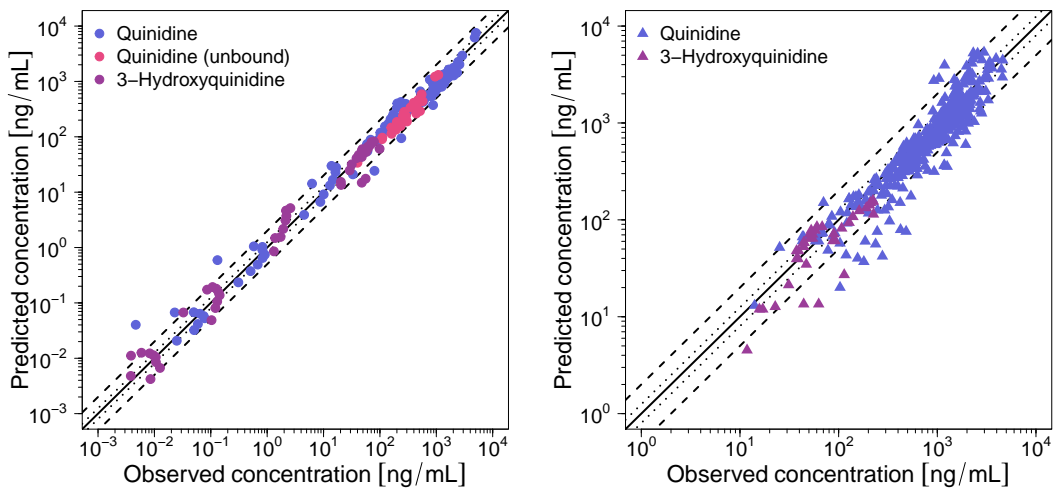


Figure S15: Goodness-of-fit plots comparing predicted and observed plasma concentration values. The solid line marks the line of identity. Dotted lines indicate 1.25-fold, dashed lines indicate 2-fold deviation.

S2.6 Mean relative deviation of plasma concentration predictions

Table S6: MRD values of quinidine plasma concentration predictions

Quinidine administration						
Dose salt [mg]	Dose base [mg]	Route	Molecule	Dataset	MRD	Reference
Quinidine						
260.3 ^a	162.2	s.d. iv 60 min inf	QUI	te	1.48	Fremstad 1979 [22]
300 ^a	187.5	s.d. iv 30 min inf	QUI	te	2.05	Darbar 1997 ^b [24]
300 ^a	187.5	s.d. iv 30 min inf	QUI	te	1.83	Darbar 1997 ^c [24]
6/kg ^a	3.74/kg	s.d. iv 25 min inf	QUI	te	1.37	Guentert 1979 [25]
6/kg ^a	3.74/kg	s.d. iv 25 min inf	QUI	te	1.32	Guentert 1979 [25]
6/kg ^a	3.74/kg	s.d. iv 25 min inf	QUI	te	1.81	Guentert 1979 [25]
6.42/kg ^a	4.00/kg	s.d. iv 20 min inf	QUI	te	1.42	Shin 2007 [27]
6.42/kg ^a	4.00/kg	s.d. iv 20 min inf	QUI	te	1.24	Shin 2007 [27]
6.42/kg ^a	4.00/kg	s.d. iv 20 min inf	QUI	te	1.56	Shin 2007 [27]
6.42/kg ^a	4.00/kg	s.d. iv 20 min inf	QUI	te	1.38	Shin 2007 [27]
481.4 ^a	300	s.d. iv 15 min inf	QUI	tr	1.40	Ochs 1980 [28]
481.4 ^a	300	s.d. iv 15 min inf	QUI	tr	1.59	Ochs 1980 [28]
520.6 ^a	324.4	s.d. iv 60 min inf	QUI	te	1.42	Fremstad 1979 [22]
0.1 ^d	0.08	s.d. po sol	QUI	tr	2.33	Maeda 2011 [30]
1 ^d	0.83	s.d. po sol	QUI	tr	1.79	Maeda 2011 [30]
10 ^d	8.29	s.d. po sol	QUI	tr	1.56	Maeda 2011 [30]
100 ^d	82.87	s.d. po sol	QUI	tr	1.49	Maeda 2011 [30]
100 ^d	82.87	s.d. po tab	QUI	te	1.28	Kaukonen 1997 [31]
200 ^d	165.7	s.d. po cap	QUI	tr	1.21	Andreasen 2007 [32]
200 ^d	165.7	s.d. po tab	QUI	te	1.27	Damkier 1999 [33]
200 ^d	165.7	s.d. po tab	QUI	te	1.18	Damkier 1999a [34]
200 ^d	165.7	s.d. po tab	QUI	te	1.49	Laganière 1996 [35]
200 ^d	165.7	s.d. po sol	QUI	te	1.30	Mason 1976 [36]
200 ^d	165.7	s.d. po cap	QUI	te	1.43	Mason 1976 [36]
200 ^d	165.7	s.d. po tab	QUI	te	1.85	Mason 1976 [36]
250 ^d	207.2	s.d. po cap	QUI	te	2.29	Rao 1995 [37]
400 ^d	331.5	s.d. po tab	QUI	te	1.44	Bleske 1990 [38]
400 ^d	331.5	s.d. po tab	QUI	te	1.49	Ching 1991 [39]
400 ^d	331.5	s.d. po tab	QUI	te	1.73	Edwards 1987 [40]
400 ^d	331.5	s.d. po tab	QUI	te	1.86	Hardy 1983 [41]
400 ^d	331.5	s.d. po tab	QUI	te	2.12	Kolb 1984 [42]
400 ^d	331.5	s.d. po tab	QUI	te	1.47	Ochs 1978 [43]
400 ^d	331.5	s.d. po tab	QUI	tr	1.33	Strum 1977 (A) [44]
400 ^d	331.5	s.d. po tab	QUI	tr	1.28	Strum 1977 (B) [44]
400 ^d	331.5	s.d. po tab	QUI	te	1.33	Strum 1977 (C) [44]
400 ^d	331.5	s.d. po tab	QUI	te	1.29	Strum 1977 (D) [44]
600 ^d	497.2	s.d. po tab	QUI	te	1.90	Darbar 1997 ^b [24]
600 ^d	497.2	s.d. po tab	QUI	te	1.50	Darbar 1997 ^c [24]
600 ^d	497.2	s.d. po tab	QUI	te	1.28	Frigo 1977 [45]
200 ^d	165.7	t.i.d. po tab	QUI	te	1.07	Bolme 1977 [46]
300 ^d	248.6	t.i.d. po tab	QUI	te	1.12	Bolme 1977 [46]
400 ^d	331.5	t.i.d. po tab	QUI	te	1.09	Bolme 1977 [46]
400 + 200 ^d	331.5 + 165.7	s.d. + q.i.d. po tab	QUI	tr	1.28	Ochs 1978 [43]
Mean QUI MRD training dataset (range):				1.53 (1.21 – 2.33), 9/10 with MRD \leq 2		
Mean QUI MRD test dataset (range):				1.51 (1.07 – 2.29), 30/33 with MRD \leq 2		
Overall QUI MRD (range):				1.51 (1.07 – 2.33), 39/43 with MRD \leq 2		

cap: capsule, inf: infusion, iv: intravenous, MRD: mean relative deviation, OHQ: 3-hydroxyquinidine, po: oral, q.i.d.: four times daily, QUB: quinidine unbound, QUI: quinidine, s.d.: single dose, sol: solution, tab: tablet, te: test dataset, t.i.d.: three times daily, tr: training dataset. Respective doses of quinidine base were calculated and incorporated in simulations. ^a Quinidine gluconate dose. ^b Low-salt diet. ^c High-salt diet. ^d Quinidine sulfate dose.

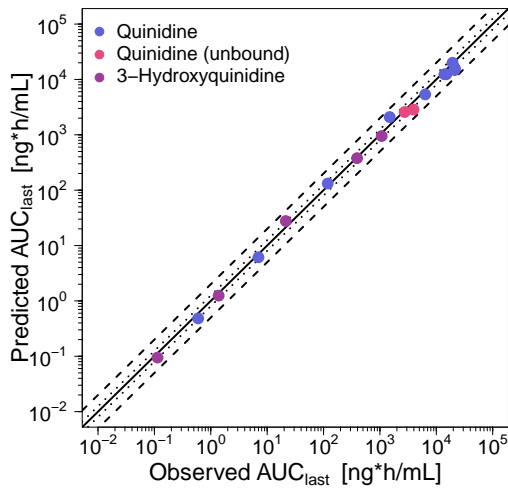
Table S6: MRD values of quinidine plasma concentration predictions (*continued*)

Quinidine administration						
Dose salt [mg]	Dose base [mg]	Route	Molecule	Dataset	MRD	Reference
Quinidine (unbound)						
481.4 ^a	300	s.d. iv 15 min inf	QUB	tr		Ochs 1980 [28]
481.4 ^a	300	s.d. iv 15 min inf	QUB	tr		Ochs 1980 [28]
Mean QUB MRD (range):					1.27 (1.12 – 1.41), 2/2 with MRD ≤ 2	
3-Hydroxyquinidine						
0.1 ^b	0.08	s.d. po sol	OHQ	tr	1.76	Maeda 2011 [30]
1 ^d	0.83	s.d. po sol	OHQ	tr	1.65	Maeda 2011 [30]
10 ^d	8.29	s.d. po sol	OHQ	tr	1.65	Maeda 2011 [30]
100 ^d	82.87	s.d. po sol	OHQ	tr	1.65	Maeda 2011 [30]
200 ^d	82.87	s.d. po cap	OHQ	tr	1.50	Andreasen 2007 [32]
200 ^d	82.87	s.d. po tab	OHQ	te	1.75	Damkier 1999 [33]
200 ^d	82.87	s.d. po tab	OHQ	te	1.55	Damkier 1999a [34]
400 ^d	331.5	s.d. po tab	OHQ	te	1.75	Ching 1991 [39]
Mean OHQ MRD training dataset (range):					1.62 (1.50 – 1.76), 5/5 with MRD ≤ 2	
Mean OHQ MRD test dataset (range):					1.68 (1.55 – 1.75), 3/3 with MRD ≤ 2	
Overall OHQ MRD (range):					1.64 (1.50 – 1.76), 8/8 with MRD ≤ 2	
Overall MRD training dataset (range):					1.52 (1.12 – 2.33), 16/17 with MRD ≤ 2	
Overall MRD test dataset (range):					1.52 (1.07 – 2.29), 33/36 with MRD ≤ 2	
Overall MRD (range):					1.52 (1.07 – 2.33), 49/53 with MRD ≤ 2	

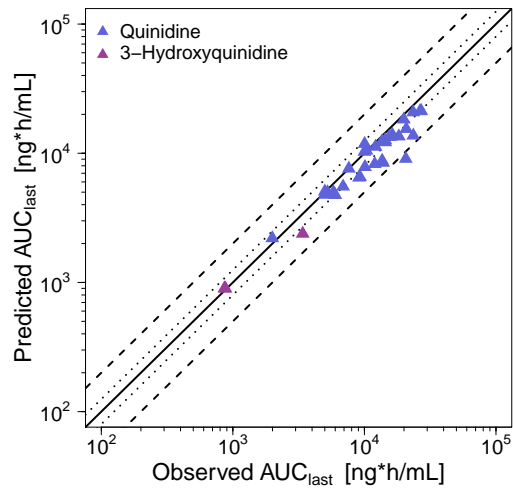
cap: capsule, inf: infusion, iv: intravenous, MRD: mean relative deviation, OHQ: 3-hydroxyquinidine, po: oral, q.i.d.: four times daily, QUB: quinidine unbound, QUI: quinidine, s.d.: single dose, sol: solution, tab: tablet, te: test dataset, t.i.d.: three times daily, tr: training dataset. Respective doses of quinidine base were calculated and incorporated in simulations. ^a Quinidine gluconate dose. ^b Low-salt diet. ^c High-salt diet. ^d Quinidine sulfate dose.

S2.7 Predicted compared to observed AUC_{last} and C_{max} values

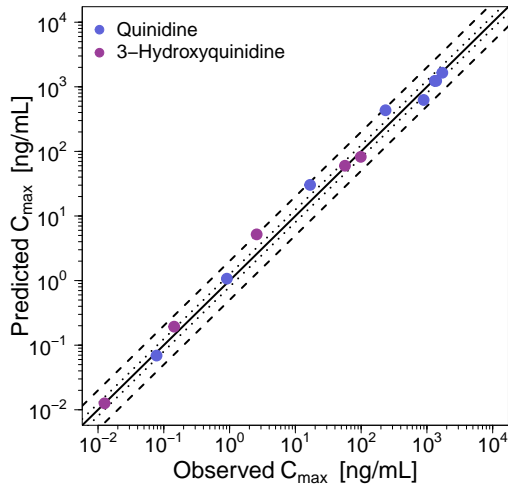
(a) AUC_{last} training dataset



(b) AUC_{last} test dataset



(c) C_{max} training dataset



(d) C_{max} test dataset

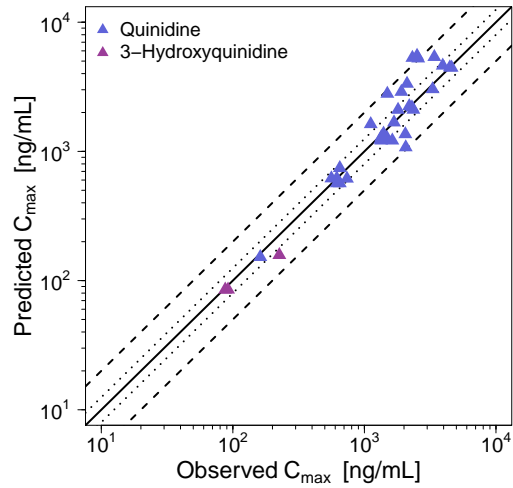


Figure S16: Goodness-of-fit plots comparing predicted and observed AUC_{last} and C_{max} values. The solid line marks the line of identity. Dotted lines indicate 1.25-fold, dashed lines indicate 2-fold deviation. AUC_{last}: area under the plasma concentration-time curve calculated between the first and last concentration measurement, C_{max}: maximum plasma concentration.

S2.8 Geometric mean fold errors of predicted AUC_{last} and C_{max} values

Table S7: Predicted and observed quinidine AUC_{last} and C_{max} values

Quinidine administration			AUC _{last}				C _{max}				Molecule	Dataset	Reference
Dose salt [mg]	Dose base [mg]	Route	t _{last} [h]	Pred [ng·h/mL]	Obs [ng·h/mL]	Pred/Obs	Pred [ng/mL]	Obs [ng/mL]	Pred/Obs	Molecule			
Quinidine													
260.3 ^a	162.2	s.d. iv 60 min inf	24	6554.71	9263.44	0.71	1626.43	1116.94	1.46	QUI	te	Fremstad 1979 [22]	
300 ^a	187.5	s.d. iv 30 min inf	28	8445.88	13853.58	0.61	2892.69	1909.17	1.52	QUI	te	Darbar 1997 ^b [24]	
300 ^a	187.5	s.d. iv 30 min inf	28	8265.50	11985.68	0.96	2794.84	1493.54	1.87	QUI	te	Darbar 1997 ^c [24]	
6/kg ^a	3.74/kg	s.d. iv 25 min inf	24	13513.46	18270.86	0.74	4613.41	3940.06	1.17	QUI	te	Guentert 1979 [25]	
6/kg ^a	3.74/kg	s.d. iv 25 min inf	24	13502.09	16073.67	0.84	4447.58	4601.00	0.97	QUI	te	Guentert 1979 [25]	
6/kg ^a	3.74/kg	s.d. iv 25 min inf	24	13715.93	23533.78	0.58	4470.83	4461.40	1.00	QUI	te	Guentert 1979 [25]	
6.42/kg ^a	4.00/kg	s.d. iv 20 min inf	12	11820.90	10039.30	1.18	5497.46	2512.40	2.19	QUI	te	Shin 2007 [27]	
6.42/kg ^a	4.00/kg	s.d. iv 20 min inf	12	11235.57	12146.47	0.93	5384.97	3399.50	1.58	QUI	te	Shin 2007 [27]	
6.42/kg ^a	4.00/kg	s.d. iv 20 min inf	12	10277.00	10002.75	1.03	5245.17	2564.50	2.05	QUI	te	Shin 2007 [27]	
481.4 ^a	300	s.d. iv 15 min inf	38	14741.64	21152.33	0.70	-	-	-	QUI	tr	Ochs 1980 [28]	
481.4 ^a	300	s.d. iv 15 min inf	36	15818.56	21417.30	0.74	-	-	-	QUI	tr	Ochs 1980 [28]	
520.6 ^a	324.4	s.d. iv 60 min inf	24	15437.76	20807.88	0.74	3340.12	2108.70	1.58	QUI	te	Fremstad 1979 [22]	
0.1 ^d	0.08	s.d. po sol	12	0.48	0.60	0.81	0.07	0.08	0.89	QUI	tr	Maeda 2011 [30]	
1 ^d	0.83	s.d. po sol	12	6.14	7.01	0.88	1.07	0.91	1.18	QUI	tr	Maeda 2011 [30]	
10 ^d	8.29	s.d. po sol	12	131.72	118.68	1.11	30.29	16.75	1.81	QUI	tr	Maeda 2011 [30]	
100 ^d	82.87	s.d. po sol	12	2090.94	1488.69	1.40	433.41	235.06	1.84	QUI	tr	Maeda 2011 [30]	
100 ^d	82.87	s.d. po tab	24	2201.88	1994.05	1.10	152.36	161.66	0.94	QUI	te	Kaukonen 1997 [31]	
200 ^d	165.7	s.d. po cap	24	5360.72	6367.26	0.84	625.51	891.66	0.70	QUI	tr	Andreasen 2007 [32]	
200 ^d	165.7	s.d. po tab	24	4991.73	5248.11	0.95	618.73	561.00	1.10	QUI	te	Damkier 1999 [33]	
200 ^d	165.7	s.d. po tab	24	4991.74	5814.42	0.86	618.73	616.40	1.00	QUI	te	Damkier 1999a [34]	
200 ^d	165.7	s.d. po tab	26	5529.71	6884.07	0.80	615.87	736.73	0.84	QUI	te	Laganière 1996 [35]	
200 ^d	165.7	s.d. po sol	24	5057.62	5002.61	1.01	743.71	650.10	1.14	QUI	te	Mason 1976 [36]	
200 ^d	165.7	s.d. po cap	24	4755.30	6002.45	0.79	566.99	616.57	0.92	QUI	te	Mason 1976 [36]	
200 ^d	165.7	s.d. po tab	24	4774.21	5002.61	0.95	566.99	650.10	0.87	QUI	te	Mason 1976 [36]	
250 ^d	207.2	s.d. po cap	30	9063.63	20629.28	0.48	1076.40	2061.28	0.52	QUI	te	Rao 1995 [37]	
400 ^d	331.5	s.d. po tab	24	12181.74	14392.00	0.85	1372.09	1398.30	0.98	QUI	te	Bleske 1990 [38]	
400 ^d	331.5	s.d. po tab	48	13381.59	15453.90	0.87	1271.53	1486.31	0.86	QUI	te	Ching 1991 [39]	
400 ^d	331.5	s.d. po tab	12	8759.10	13634.29	0.64	1359.68	2046.99	0.66	QUI	te	Edwards 1987 [40]	
400 ^d	331.5	s.d. po tab	12	7831.41	10096.53	0.78	1214.62	1343.16	0.90	QUI	te	Hardy 1983 [41]	
400 ^d	331.5	s.d. po tab	9	6486.18	9100.55	0.71	1214.56	1629.89	0.75	QUI	te	Kolb 1984 [42]	
400 ^d	331.5	s.d. po tab	30	13958.36	16286.56	0.86	1676.78	1679.06	1.00	QUI	te	Ochs 1978 [43]	
400 ^d	331.5	s.d. po tab	32	12395.93	13954.84	0.89	1234.30	1317.65	0.94	QUI	tr	Strum 1977 (A) [44]	
400 ^d	331.5	s.d. po tab	32	12395.93	15040.31	0.82	1234.30	1383.33	0.89	QUI	tr	Strum 1977 (B) [44]	
400 ^d	331.5	s.d. po tab	32	12395.93	14253.64	0.87	1234.30	1386.25	0.89	QUI	te	Strum 1977 (C) [44]	
400 ^d	331.5	s.d. po tab	32	12395.93	13617.59	0.91	1234.30	1322.02	0.93	QUI	te	Strum 1977 (D) [44]	
600 ^d	497.2	s.d. po tab	28	21298.05	27000.85	0.79	2190.62	2297.91	0.95	QUI	te	Darbar 1997 ^b [24]	
600 ^d	497.2	s.d. po tab	28	20762.60	23458.79	0.89	2099.90	1802.24	1.17	QUI	te	Darbar 1997 ^c [24]	
600 ^d	497.2	s.d. po tab	24	21174.82	26466.89	0.80	2243.14	2193.19	1.02	QUI	te	Frigo 1977 [45]	
200 ^d	165.7	t.i.d. po tab	8	7608.27	7615.63	1.00	1292.21	1345.63	0.96	QUI	te	Bolme 1977 [46]	
300 ^d	248.6	t.i.d. po tab	8	12648.11	14391.95	0.88	2103.04	2354.96	0.89	QUI	te	Bolme 1977 [46]	
400 ^d	331.5	t.i.d. po tab	8	18276.65	19912.52	0.92	3033.61	3301.62	0.92	QUI	te	Bolme 1977 [46]	
400 + 200 ^d	331.5 + 165.7	s.d. + q.i.d. po tab	72	20002.91	19396.58	1.03	1650.11	1714.69	0.96	QUI	tr	Ochs 1978 [43]	
Mean QUI GMFE training dataset (range):				1.22 (1.03 – 1.43), 10/10 with GMFE ≤ 2			1.33 (1.04 – 1.84), 8/8 with GMFE ≤ 2						
Mean QUI GMFE test dataset (range):				1.26 (1.00 – 2.28), 32/33 with GMFE ≤ 2			1.31 (1.00 – 2.29), 30/33 with GMFE ≤ 2						
Overall QUI GMFE (range):				1.25 (1.00 – 2.28), 42/43 with GMFE ≤ 2			1.31 (1.00 – 2.29), 38/41 with GMFE ≤ 2						

AUC_{last}: area under the plasma concentration-time curve calculated between the first and last concentration measurement, cap: capsule, C_{max}: maximum plasma concentration, GMFE: geometric mean fold error, inf: infusion, i.v.: intravenous, obs: observed, OHQ: 3-hydroxyquinidine, po: oral, q.i.d.: four times daily, QUB: quinidine unbound, QUI: quinidine, s.d.: single dose, tab: tablet, te: test dataset, t.i.d.: three times daily, t_{last}: time of the last concentration measurement, tr: training dataset, -: not available. Respective doses of quinidine base were calculated and incorporated in simulations. ^a Quinidine gluconate dose. ^b Low-salt diet. ^c High-salt diet. ^d Quinidine sulfate dose.

Table S7: Predicted and observed quinidine AUC_{last} and C_{max} values (*continued*)

Quinidine administration				AUC _{last}			C _{max}			Molecule	Dataset	Reference
Dose salt [mg]	Dose base [mg]	Route	t _{last} [h]	Pred [ng·h/mL]	Obs [ng·h/mL]	Pred/Obs	Pred [ng/mL]	Obs [ng/mL]	Pred/Obs			
Quinidine (unbound)												
481.4 ^a	300	s.d. iv 15 min inf	24	2853.55	3956.09	0.72	-	-	-	QUB	tr	Ochs 1980 [28]
481.4 ^a	300	s.d. iv 15 min inf	12	2577.23	2748.57	0.94	-	-	-	QUB	tr	Ochs 1980 [28]
Mean QUB GMFE (range):												
1.23 (1.07 – 1.39), 2/2 with GMFE ≤ 2												
3-Hydroxyquinidine												
0.1 ^d	0.08	s.d. po sol	12	0.09	0.11	0.83	0.01	0.01	1.00	OHQ	tr	Maeda 2011 [30]
1 ^d	0.83	s.d. po sol	12	1.25	1.38	0.90	0.19	0.14	1.35	OHQ	tr	Maeda 2011 [30]
10 ^d	8.29	s.d. po sol	12	27.66	21.42	1.29	5.19	2.58	2.01	OHQ	tr	Maeda 2011 [30]
100 ^d	82.87	s.d. po sol	12	379.09	393.81	0.96	59.94	56.77	1.06	OHQ	tr	Maeda 2011 [30]
200 ^d	165.7	s.d. po cap	24	948.78	1074.81	0.88	82.29	98.72	0.83	OHQ	tr	Andreasen 2007 [32]
200 ^d	165.7	s.d. po tab	24	898.21	862.40	1.04	85.22	87.51	0.97	OHQ	te	Damkier 1999 [33]
200 ^d	165.7	s.d. po tab	24	898.21	878.23	1.02	85.22	91.91	0.93	OHQ	te	Damkier 1999a [34]
400 ^d	331.5	s.d. po tab	48	2385.10	3397.45	0.70	157.86	225.59	0.70	OHQ	te	Ching 1991 [39]
Mean OHQ GMFE training dataset (range):												
1.15 (1.04 – 1.29), 5/5 with GMFE ≤ 2												
Mean OHQ GMFE test dataset (range):												
1.16 (1.02 – 1.42), 3/3 with GMFE ≤ 2												
Overall OHQ GMFE (range):												
1.16 (1.02 – 1.42), 8/8 with GMFE ≤ 2												
1.27 (1.00 – 2.07), 7/8 with GMFE ≤ 2												
Mean GMFE training dataset (range):												
1.20 (1.03 – 1.43), 17/17 with GMFE ≤ 2												
1.32 (1.00 – 2.01), 12/13 with GMFE ≤ 2												
Mean GMFE test dataset (range):												
1.25 (1.00 – 2.28), 35/36 with GMFE ≤ 2												
1.30 (1.00 – 2.29), 33/36 with GMFE ≤ 2												
Overall GMFE (range):												
1.23 (1.00 – 2.28), 52/53 with GMFE ≤ 2												
1.31 (1.00 – 2.29), 45/49 with GMFE ≤ 2												

AUC_{last}: area under the plasma concentration-time curve calculated between the first and last concentration measurement, cap: capsule, C_{max}: maximum plasma concentration, GMFE: geometric mean fold error, inf: infusion, iv: intravenous, obs: observed, OHQ: 3-hydroxyquinidine, po: oral, q.i.d.: four times daily, QUB: quinidine unbound, QUI: quinidine, s.d.: single dose, tab: tablet, te: test dataset, t.i.d.: three times daily, t_{last}: time of the last concentration measurement, tr: training dataset, -: not available. Respective doses of quinidine base were calculated and incorporated in simulations. ^a Quinidine gluconate dose. ^b Low-salt diet. ^c High-salt diet. ^d Quinidine sulfate dose.

S2.9 Geometric mean fold errors of predicted V_d and half-life values

Table S8: Predicted and observed quinidine V_d values

Quinidine administration			V_d			Molecule	Dataset	Reference
Dose salt [mg]	Dose base [mg]	Route	Pred [L/kg]	Obs [L/kg]	Pred/Obs			
Quinidine								
260.3 ^a	162.2	s.d. iv 60 min inf	3.03	2.27	1.33	QUI	te	Fremstad 1979 [22]
6/kg ^a	3.74/kg	s.d. iv 25 min inf	2.72	2.04	1.33	QUI	te	Guentert 1979 [25]
6/kg ^a	3.74/kg	s.d. iv 25 min inf	2.44	1.6	1.39	QUI	te	Guentert 1979 [25]
6/kg ^a	3.74/kg	s.d. iv 25 min inf	2.46	1.27	1.94	QUI	te	Guentert 1979 [25]
6.42/kg ^a	4.00/kg	s.d. iv 20 min inf	2.36 ^b	2.85 ^b	0.83	QUI	te	Shin 2007 [27]
6.42/kg ^a	4.00/kg	s.d. iv 20 min inf	2.20 ^b	2.18 ^b	1.01	QUI	te	Shin 2007 [27]
6.42/kg ^a	4.00/kg	s.d. iv 20 min inf	2.44 ^b	2.70 ^b	0.91	QUI	te	Shin 2007 [27]
6.42/kg ^a	4.00/kg	s.d. iv 20 min inf	2.36 ^b	2.66 ^b	0.89	QUI	te	Shin 2007 [27]
481.4 ^a	300	s.d. iv 15 min inf	2.65	1.84	1.44	QUI	tr	Ochs 1980 [28]
481.4 ^a	300	s.d. iv 15 min inf	2.97	2.55	1.16	QUI	tr	Ochs 1980 [28]
520.6 ^a	324.4	s.d. iv 60 min inf	2.64	2.27	1.16	QUI	te	Fremstad 1979 [22]
Mean QUI GMFE training dataset (range):			1.30 (1.16 – 1.44), 2/2 with GMFE ≤ 2					
Mean QUI GMFE test dataset (range):			1.27 (1.01 – 1.94), 9/9 with GMFE ≤ 2					
Overall QUI GMFE (range):			1.27 (1.01 – 1.94), 11/11 with GMFE ≤ 2					

GMFE: geometric mean fold error, inf: infusion, iv: intravenous, obs: observed, pred: predicted, QUI: quinidine, s.d.: single dose, te: test dataset, tr: training dataset, V_d : apparent volume of distribution. Respective doses of quinidine base were calculated and incorporated in simulations. ^a Quinidine gluconate dose. ^b volume of distribution at steady state (V_{ss}).

Table S9: Predicted and observed quinidine half-life values

Quinidine administration			Half-life					
Dose salt [mg]	Dose base [mg]	Route	Pred [h]	Obs [h]	Pred/Obs	Molecule	Dataset	Reference
Quinidine								
260.3 ^a	162.2	s.d. iv 60 min inf	6.84	6.42	1.07	QUI	te	Fremstad 1979 [22]
300 ^a	187.5	s.d. iv 30 min inf	6.92	10.20	0.68	QUI	te	Darbar 1997 ^b [24]
300 ^a	187.5	s.d. iv 30 min inf	7.11	9.67	0.74	QUI	te	Darbar 1997 ^c [24]
481.4 ^a	300	s.d. iv 15 min inf	8.04	7.52	1.07	QUI	tr	Ochs 1980 [28]
481.4 ^a	300	s.d. iv 15 min inf	7.10	7.88	0.90	QUI	tr	Ochs 1980 [28]
520.6 ^a	324.4	s.d. iv 60 min inf	6.80	6.42	1.06	QUI	te	Fremstad 1979 [22]
0.1 ^d	0.08	s.d. po sol	7.29	5.07	1.44	QUI	tr	Maeda 2011 [30]
1 ^d	0.83	s.d. po sol	6.82	5.73	1.19	QUI	tr	Maeda 2011 [30]
10 ^d	8.29	s.d. po sol	5.79	5.24	1.10	QUI	tr	Maeda 2011 [30]
100 ^d	82.87	s.d. po sol	6.06	5.59	1.08	QUI	tr	Maeda 2011 [30]
100 ^d	82.87	s.d. po tab	11.38	7.40	1.54	QUI	te	Kaukonen 1997 [31]
200 ^d	165.7	s.d. po cap	7.92	6.88	1.15	QUI	tr	Andreasen 2007 [32]
200 ^d	165.7	s.d. po tab	8.03	7.90	1.02	QUI	te	Damkier 1999 [33]
200 ^d	165.7	s.d. po tab	8.03	8.10	0.99	QUI	te	Damkier 1999a [34]
200 ^d	165.7	s.d. po tab	8.19	6.80	1.20	QUI	te	Laganière 1996 [35]
200 ^d	165.7	s.d. po sol	8.23	5.68	1.45	QUI	te	Mason 1976 [36]
200 ^d	165.7	s.d. po cap	8.84	5.74	1.54	QUI	te	Mason 1976 [36]
200 ^d	165.7	s.d. po tab	8.84	7.35	1.20	QUI	te	Mason 1976 [36]
250 ^d	207.2	s.d. po cap	6.67	7.00	0.95	QUI	te	Rao 1995 [37]
400 ^d	331.5	s.d. po tab	7.51	7.90	0.95	QUI	te	Bleske 1990 [38]
400 ^d	331.5	s.d. po tab	8.71	7.91	1.10	QUI	te	Ching 1991 [39]
400 ^d	331.5	s.d. po tab	8.72	6.90	1.26	QUI	te	Edwards 1987 [40]
400 ^d	331.5	s.d. po tab	10.14	5.80	1.75	QUI	te	Hardy 1983 [41]
400 ^d	331.5	s.d. po tab	9.61	14.91	0.64	QUI	te	Kolb 1984 [42]
400 ^d	331.5	s.d. po tab	6.38	6.10	1.05	QUI	te	Ochs 1978 [43]
400 ^d	331.5	s.d. po tab	8.09	5.36	1.51	QUI	tr	Strum 1977 (A) [44]
400 ^d	331.5	s.d. po tab	8.09	5.36	1.51	QUI	tr	Strum 1977 (B) [44]
400 ^d	331.5	s.d. po tab	8.09	5.36	1.51	QUI	te	Strum 1977 (C) [44]
400 ^d	331.5	s.d. po tab	8.09	5.36	1.51	QUI	te	Strum 1977 (D) [44]
600 ^d	497.2	s.d. po tab	7.08	7.93	0.89	QUI	te	Darbar 1997 ^b [24]
600 ^d	497.2	s.d. po tab	7.41	8.12	0.91	QUI	te	Darbar 1997 ^c [24]
600 ^d	497.2	s.d. po tab	7.32	7.87	0.93	QUI	te	Frigo 1977 [45]
Mean QUI GMFE training dataset (range):			1.23 (1.07 – 1.51), 9/9 with GMFE ≤ 2					
Mean QUI GMFE test dataset (range):			1.24 (1.01 – 1.75), 23/23 with GMFE ≤ 2					
Overall QUI GMFE (range):			1.24 (1.01 – 1.75), 32/32 with GMFE ≤ 2					

cap: capsule, GMFE: geometric mean fold error, inf: infusion, iv: intravenous, obs: observed, po: oral, pred: predicted, q.i.d.: four times daily, QUI: quinidine, s.d.: single dose, tab: tablet, te: test dataset, t.i.d.: three times daily, tr: training dataset. Respective doses of quinidine base were calculated and incorporated in simulations. ^a Quinidine gluconate dose. ^b Low-salt diet. ^c High-salt diet. ^d Quinidine sulfate dose.

S2.10 Sensitivity Analyses

Sensitivity of the quinidine and 3-hydroxyquinidine models to single model parameters was calculated, determined as relative change of AUC_{0-6h} at steady state in a four-times daily regimen of 200 mg (first dose 400 mg) quinidine (sulfate) according to Equation S2. A relative perturbation of 1000% (variation range 10.0, maximum number of 2 steps) was applied. Parameters were included into the analysis if (i) they have been optimized, (ii) they are associated with optimized parameters or (iii) they could have a strong impact due to their use in the calculation of permeabilities or partition coefficients (Table S10).

$$S = \frac{\Delta AUC}{AUC} \cdot \frac{p}{\Delta p} \quad (\text{S2})$$

S = sensitivity of the AUC to the examined model parameter, ΔAUC = change of the AUC, AUC = simulated AUC with the original parameter value, Δp = change of the examined parameter value and p = original parameter value. Parameters were considered sensitive, if their sensitivity value was equal or greater than 0.5.

Table S10: Parameters evaluated during quinidine and 3-hydroxyquinidine sensitivity analyses

Parameter	Quinidine		3-Hydroxyquinidine	
	Value	Source	Value	Source
Solubility (pH 7.0) [g/L]	11.11	Literature	12.57	Literature
Lipophilicity	2.51	Literature	1.66	Literature
$f_{u,p}$ [%]	21	Literature	31	Literature
P-gp K_M [$\mu\text{mol}/\text{L}$]	0.23	Literature	-	-
P-gp k_{cat} [1/min]	0.77	Optimized	-	-
CYP3A4 (QUI \rightarrow OHQ) K_M [$\mu\text{mol}/\text{L}$]	51.8	Literature	-	-
CYP3A4 (QUI \rightarrow OHQ) k_{cat} [1/min]	2.21	Optimized	-	-
CYP3A4 (QUI \rightarrow sink) K_M [$\mu\text{mol}/\text{L}$]	65.03	Literature	-	-
CYP3A4 (QUI \rightarrow sink) k_{cat} [1/min]	3.84	Optimized	-	-
CYP3A4 CL [1/min]	-	-	0.08	Optimized
CL_{hep} [1/min]	-	-	0.45	Optimized
P-gp K_i [$\mu\text{mol}/\text{L}$]	0.10	Literature	-	-
Intestinal permeability [cm/min]	$6.47 \cdot 10^{-6}$	Optimized	-	-
Weibull dissolution time (50% dissolved) [min]	8.76	Literature	-	-
Weibull dissolution shape	0.42	Literature	-	-

CL: clearance, CL_{hep} : hepatic metabolic clearance, CYP: cytochrome P450, $f_{u,p}$: fraction unbound plasma, k_{cat} : catalytic or transport rate constant, K_i : concentration for 50% inhibition (competitive), K_M : Michaelis-Menten constant, OHQ: 3-hydroxyquinidine, P-gp: P-glycoprotein, QUI: quinidine, -: not available.

Quinidine sensitivity analysis

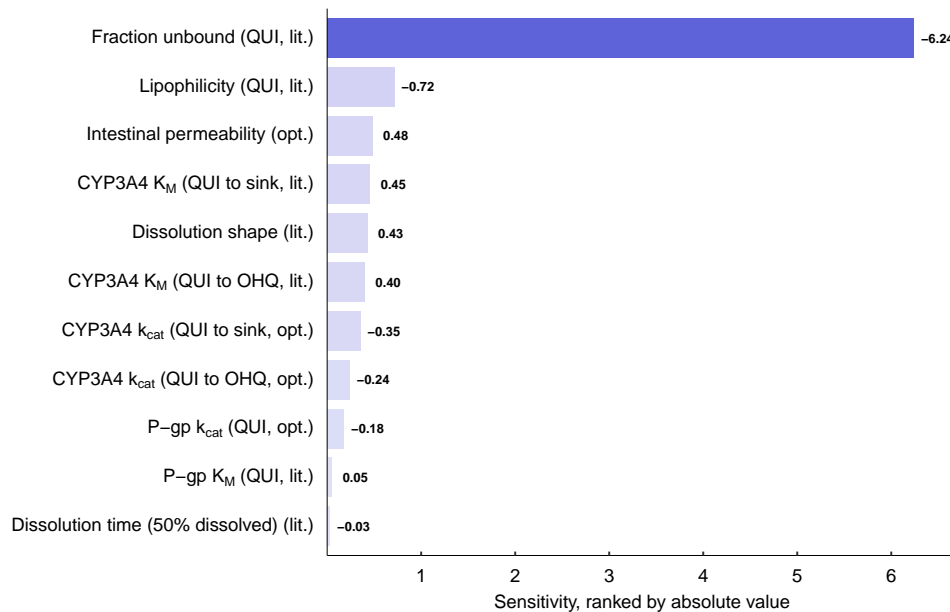


Figure S17: Local sensitivity analysis results of the quinidine PBPK model (parent quinidine), determined as relative change of AUC_{0-6h} at steady state in a four-times daily regimen of 200 mg (first dose 400 mg) quinidine (sulfate). CYP: cytochrome P450, k_{cat} : catalytic or transport rate constant, K_M : Michaelis-Menten constant, lit.: literature value, OHQ: 3-hydroxyquinidine, opt.: optimized, P-gp: P-glycoprotein, QUI: quinidine.

3-Hydroxyquinidine sensitivity analysis

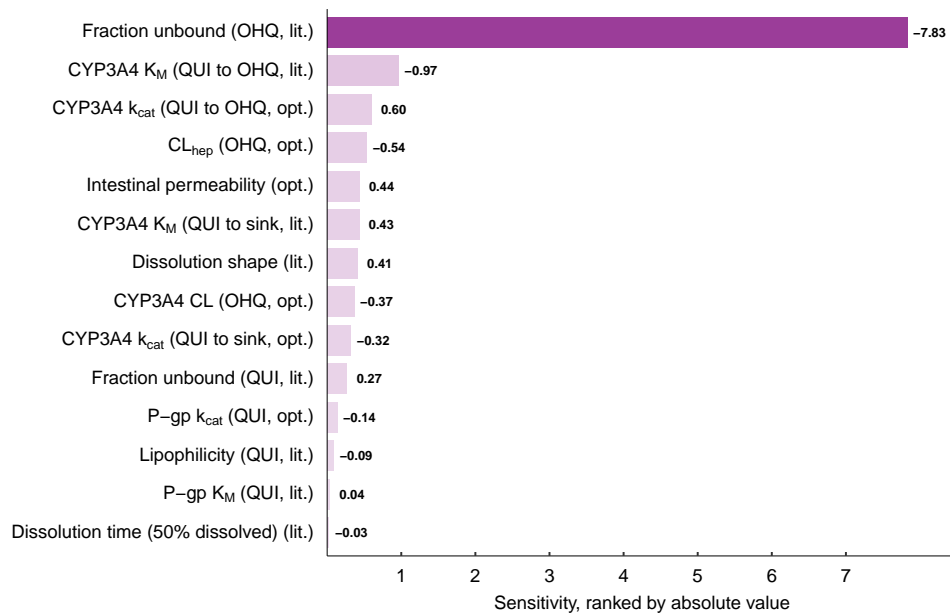


Figure S18: Local sensitivity analysis results of the quinidine PBPK model (metabolite 3-hydroxyquinidine), determined as relative change of AUC_{0-6h} at steady state in a four-times daily regimen of 200 mg (first dose 400 mg) quinidine (sulfate). CL: clearance, CL_{hep} : hepatic metabolic clearance, CYP: cytochrome P450, k_{cat} : catalytic or transport rate constant, K_M : Michaelis-Menten constant, lit.: literature value, OHQ: 3-hydroxyquinidine, opt.: optimized, P-gp: P-glycoprotein, QUI: quinidine.

S3 DD(G)I Modeling

S3.1 Types of Interaction

S3.1.1 Competitive inhibition

$$K_{M,app} = K_M * \left(1 + \frac{[I]}{K_i}\right) \quad (\text{S3})$$

$$v = \frac{v_{max} * [S]}{K_{M,app} + [S]} = \frac{k_{cat} * [E] * [S]}{K_{M,app} + [S]} \quad (\text{S4})$$

$K_{M,app}$ = Michaelis-Menten constant in the presence of inhibitor, K_M = Michaelis-Menten constant, $[I]$ = free inhibitor concentration, K_i = dissociation constant of the inhibitor-enzyme/transporter complex, v = reaction velocity, $[S]$ = free substrate concentration, k_{cat} = catalytic or transport rate constant and $[E]$ = enzyme concentration.

S3.1.2 Non-competitive inhibition

$$v_{max,app} = \frac{v_{max}}{1 + \frac{[I]}{K_i}} \quad (\text{S5})$$

$$v = \frac{v_{max,app} * [S]}{K_M + [S]} \quad (\text{S6})$$

$v_{max,app}$ = maximum reaction velocity in the presence of inhibitor, v_{max} = maximum reaction velocity, $[I]$ = free inhibitor concentration, K_i = dissociation constant of the inhibitor-enzyme/transporter complex, v = reaction velocity, $[S]$ = free substrate concentration and K_M = Michaelis-Menten constant.

S3.1.3 Mechanism-based inactivation

$$\frac{d[E]}{dt} = k_{deg} * E_0 - \frac{k_{deg} + k_{inact} * [I]}{K_I + [I]} * [E] \quad (\text{S7})$$

$\frac{d[E]}{dt}$ = enzyme turnover, k_{deg} = degradation rate constant, E_0 = enzyme concentration at time 0, $[I]$ = free mechanism-based inactivator concentration, k_{inact} = maximum inactivation rate constant, K_I = concentration for half-maximal inactivation and $[E]$ = enzyme concentration.

S3.1.4 Induction

$$\frac{d[E]}{dt} = k_{deg} * E_0 * \frac{1 + (E_{max} * [Ind])}{EC50 + [Ind]} \quad (\text{S8})$$

$\frac{d[E]}{dt}$ = enzyme turnover, k_{deg} = degradation rate constant, E_0 = enzyme concentration at time 0, E_{max} = maximal induction effect *in vivo*, $[Ind]$ = free inducer concentration and $EC50$ = concentration for half maximal induction *in vivo*.

S3.2 Published PBPK DDI models

Table S11: Published perpetrator models and included relevant interaction constants

Model (PK-Sim® Version)	Mechanism	Parameter	Value	Publication	Model repository
Carbamazepine (V11)				Fuhr et al. 2021 [65]	Carbamazepine-Model (OSP, v1.0) ^a
Carbamazepine	Induction	CYP3A4 E _{max}	6.00		
Carbamazepine	Induction	CYP3A4 EC ₅₀ [$\mu\text{mol/L}$]	20.00		
Carbamazepine-10,11-epoxide	-	-	-		
Cimetidine (V11)				Hanke et al. 2020 [66]	Cimetidine-Model (OSP, v1.1) ^a
Cimetidine	Competitive inhibition	CYP3A4 K _i [$\mu\text{mol/L}$]	268.00		
Fluvoxamine (V11)				Britz et al. 2019 [67]	Fluvoxamine-Model (OSP, v1.2) ^a
Fluvoxamine	Competitive inhibition	CYP3A4 K _i [$\mu\text{mol/L}$]	1.60		
Itraconazole (V11)				Hanke et al. 2018 [17]	Itraconazole-Model (OSP, v1.3) ^a
Itraconazole	Competitive inhibition	CYP3A4 K _i [nmol/L]	1.30		
	Competitive inhibition	P-gp K _i [nmol/L]	8.00		
Hydroxy-itraconazole	Competitive inhibition	CYP3A4 K _i [nmol/L]	14.40		
Keto-itraconazole	Competitive inhibition	CYP3A4 K _i [nmol/L]	5.12		
N-Desalkyl-itraconazole	Competitive inhibition	CYP3A4 K _i [nmol/L]	0.32		
Omeprazole (V11)				Kanacher et al. 2020 [20]	Omeprazole-Model (OSP, v1.1) ^a
R-Omeprazole	Competitive inhibiton	CYP3A4 K _i [$\mu\text{mol/L}$]	44.50 [68]		
S-Omeprazole	Competitive inhibiton	CYP3A4 K _i [$\mu\text{mol/L}$]	46.60 [68]		
Rifampicin (V11)				Hanke et al. 2018 [17]	Rifampicin-Model (OSP, v1.2) ^a
Rifampicin	Induction	CYP3A4 E _{max}	9.00		
	Induction	CYP3A4 EC ₅₀ [$\mu\text{mol/L}$]	0.34		
	Competitive inhibition	CYP3A4 K _i [$\mu\text{mol/L}$]	18.50		
	Induction	P-gp E _{max}	2.50		
	Induction	P-gp EC ₅₀ [$\mu\text{mol/L}$]	0.34		
	Competitive inhibition	P-gp K _i [$\mu\text{mol/L}$]	169.00		
Verapamil (V11)				Hanke et al. 2020a [69]	Verapamil-Norverapamil-Model
R-Verapamil	Mechanism-based inactivation	CYP3A4 K _i	27.63		
	Mechanism-based inactivation	CYP3A4 k _{inact} [$\mu\text{mol/L}$]	0.038		
	Non-competitive inhibition	P-gp K _i [$\mu\text{mol/L}$]	0.038		
S-Verapamil	Mechanism-based inactivation	CYP3A4 K _i	3.85		
	Mechanism-based inactivation	CYP3A4 k _{inact} [$\mu\text{mol/L}$]	0.034		
	Non-competitive inhibition	P-gp K _i [$\mu\text{mol/L}$]	0.038		
R-Norverapamil	Mechanism-based inactivation	CYP3A4 K _i	6.10		
	Mechanism-based inactivation	CYP3A4 k _{inact} [$\mu\text{mol/L}$]	0.048		
	Non-competitive inhibition	P-gp K _i [$\mu\text{mol/L}$]	0.038		

CYP: cytochrome P450, EC₅₀: concentration for half maximal induction, E_{max}: maximal induction effect, K_i: dissociation constant of the inhibitor-enzyme/transporter (competitive) and inhibitor-enzyme/transporter(-substrate) complex (non-competitive), K_i: concentration for 50% inactivation (mechanism-based inactivation), k_{inact}: maximum inactivation rate (mechanism-based inactivation), OSP: Open Systems Pharmacology, P-gp: P-glycoprotein. If not otherwise indicated, interaction constants were adopted from the respective published models. Hyperlinks refer to the respective model repositories. ^a Open Systems Pharmacology model repository (<https://github.com/Open-Systems-Pharmacology>).

Table S11: (continued)

Model (PK-Sim® Version)	Mechanism	Parameter	Value	Publication	Model repository
S-Norverapamil	Mechanism-based inactivation	CYP3A4 KI	2.90		
	Mechanism-based inactivation	CYP3A4 k_{inact} [$\mu\text{mol/L}$]	0.080		
	Non-competitive inhibition	P-gp K _i [$\mu\text{mol/L}$]	0.038		

CYP: cytochrome P450, EC₅₀: concentration for half maximal induction, E_{max}: maximal induction effect, K_i: dissociation constant of the inhibitor-enzyme/transporter (competitive) and inhibitor-enzyme/transporter(-substrate) complex (non-competitive), KI: concentration for 50% inactivation (mechanism-based inactivation), k_{inact} : maximum inactivation rate (mechanism-based inactivation), OSP: Open Systems Pharmacology, P-gp: P-glycoprotein. If not otherwise indicated, interaction constants were adopted from the respective published models. Hyperlinks refer to the respective model repositories. ^a Open Systems Pharmacology model repository (<https://github.com/Open-Systems-Pharmacology>).

Table S12: Published victim models and affected metabolism and transport pathways

Model (PK-Sim® Version)	Mechanism	Parameter	Value	Publication	Model repository
Dextromethorphan (V11)				Rüdesheim et al. 2022 [70]	Dextromethorphan-Model
Dextromethorphan	Metabolism to DXT	CYP2D6 K_M [$\mu\text{mol/L}$]	4.65		
	Metabolism to DXT	CYP2D6 k_{cat} [1/min] (NM)	90.89		
	Metabolism to DXT	CYP2D6 k_{cat} [1/min] (PM)	0.00		
Dextrorphan	-	-	-		
Dextrorphan-O-glucuronide	-	-	-		
Digoxin (V11)				Hanke et al. 2018 [17]	Digoxin-Model (OSP) ^a
Digoxin	Transport	P-gp K_M [$\mu\text{mol/L}$]	177.00		
	Transport	P-gp k_{cat} [1/min]	71.20		
Metoprolol (V11)				Rüdesheim et al. 2020 [71]	Metoprolol-Model
R-Metoprolol	Metabolism to α HM	CYP2D6 K_M [$\mu\text{mol/L}$]	10.08		
	Metabolism to α HM	CYP2D6 k_{cat} [1/min] (NM)	6.02		
	Metabolism to α HM	CYP2D6 k_{cat} [1/min] (PM)	0.00		
	Metabolism (ODM)	CYP2D6 K_M [$\mu\text{mol/L}$]	8.82		
	Metabolism (ODM)	CYP2D6 k_{cat} [1/min] (NM)	9.87		
	Metabolism (ODM)	CYP2D6 k_{cat} [1/min] (PM)	0.00		
S-Metoprolol	Metabolism to α HM	CYP2D6 K_M [$\mu\text{mol/L}$]	10.75		
	Metabolism to α HM	CYP2D6 k_{cat} [1/min] (NM)	6.55		
	Metabolism to α HM	CYP2D6 k_{cat} [1/min] (PM)	0.00		
	Metabolism (ODM)	CYP2D6 K_M [$\mu\text{mol/L}$]	12.43		
	Metabolism (ODM)	CYP2D6 k_{cat} [1/min] (NM)	8.21		
	Metabolism (ODM)	CYP2D6 k_{cat} [1/min] (PM)	0.00		
α -Hydroxymetoprolol	-	-	-		
Mexiletine (V11)				Kanacher et al. 2020 [20]	Mexiletine-Model (OSP, v1.1) ^a
Mexiletine	Metabolism	CYP2D6 clearance [1/min]	0.46		
Paroxetine (V11)				Rüdesheim et al. 2022 [72]	Paroxetine-Model
Paroxetine	Metabolism	CYP2D6 K_M [$\mu\text{mol/L}$]	0.03		
	Metabolism	CYP2D6 k_{cat} [1/min] (NM)	1.37		

α HM: α -hydroxymetoprolol, CYP: cytochrome P450, DXT: dextrorphan, NM: normal metabolizer, ODM: O-demethylation OSP: Open Systems Pharmacology, P-gp: P-glycoprotein, PM: poor metabolizer. Interaction constants were adopted from the respective published models. Hyperlinks refer to the respective model repositories. ^a Open Systems Pharmacology model repository (<https://github.com/Open-Systems-Pharmacology>).

S3.3 DD(G)I – Clinical studies

S3.3.1 Quinidine as victim

Table S13: Clinical study data used for DDI model development with quinidine as victim

Drug administration		Perpetrator									
Perpetrator	Quinidine	C _{max,u} [μmol/L] ^a	n	Population ^b	Fem. [%]	Age [years]	Weight [kg]	BMI [kg/m ²]	Molecule	Dataset	Reference
Carbamazepine											
200/400 mg b.i.d. po	200 mg ^c s.d. po	13.88	10	European [21]	0	(21-26)	(62-85)	(19-26)	QUI, OHQ	tr	Andreasen 2007 [32]
Cimetidine											
300 mg q.d. po	400 mg ^c s.d. po	3.58	9	American [23]	0	(21-35)	-	-	QUI	te	Kolb 1984 [42]
300 mg q.i.d. po	400 mg ^c s.d. po	4.52	9	American [23]	0	(21-35)	-	-	QUI	te	Hardy 1983 [41]
Fluvoxamine											
100 mg q.d. po	200 mg ^c s.d. po	0.06	6	American [23]	0	-	-	-	QUI, OHQ	te	Damkier 1999a [34]
Itraconazole											
200 mg q.d. po	100 mg ^c s.d. po	3.20 · 10 ⁻³	9	European [21]	56	25 (21-32)	64 (41-80)	-	QUI	te	Kaukonen 1997 [31]
Omeprazole											
40 mg q.d. po	400 mg ^c s.d. po	0.02 (R-omep) 0.03 (S-omep)	8	European [21]	0	(22-29)	(60-94)	-	QUI, OHQ	te	Ching 1991 [39]
Rifampicin											
600 mg q.d. po	200 mg ^c s.d. po	2.13	6	European [21]	0	-	-	-	QUI, OHQ	te	Damkier 1999 [33]
Verapamil											
80 mg t.i.d. po	400 mg ^c s.d. po	0.01 (R-vera) 8.69 · 10 ⁻³ (S-vera)	6	European [21]	0	(23-34)	-	-	QUI	te	Edwards 1987 [40]
120 mg t.i.d. po	400 mg ^c s.d. po	0.03 (R-vera) 0.02 (S-vera)	6	European [21]	0	(23-34)	-	-	QUI	te	Edwards 1987 [40]

b.i.d.: twice daily, BMI: body mass index, cap: capsule, C_{max,u}: unbound maximum plasma concentration, DDI: drug-drug interaction, fem: females, inf: infusion, n: number of study participants, OHQ: 3-hydroxyquinidine, omeprazole: oral, q.d.: once daily, q.i.d.: four times daily, QUI: quinidine, s.d: single dose, te: test dataset, t.i.d.: three times daily, tr: training dataset, vera: verapamil, -: not available. Values are given as mean (range). If perpetrator and victim drugs were applied in form of salts, the respective dose of bases were calculated and incorporated in simulations. ^a Calculated from model-predicted perpetrator concentrations in the respective DDI simulations. ^b Population used in simulations. ^c Quinidine sulfate dose.

S3.3.2 Quinidine as perpetrator

Table S14: Clinical study data used for DD(G)I model development with quinidine as perpetrator

Drug administration		Quinidine										
Quinidine	Victim	C _{max,u} [μmol/L] ^a	n	Population ^b	Fem. [%]	Age [years]	Weight [kg]	BMI [kg/m ²]	Phenotype	Molecule	Dataset	Reference
Dextromethorphan												
50 mg ^c s.d. po	30 mg s.d. po ^d	0.09	6	European [21]	33.3	22.4 (20-26)	70 (49-86)	-	CYP2D6 NM	DEX, DTT	te	Capon 1996 [73]
100 mg ^c s.d. po	30 mg s.d. po	0.20	5	American [23]	80	26.4 (22-31)	-	-	CYP2D6 NM	DEX, DXT, DXG	te	Schadel 1995 [74]
30 mg ^c b.i.d. po ^e	30 mg b.i.d. po ^f	0.07	13	American [23]	14.3	33.5 (23-50)	73.3	25.1	CYP2D6 NM	DEX	te	Schoedel 2012 [75]
Digoxin												
200 mg ^c b.i.d. po	10 μg/kg s.d. iv ^g	0.52	6	European [21]	33	(21-28)	-	-	-	DIG	te	Steiness 1980 [76]
200 mg ^c q.i.d. po	1 mg s.d. iv	1.01	7	European [21]	-	-	-	-	-	DIG	te	Ochs 1981 [77]
Metoprolol												
50 mg ^c s.d. po	20 mg s.d. iv	0.08	4	European [21]	0	(22-34)	(58-80)	-	CYP2D6 NM	MET	te	Leemann 1993 [78]
50 mg ^c s.d. po	20 mg s.d. iv ^h	0.08	3	European [21]	0	(25-38)	(65-86)	-	CYP2D6 PM	MET	te	Leemann 1993 [78]
250 mg ^c b.i.d. po	20 mg s.d. iv	0.81	4	European [21]	0	(22-34)	(58-80)	-	CYP2D6 NM	MET	te	Leemann 1993 [78]
250 mg ^c b.i.d. po	20 mg s.d. iv ^h	0.81	3	European [21]	0	(25-38)	(65-86)	-	CYP2D6 PM	MET	te	Leemann 1993 [78]
100 mg ^c q.d. po	200 mg s.d. po	0.20	10	American [23]	0	28.9 (24-40)	85.2	-	CYP2D6 NM	RME, SME	te	Johnson 1996 [79]
100 mg ^c q.d. po	200 mg s.d. po	0.20	10	American [23]	0	28.5 (24-36)	82.2	-	CYP2D6 NM	RME, SME	te	Johnson 1996 [79]
Mexiletine												
50 mg ^c q.i.d. po	200 mg s.d. po	0.21	6	American [23]	33.3	22.4 (20-26)	71 (49-86)	-	CYP2D6 NM	MEX	te	Abolfathi 1993 [80]
50 mg ^c q.i.d. po	200 mg s.d. po	0.21	10	American [23]	7	26	74	-	CYP2D6 PM	MEX	te	Abolfathi 1993 [80]
Paroxetine												
30 mg ^c b.i.d. po	20 mg q.d. po ⁱ	0.07	14	American [23]	14.3	33.6 (19-55)	75.3	25.3	CYP2D6 NM	PAR	te	Schoedel 2012 [75]

b.i.d.: twice daily, BMI: body mass index, C_{max,u}: unbound maximum plasma concentration, DD(G)I: drug-drug(-gene) interaction, DEX: dextromethorphan, DIG: digoxin, DTT: total dextrophan-O-glucuronide, fem: females, iv: intravenous, MET: metoprolol (racemate), MEX: mexiletine, n: number of study participants, NM: normal metabolizer, PAR: paroxetine, PM: poor metabolizer, po: oral, q.d.: once daily, q.i.d.: four times daily, RME: R-metoprolol, s.d.: single dose, SME: S-metoprolol, te: test dataset, -: not available. Values are given as mean (range). If perpetrator and victim drugs were applied in form of salts, the respective doses of bases were calculated and incorporated in simulations. ^a Calculated from model-predicted quinidine concentrations in the respective DDI simulations. ^b Population used in simulations. ^c Quinidine sulfate dose. ^d CYP2D6 catalytic rate constant estimated for control to account for unexplained interindividual variability in CYP2D6 activity (57% of original model value). ^e Plus paroxetine (20 mg q.d. po). ^f CYP2D6 catalytic rate constant estimated for control to account for unexplained interindividual variability in CYP2D6 activity (26% of original model value). ^g Digoxin dose of 15 μg/kg before DDI, normalized to 15 μg/kg for evaluation. ^h CYP2D6 catalytic rate constant estimated for control to account for unexplained interindividual variability in CYP2D6 activity (300% for sink metabolism and 200% for formation of α-hydroxymetoprolol of original model value). ⁱ Plus dextromethorphan (30 mg b.i.d. po).

S3.4 Plasma concentration-time profiles (semilogarithmic representation)

S3.4.1 Quinidine as victim

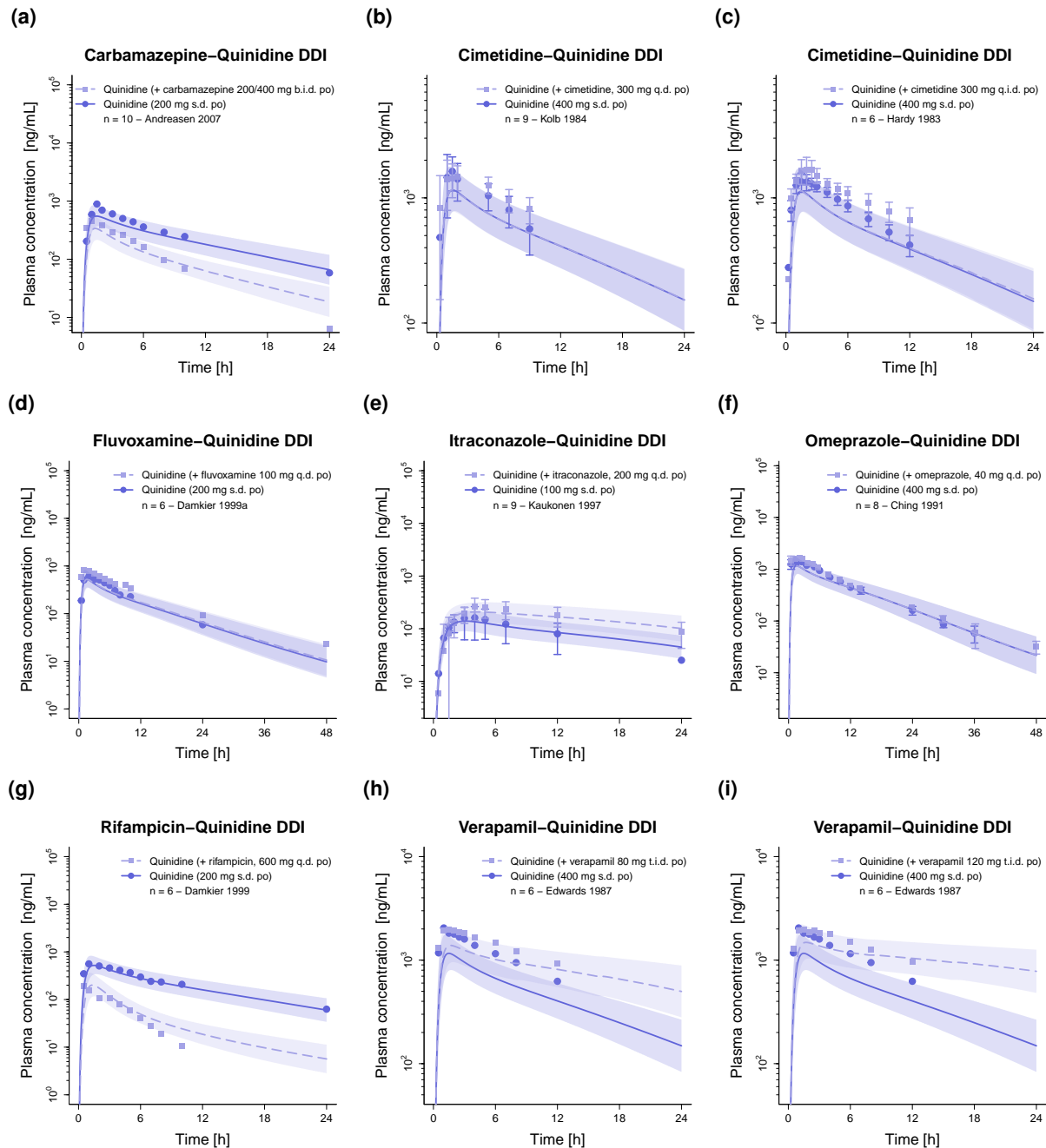


Figure S19: Predicted compared to observed plasma concentration-time profiles of quinidine alone and after pretreatment and/or concomitant administration of (a) carbamazepine, (b–c) cimetidine, (d) fluvoxamine, (e) itraconazole, (f) R-/S-omeprazole, (g) rifampicin and (h–i) R-/S-verapamil (semilogarithmic representation). Population predicted geometric means are shown as lines, corresponding geometric standard deviations are shown as shaded areas and observed data are shown as dots (control) and squares (DDI) (\pm standard deviation, if reported). b.i.d.: twice daily, DDI: drug-drug interaction, n: number of study participants, po: oral, q.d.: once daily, q.i.d.: four times daily, s.d.: single dose, t.i.d.: three times daily.

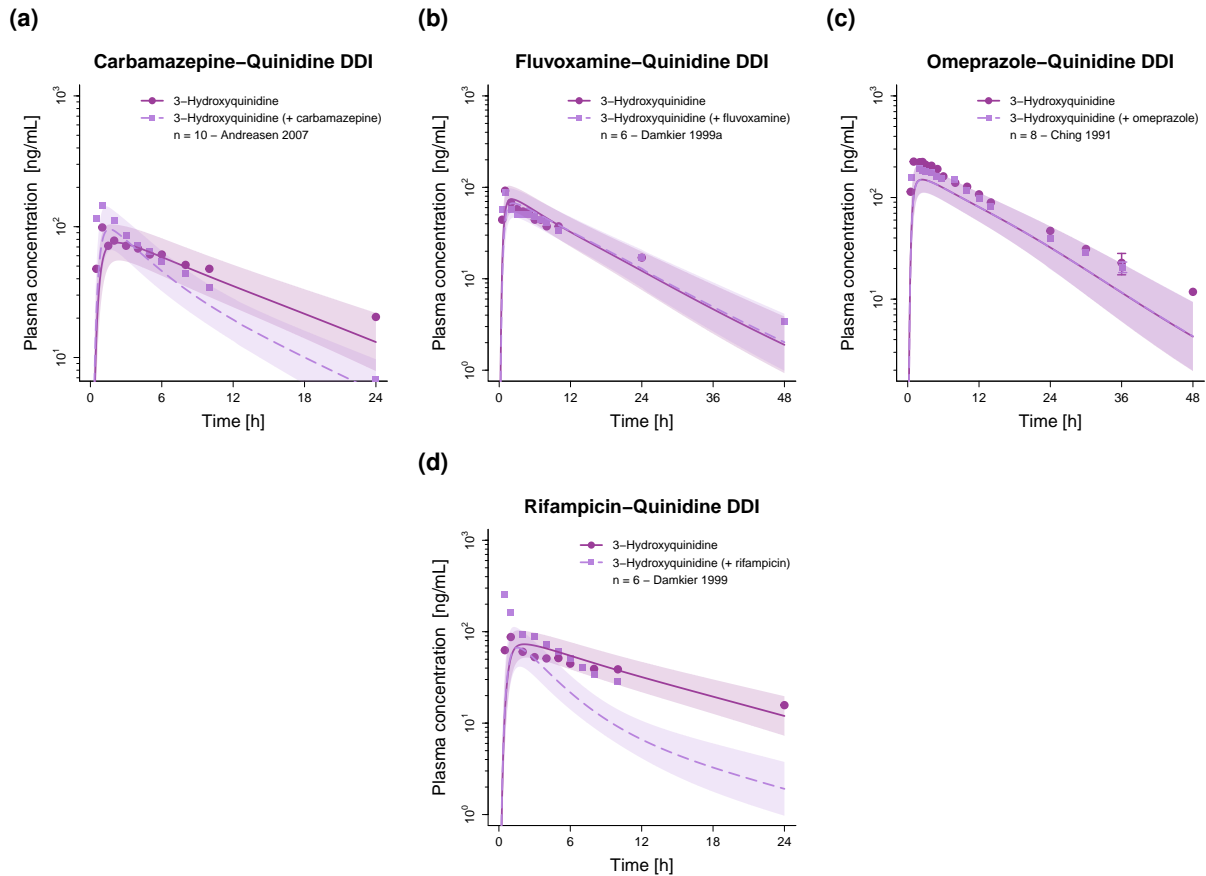


Figure S20: Predicted compared to observed plasma concentration-time profiles of 3-hydroxyquinidine alone and after pretreatment and/or concomitant administration of (a) carbamazepine, (b) fluvoxamine, (c) R-/S-omeprazole and (d) rifampicin (semilogarithmic representation). Population predicted geometric means are shown as lines, corresponding geometric standard deviations are shown as shaded areas and observed data are shown as dots (control) and squares (DDI). DDI: drug-drug interaction, n: number of study participants.

S3.4.2 Quinidine as perpetrator

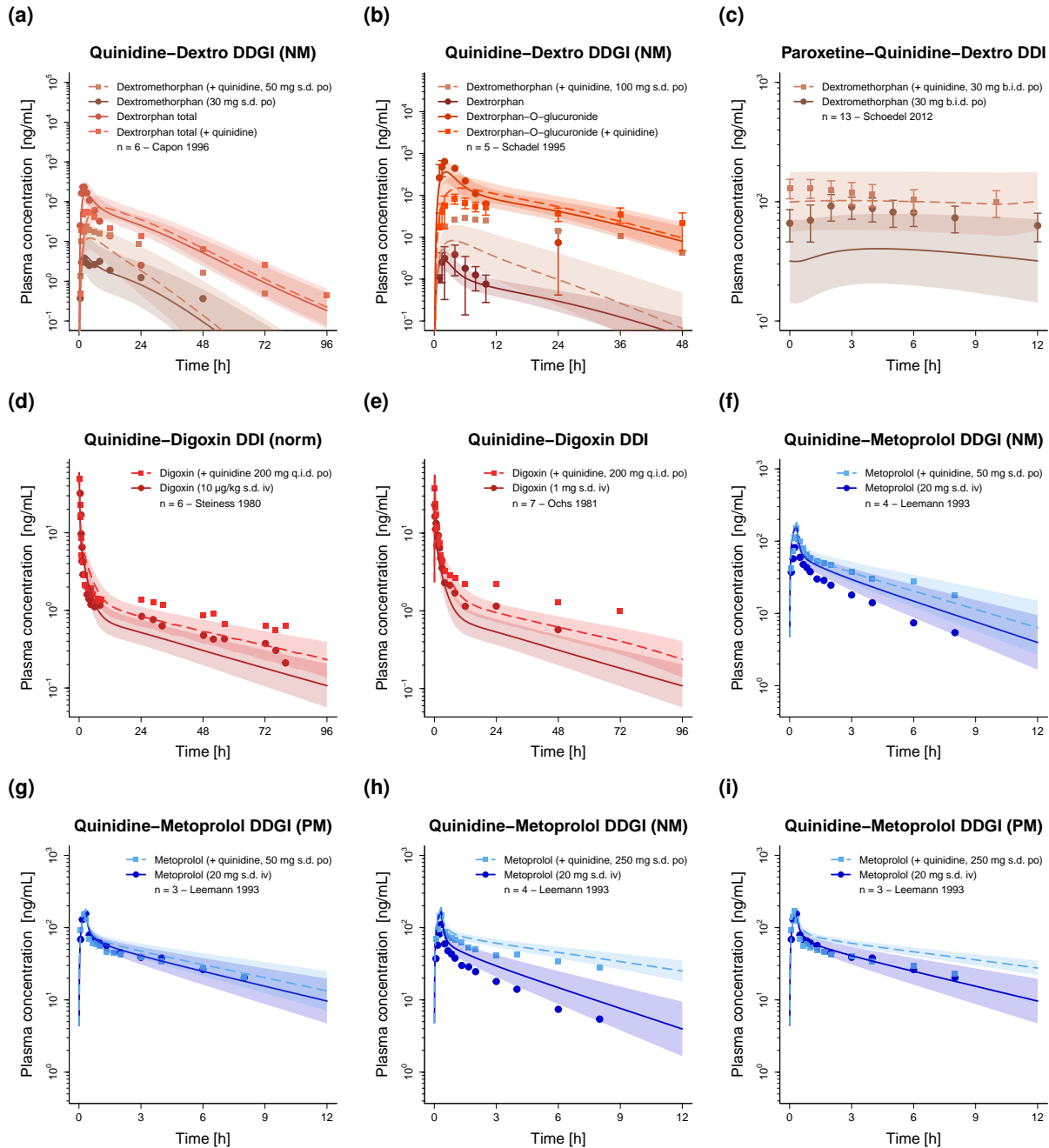


Figure S21: Predicted compared to observed plasma concentration-time profiles of (a–c) dextromethorphan (+ metabolites), (d–e) digoxin and (f–i) metoprolol alone and after pretreatment with and/or concomitant administration of quinidine (semilogarithmic representation). Population predicted geometric means are shown as lines, corresponding geometric standard deviations are shown as shaded areas and observed data are shown as dots (control) and squares (DDI) (\pm standard deviation, if reported). b.i.d.: twice daily, DDI: drug-drug interaction, DDGI: drug-drug-gene interaction, iv: intravenous, n: number of study participants, NM: CYP2D6 normal metabolizer, norm: dose-normalized, PM: CYP2D6 poor metabolizer, po: oral, q.i.d.: four times daily, s.d.: single dose.

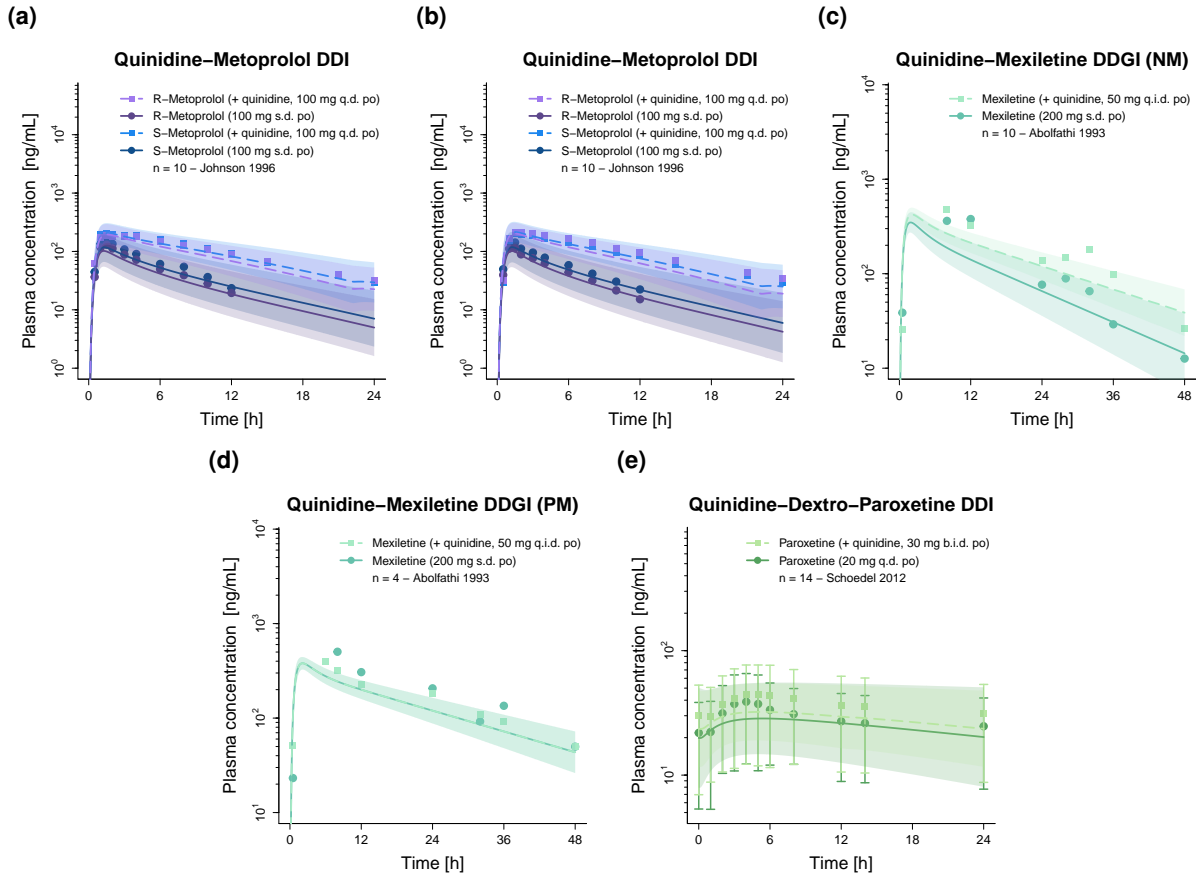


Figure S22: Predicted compared to observed plasma concentration-time profiles of (a–b) R-/S- metoprolol (comparison of different ethnic backgrounds), (c–d) mexiletine (observed data of representative subjects) and (e) paroxetine alone and after pretreatment with and/or concomitant administration of quinidine (semilogarithmic representation). Population predicted geometric means are shown as lines, corresponding geometric standard deviations are shown as shaded areas and observed data are shown as dots(control) and squares (DDI). b.i.d.: twice daily, DDI: drug-drug interaction, DDGI: drug-drug-gene interaction, n: number of study participants, NM: CYP2D6 normal metabolizer, PM: CYP2D6 poor metabolizer, po: oral, q.d.: once daily, q.i.d.: four times daily.

S3.5 Amount excreted unchanged in urine profiles (semilogarithmic representation)

S3.5.1 Quinidine as victim

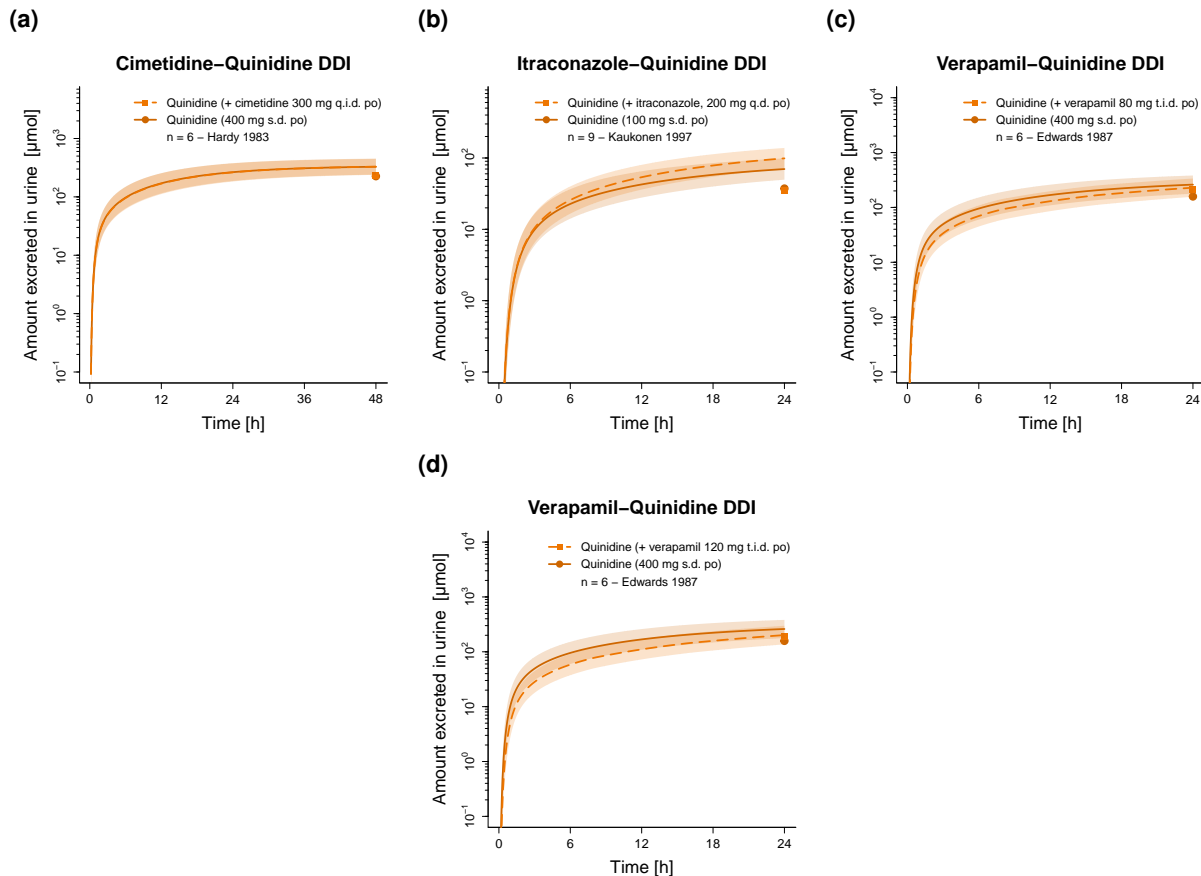


Figure S23: Predicted compared to observed plasma amount excreted unchanged in urine profiles of quinidine alone and after pretreatment and/or concomitant administration of (a) cimetidine, (b) itraconazole and (c–d) R-/S-verapamil (semilogarithmic representation). Population predicted geometric means are shown as lines, corresponding geometric standard deviations are shown as shaded areas and observed data are shown as dots (control) and squares (DDI). DDI: drug-drug interaction, n: number of study participants, po: oral, q.d.: once daily, q.i.d.: four times daily, s.d.: single dose, t.i.d.: three times daily.

S3.6 Plasma concentration-time profiles (linear representation)

S3.6.1 Quinidine as victim

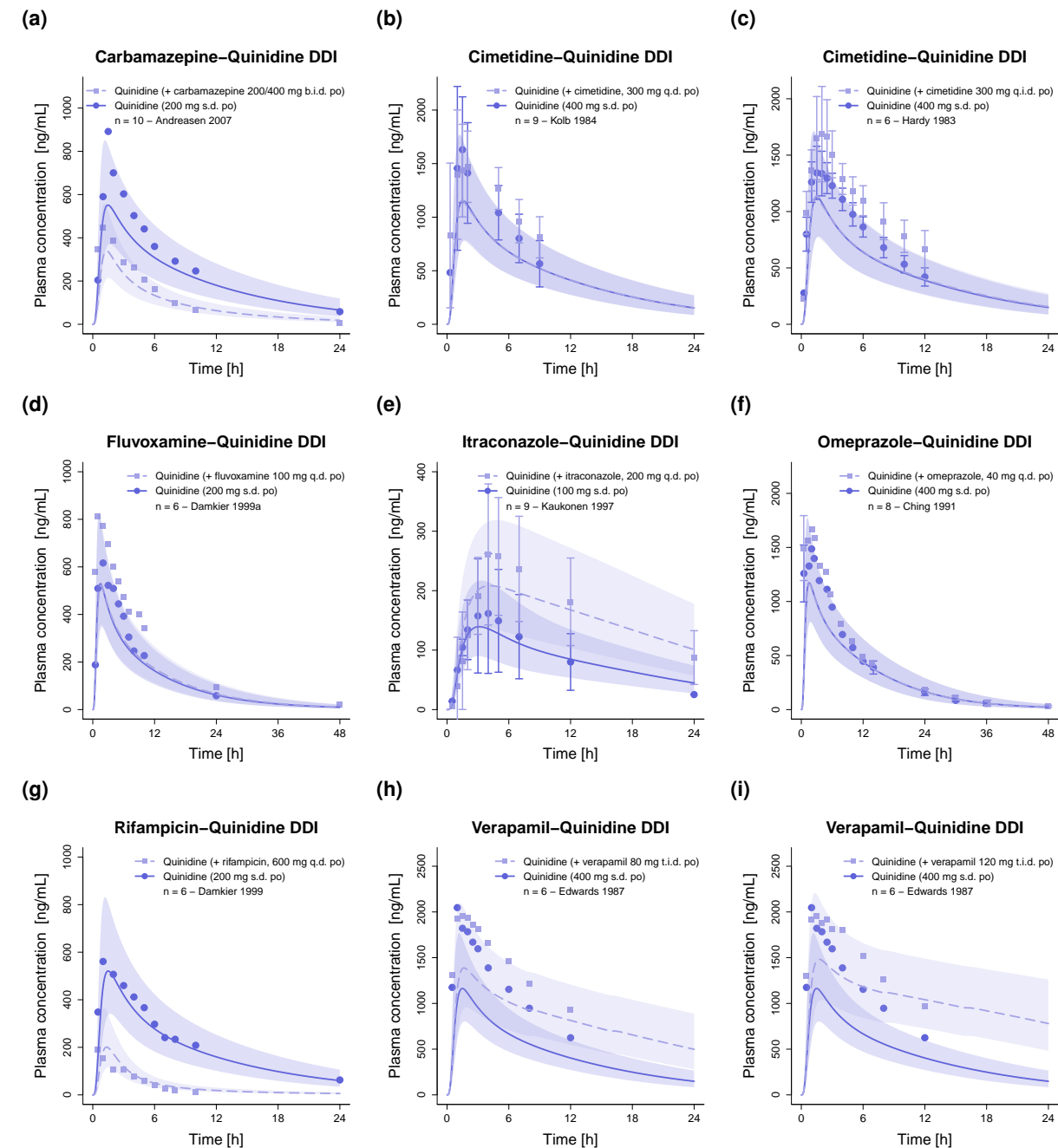


Figure S24: Predicted compared to observed plasma concentration-time profiles of quinidine and 3-hydroxyquinidine alone and after pretreatment and/or concomitant administration of (a) carbamazepine, (b–c) cimetidine, (d) fluvoxamine, (e) itraconazole, (f) R-/S-omeprazole, (g) rifampicin and (h–i) R-/S-verapamil (linear representation). Population predicted geometric means are shown as lines, corresponding geometric standard deviations are shown as shaded areas and observed data are shown as dots (\pm standard deviation, if reported). b.i.d.: twice daily, DDI: drug-drug interaction, n: number of study participants, po: oral, q.d.: once daily, q.i.d.: four times daily, s.d.: single dose, t.i.d.: three times daily.

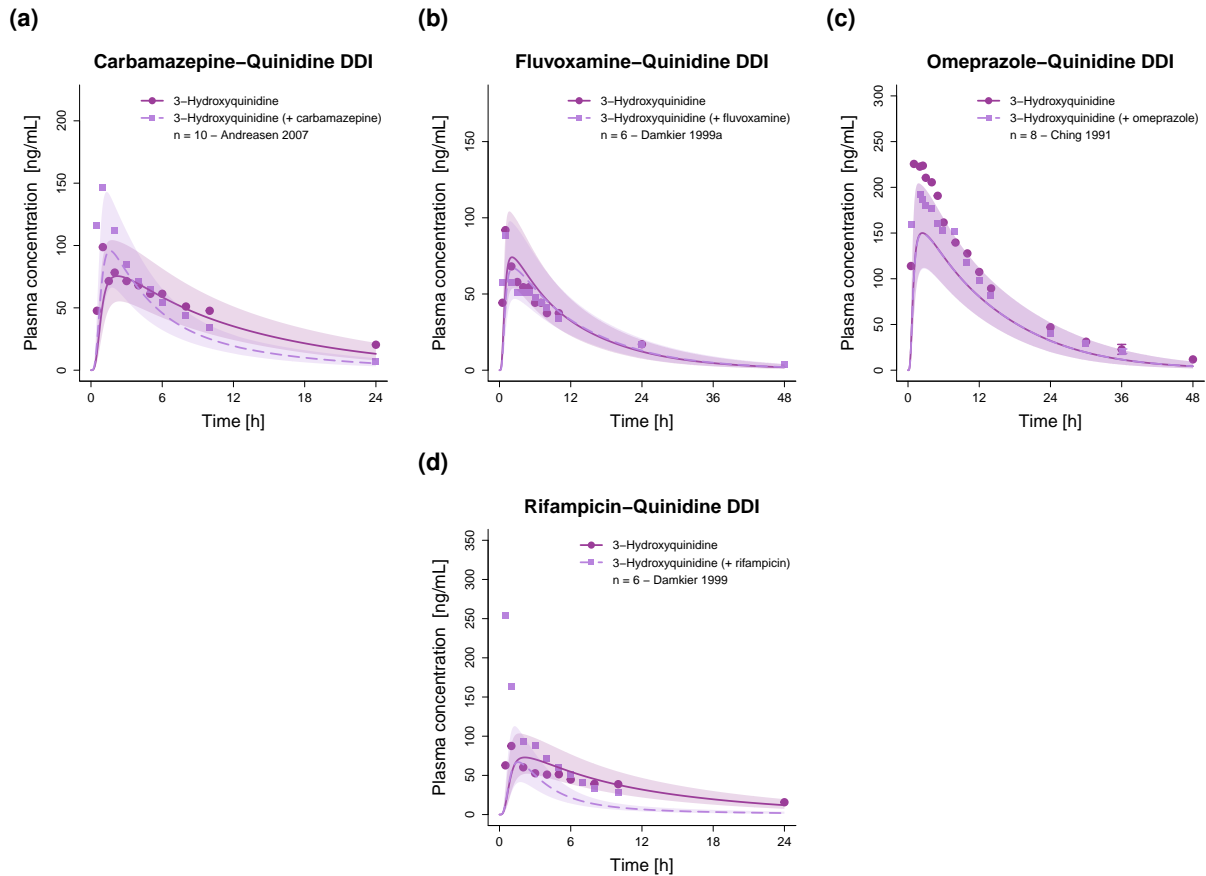


Figure S25: Predicted compared to observed plasma concentration-time profiles of 3-hydroxyquinidine alone and after pretreatment and/or concomitant administration of (a) carbamazepine, (b) fluvoxamine, (c) R-/S-omeprazole and (d) rifampicin (linear representation). Population predicted geometric means are shown as lines, corresponding geometric standard deviations are shown as shaded areas and observed data are shown as dots (\pm standard deviation, if reported). DDI: drug-drug interaction, n: number of study participants.

S3.6.2 Quinidine as perpetrator

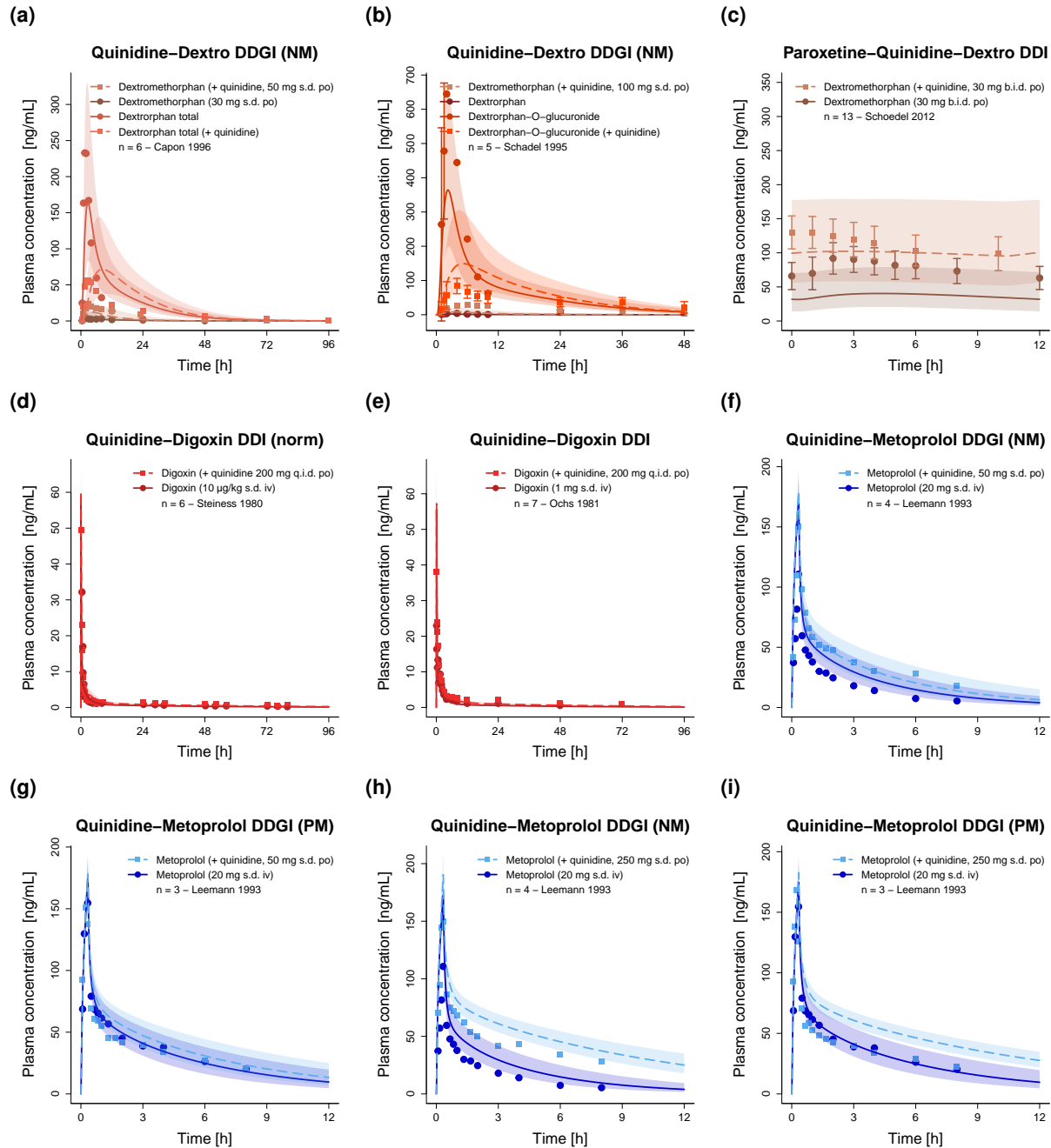


Figure S26: Predicted compared to observed plasma concentration-time profiles of (a–c) dextromethorphan (+ metabolites), (d–e) digoxin and (f–i) metoprolol alone and after pretreatment with and/or concomitant administration of quinidine (linear representation). Population predicted geometric means are shown as lines, corresponding geometric standard deviations are shown as shaded areas and observed data are shown as dots (\pm standard deviation, if reported). b.i.d.: twice daily, DDI: drug-drug interaction, DDGI: drug-drug-gene interaction, iv: intravenous, n: number of study participants, NM: CYP2D6 normal metabolizer, norm: dose-normalized, PM: CYP2D6 poor metabolizer, po: oral, q.i.d.: four times daily, s.d.: single dose.

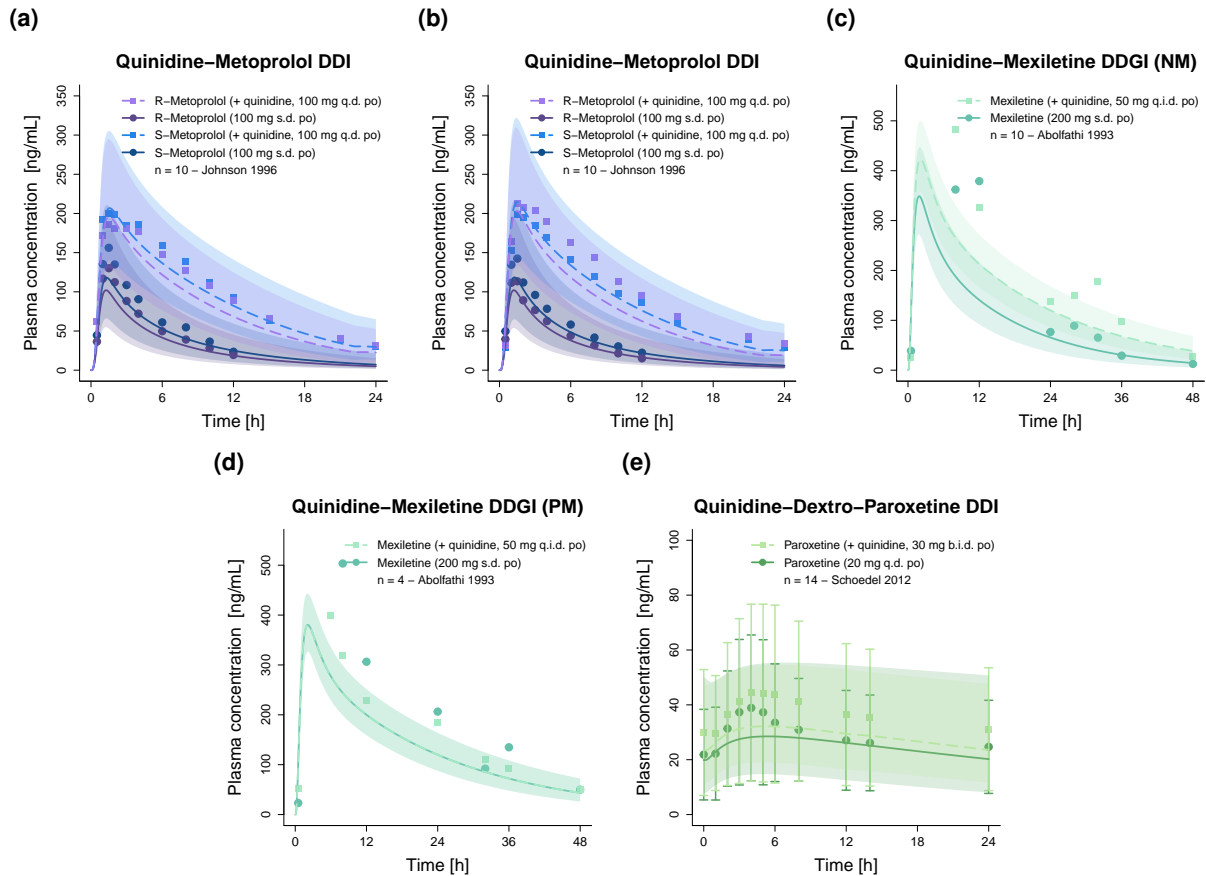


Figure S27: Predicted compared to observed plasma concentration-time profiles of (a–b) R-/S- metoprolol (comparison of different ethnic backgrounds), (c–d) mexiletine (observed data of representative subjects) and (e) paroxetine alone and after pretreatment with and/or concomitant administration of quinidine (linear representation). Population predicted geometric means are shown as lines, corresponding geometric standard deviations are shown as shaded areas and observed data are shown as dots (\pm standard deviation, if reported). b.i.d.: twice daily, DDI: drug-drug interaction, DDGI: drug-drug-gene interaction, n: number of study participants, NM: CYP2D6 normal metabolizer, PM: CYP2D6 poor metabolizer, po: oral, q.d.: once daily, q.i.d.: four times daily.

S3.7 Amount excreted unchanged in urine profiles (linear representation)

S3.7.1 Quinidine as victim

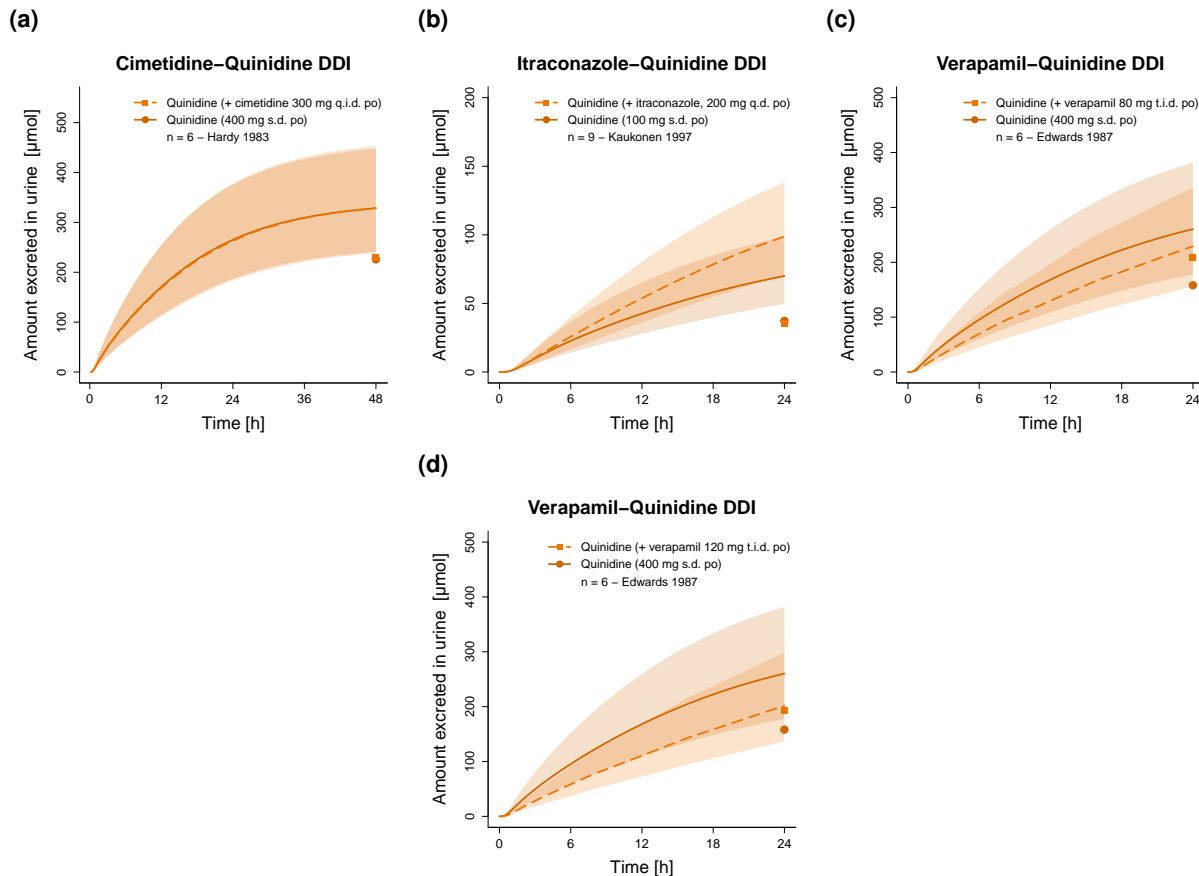


Figure S28: Predicted compared to observed plasma amount excreted unchanged in urine profiles of quinidine alone and after pretreatment and/or concomitant administration of (a) cimetidine, (b) itraconazole and (c–d) R-/S-verapamil (linear representation). Population predicted geometric means are shown as lines, corresponding geometric standard deviations are shown as shaded areas and observed data are shown as dots (control) and squares (DDI). DDI: drug-drug interaction, n: number of study participants, po: oral, q.d.: once daily, q.i.d.: four times daily, s.d.: single dose, t.i.d.: three times daily.

S3.8 DDI AUC_{last} and C_{max} ratios

S3.8.1 Quinidine as victim

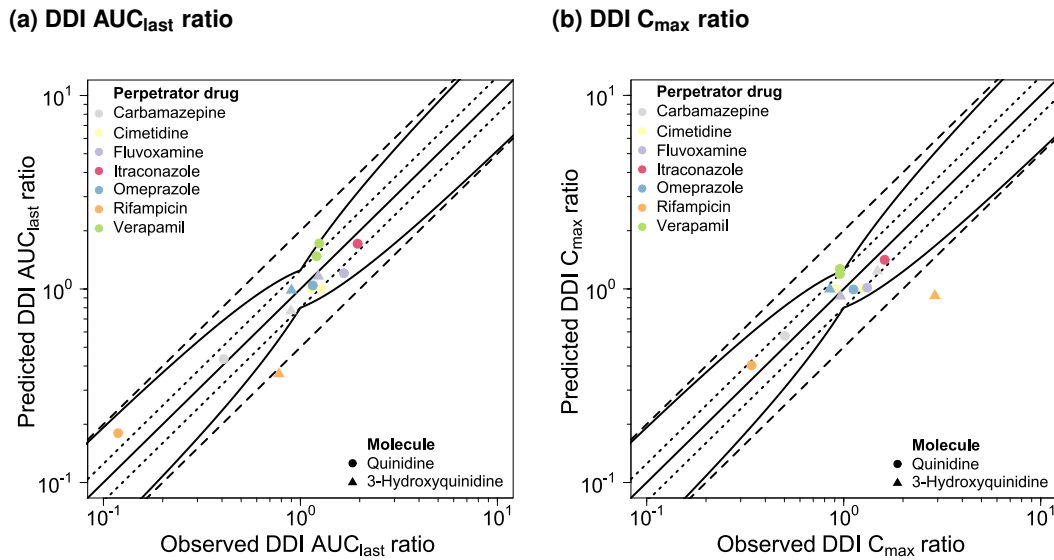


Figure S29: Goodness-of-fit plots comparing predicted and observed DDI AUC_{last} and C_{max} ratios. The solid line marks the line of identity. Dotted lines indicate 1.25-fold, dashed lines indicate 2-fold deviation. Prediction success limits proposed by Guest et al. [81] are shown as curved lines (including 20% variability). AUC_{last}: area under the plasma concentration-time curve calculated between the first and last concentration measurement, C_{max}: maximum plasma concentration, DDI: drug-drug interaction.

S3.8.2 Quinidine as perpetrator

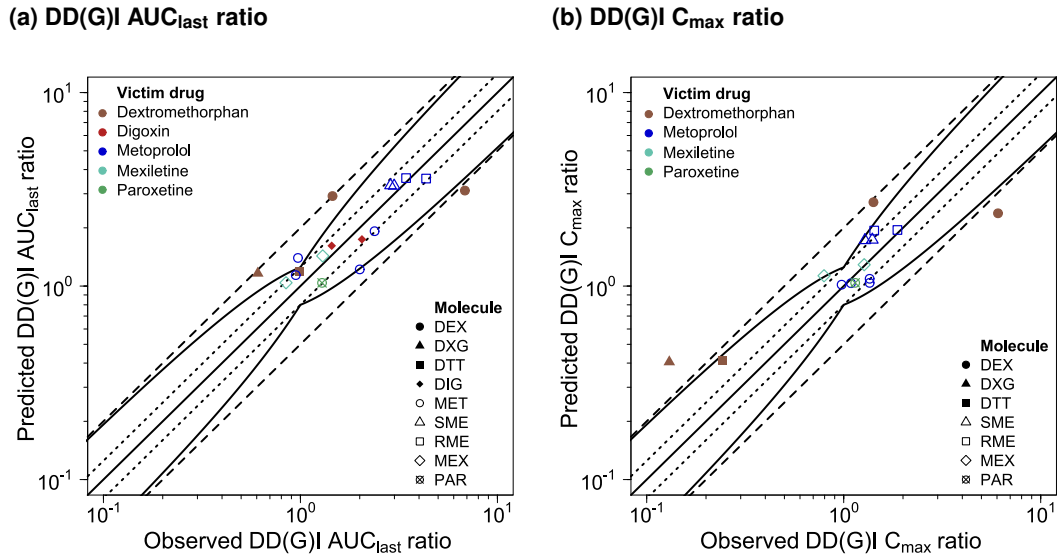


Figure S30: Goodness-of-fit plots comparing predicted and observed DD(G)I AUC_{last} and C_{max} ratios. The solid line marks the line of identity. Dotted lines indicate 1.25-fold, dashed lines indicate 2-fold deviation. Prediction success limits proposed by Guest et al. [81] are shown as curved lines (including 20% variability). AUC_{last} : area under the plasma concentration-time curve calculated between first and last concentration measurement, C_{max} : maximum plasma concentration, DD(G)I: drug-drug(-gene) interaction. DEX: dextromethorphan, DXG: dextrorphan-O-glucuronide, DTT: total dextrorphan, DIG: digoxin, MET: metoprolol, MEX: mexiletine, PAR: paroxetine, RME: R-metoprolol, SME: S-metoprolol.

S3.9 Geometric mean fold errors of predicted DD(G)I AUC_{last} and C_{max} ratios

S3.9.1 Quinidine as victim

Table S15: Predicted and observed DDI AUC_{last} and C_{max} ratios involving quinidine as victim drug

Drug administration			DDI AUC _{last} ratio			DDI C _{max} ratio			Molecule	Dataset	Reference
Perpetrator	Quinidine	t _{last} [h]	Pred	Obs	Pred/Obs	Pred	Obs	Pred/Obs			
Carbamazepine											
200/400 mg b.i.d. po	200 mg ^a s.d. po	24	0.43	0.41	1.07	0.57	0.50	1.14	QUI	tr	Andreasen 2007 [32]
200/400 mg b.i.d. po	200 mg ^a s.d. po	24	0.77	0.90	0.86	1.24	1.48	0.83	OHQ	tr	Andreasen 2007 [32]
Mean GMFE (range):			1.11 (1.07 – 1.16), 2/2 with GMFE ≤ 2			1.17 (1.14 – 1.20), 2/2 with GMFE ≤ 2					
Cimetidine											
300 mg q.d. po	400 mg ^a s.d. po	9	1.00	1.13	0.88	1.00	0.90	1.11	QUI	te	Kolb 1984 [42]
300 mg q.i.d. po	400 mg ^a s.d. po	12	1.00	1.28	0.79	1.01	1.26	0.80	QUI	te	Hardy 1983 [41]
Mean GMFE (range):			1.20 (1.14 – 1.27), 2/2 with GMFE ≤ 2			1.18 (1.11 – 1.25), 2/2 with GMFE ≤ 2					
Fluvoxamine											
100 mg q.d. po	200 mg ^a s.d. po	48	1.21	1.66	0.73	1.01	1.32	0.77	QUI	te	Damkier 1999a [34]
100 mg q.d. po	200 mg ^a s.d. po	48	1.16	1.23	0.94	0.92	0.96	0.95	OHQ	te	Damkier 1999a [34]
Mean GMFE (range):			1.22 (1.06 – 1.38), 2/2 with GMFE ≤ 2			1.17 (1.05 – 1.30), 2/2 with GMFE ≤ 2					
Itraconazole											
200 mg q.d. po	100 mg ^a s.d. po	24	1.71	1.95	0.88	1.41	1.61	0.88	QUI	te	Kaukonen 1997 [31]
Mean GMFE:			1.14, 1/1 with GMFE ≤ 2			1.14, 1/1 with GMFE ≤ 2					
Omeprazole											
40 mg q.d. po	400 mg ^a s.d. po	48	1.04	1.15	0.90	0.99	1.12	0.89	QUI	te	Ching 1991 [39]
40 mg q.d. po	400 mg ^a s.d. po	48	0.98	0.90	1.09	1.00	0.85	1.17	OHQ	te	Ching 1991 [39]
Mean GMFE (range):			1.10 (1.09 – 1.11), 2/2 with GMFE ≤ 2			1.15 (1.13 – 1.17), 2/2 with GMFE ≤ 2					
Rifampicin											
600 mg q.d. po	200 mg ^a s.d. po	10	0.18	0.12	1.52	0.40	0.34	1.18	QUI	te	Damkier 1999 [33]
600 mg q.d. po	200 mg ^a s.d. po	10	0.36	0.78	0.47	0.92	2.90	0.32	OHQ	te	Damkier 1999 [33]
Mean GMFE (range):			1.83 (1.52 – 2.13), 1/2 with GMFE ≤ 2			2.17 (1.18 – 3.15), 1/2 with GMFE ≤ 2					
Verapamil											
80 mg t.i.d. po	400 mg ^a s.d. po	12	1.48	1.21	1.22	1.19	0.96	1.25	QUI	te	Edwards 1987 [40]
120 mg t.i.d. po	400 mg ^a s.d. po	12	1.72	1.25	1.38	1.27	0.96	1.33	QUI	te	Edwards 1987 [40]
Mean GMFE (range):			1.34 (1.30 – 1.38), 2/2 with GMFE ≤ 2			1.31 (1.29 – 1.33), 2/2 with GMFE ≤ 2					
Overall GMFE (range):			1.29 (1.06 – 2.19), 12/13 with GMFE ≤ 2			1.34 (1.05 – 3.15), 12/13 with GMFE ≤ 2					

AUC_{last}: area under the plasma concentration-time curve calculated between the first and last concentration measurement, b.i.d.: twice daily, C_{max}: maximum plasma concentration, DDI: drug-drug interaction, GMFE: geometric mean fold error, obs: observed, OHQ: 3-hydroxyquinidine, po: oral, pred: predicted, q.d.: once daily, QUI: quinidine, s.d.: single dose, te: test dataset, t.i.d.: three times daily, t_{last}: time of the last concentration measurement, tr: training dataset. Respective doses of quinidine base were calculated and incorporated in simulations. ^a Quinidine sulfate dose.

S3.9.2 Quinidine as perpetrator

Table S16: Predicted and observed DD(G)I AUC_{last} and C_{max} ratios involving quinidine as perpetrator drug

Drug administration		DD(G)I AUC _{last} ratio			DD(G)I C _{max} ratio			Phenotype	Molecule	Dataset	Reference	
Quinidine	Victim	t _{last} [h]	Pred	Obs	Pred/Obs	Pred	Obs	Pred/Obs				
Dextromethorphan												
50 mg ^a s.d. po	30 mg s.d. po ^b	72	3.12	6.84	0.46	2.38	6.07	0.39	CYP2D6 NM	DEX	te	Capon 1996 [73]
50 mg ^a s.d. po	30 mg s.d. po	96	1.19	0.99	1.20	0.41	0.24	1.69	CYP2D6 NM	DTT	te	Capon 1996 [73]
100 mg ^a s.d. po	30 mg s.d. po	48	1.16	0.61	1.92	0.41	0.13	3.11	CYP2D6 NM	DXG	te	Schadel 1995 [74]
30 mg ^a b.i.d. po ^c	30 mg b.i.d. po ^d	12	2.92	1.45	2.01	2.71	1.42	1.92	CYP2D6 NM	DEX	te	Schoedel 2012 [75]
Mean GMFE (range):			1.83 (1.20 – 2.19), 2/4 with GMFE ≤ 2			2.32 (1.69 – 3.11), 2/4 with GMFE ≤ 2						
Digoxin												
200 mg ^a q.i.d. po	10 µg/kg s.d. iv ^e	80	1.62	1.44	1.12	-	-	-	DIG	te	Steiness 1980 [76]	
200 mg ^a q.i.d. po	1 mg s.d. iv	72	1.74	2.05	0.85	-	-	-	DIG	te	Ochs 1981 [77]	
Mean GMFE (range):			1.15 (1.12 – 1.18), 2/2 with GMFE ≤ 2			-						
Metoprolol												
50 mg ^a s.d. po	20 mg s.d. iv	8	1.22	2.00	0.61	1.04	1.35	0.77	CYP2D6 NM	MET	te	Leemann 1993 [78]
50 mg ^a s.d. po	20 mg s.d. iv ^f	8	1.14	0.95	1.20	1.02	0.98	1.04	CYP2D6 PM	MET	te	Leemann 1993 [78]
250 mg ^a b.i.d. po	20 mg s.d. iv	8	1.92	2.38	0.81	1.09	1.35	0.81	CYP2D6 NM	MET	te	Leemann 1993 [78]
250 mg ^a b.i.d. po	20 mg s.d. iv ^f	8	1.40	0.97	1.44	1.03	1.09	0.95	CYP2D6 PM	MET	te	Leemann 1993 [78]
100 mg ^a q.d. po	200 mg s.d. po	24	3.61	3.44	1.05	1.94	1.43	1.36	CYP2D6 NM	RME	te	Johnson 1996 [79]
100 mg ^a q.d. po	200 mg s.d. po	24	3.31	2.87	1.16	1.73	1.28	1.35	CYP2D6 NM	SME	te	Johnson 1996 [79]
100 mg ^a q.d. po	200 mg s.d. po	24	3.59	4.35	0.83	1.95	1.87	1.04	CYP2D6 NM	RME	te	Johnson 1996 [79]
100 mg ^a q.d. po	200 mg s.d. po	24	3.30	2.99	1.10	1.74	1.40	1.24	CYP2D6 NM	SME	te	Johnson 1996 [79]
Mean GMFE (range):			1.24 (1.05 – 1.44), 8/8 with GMFE ≤ 2			1.20 (1.04 – 1.36), 8/8 with GMFE ≤ 2						
Mexiletine												
50 mg ^a q.i.d. po	200 mg s.d. po	48	1.43	1.30	1.10	1.29	1.27	1.01	CYP2D6 NM	MEX	te	Abolfathi 1993 [80]
50 mg ^a q.i.d. po	200 mg s.d. po	48	1.04	0.85	1.23	1.13	0.79	1.42	CYP2D6 PM	MEX	te	Abolfathi 1993 [80]
Mean GMFE (range):			1.17 (1.10 – 1.23), 2/2 with GMFE ≤ 2			1.22 (1.01 – 1.42), 2/2 with GMFE ≤ 2						
Paroxetine												
30 mg ^a b.i.d. po	20 mg q.d. po ^g	24	1.04	1.29	0.81	1.04	1.14	0.91	CYP2D6 NM	PAR	te	Schoedel 2012 [75]
Mean GMFE:			1.24, 1/1 with GMFE ≤ 2			1.10, 1/1 with GMFE ≤ 2						
Overall GMFE (range):			1.36 (1.05 – 2.19), 15/17 with GMFE ≤ 2			1.49 (1.01 – 3.11), 13/15 with GMFE ≤ 2						

AUC_{last}: area under the plasma concentration-time curve calculated between the first and last concentration measurement, b.i.d.: twice daily, C_{max}: maximum plasma concentration, DD(G)I: drug-drug(-gene) interaction, DEX: dextromethorphan, DIG: digoxin, DTT: total dextrorphan, DXG: dextrorphan-O-glucuronide, GMFE: geometric mean fold error, iv: intravenous, MET: metoprolol (racemate), MEX: mexiletine, n: number of individuals studied, NM: normal metabolizer, PM: poor metabolizer, PAR: paroxetine, po: oral, pred: predicted, q.d.: once daily, q.i.d.: four times daily, RME: R-metoprolol, s.d.: single dose, SME: S-metoprolol, te: test dataset, t_{last}: time of the last concentration measurement. If perpetrator and victim drugs were applied in form of salts, the respective doses of bases were calculated and incorporated in simulations. ^a Quinidine sulfate dose. ^b CYP2D6 catalytic rate constant estimated for control to account for unexplained interindividual variability in CYP2D6 activity (57% of original model value). ^c Plus paroxetine (20 mg q.d. po). ^d CYP2D6 catalytic rate constant estimated for control to account for unexplained interindividual variability in CYP2D6 activity (26% of original model value). ^e Digoxin dose of 15 µg/kg before DDI, normalized to 15 µg/kg for evaluation. ^f CYP2D6 catalytic rate constant estimated for control to account for unexplained interindividual variability in CYP2D6 activity (300% for sink metabolism and 200% for formation of α-hydroxymetoprolol of original model value). ^g Plus dextromethorphan (30 mg b.i.d. po).

References

- [1] M. Nishimura and S. Naito. Tissue-specific mRNA expression profiles of human phase I metabolizing enzymes except for cytochrome P450 and phase II metabolizing enzymes. *Drug metabolism and pharmacokinetics*, 21(5):357–74, 2006. doi: 10.2133/dmpk.21.357.
- [2] M. Meyer, S. Schneckener, B. Ludewig, L. Kuepfer, and J. Lippert. Using expression data for quantification of active processes in physiologically based pharmacokinetic modeling. *Drug metabolism and disposition: the biological fate of chemicals*, 40(5):892–901, 2012. doi: 10.1124/dmd.111.043174.
- [3] M. Nishimura, H. Yaguti, H. Yoshitsugu, S. Naito, and T. Satoh. Tissue distribution of mRNA expression of human cytochrome P450 isoforms assessed by high-sensitivity real-time reverse transcription PCR. *Journal of the Pharmaceutical Society of Japan*, 123(5):369–75, 2003. doi: 10.1248/yakushi.123.369.
- [4] A. D. Rodrigues. Integrated cytochrome P450 reaction phenotyping: attempting to bridge the gap between cDNA-expressed cytochromes P450 and native human liver microsomes. *Biochemical pharmacology*, 57(5):465–80, 1999. doi: 10.1016/S0006-2952(98)00268-8.
- [5] Open Systems Pharmacology Suite Community. Open Systems Pharmacology Suite Manual, 2018. URL <https://docs.open-systems-pharmacology.org/>.
- [6] National Center for Biotechnology Information (NCBI). Expressed Sequence Tags (EST) from UniGene, 2019.
- [7] G. Margallan, M. Rouleau, J. K. Fallon, P. Caron, L. Villeneuve, V. Turcotte, P. C. Smith, M. S. Joy, and C. Guillemette. Quantitative profiling of human renal UDP-glucuronosyltransferases and glucuronidation activity: A comparison of normal and tumoral kidney tissues. *Drug Metabolism and Disposition*, 43(4):611–19, 2015. doi: 10.1124/dmd.114.062877.
- [8] B. Achour, M. R. Russell, J. Barber, and A. Rostami-Hodjegan. Simultaneous quantification of the abundance of several cytochrome P450 and uridine 5'-diphospho-glucuronosyltransferase enzymes in human liver microsomes using multiplexed targeted proteomics. *Drug metabolism and disposition: the biological fate of chemicals*, 42(4):500–510, 2014. doi: 10.1124/dmd.113.055632.
- [9] D. Scotcher, S. Billington, J. Brown, C. R. Jones, C. D. Brown, A. Rostami-Hodjegan, and A. Galetin. Microsomal and cytosolic scaling factors in dog and human kidney cortex and application for in vitro-in vivo extrapolation of renal metabolic clearance. *Drug Metabolism and Disposition*, 45(5):556–568, 2017. doi: 10.1124/dmd.117.075242.
- [10] M. Otsuka, T. Matsumoto, R. Morimoto, S. Arioka, H. Omote, and Y. Moriyama. A human transporter protein that mediates the final excretion step for toxic organic cations. *Proceedings of the National Academy of Sciences of the United States of America*, 102(50):17923–8, 2005. doi: 10.1073/pnas.0506483102.
- [11] S. Masuda, T. Terada, A. Yonezawa, Y. Tanihara, K. Kishimoto, T. Katsura, O. Ogawa, and K.-i. Inui. Identification and functional characterization of a new human kidney-specific H+/organic cation antiporter, kidney-specific multidrug and toxin extrusion 2. *Journal of the American Society of Nephrology : JASN*, 17(8):2127–35, 2006. doi: 10.1681/ASN.2006030205.
- [12] B. Prasad, K. Johnson, S. Billington, C. Lee, G. W. Chung, C. D. Brown, E. J. Kelly, J. Himmelfarb, and J. D. Unadkat. Abundance of drug transporters in the human kidney cortex as quantified by quantitative targeted proteomics. *Drug Metabolism and Disposition*, 44(12):1920–1924, 2016. doi: 10.1124/dmd.116.072066.
- [13] M. Nishimura and S. Naito. Tissue-specific mRNA expression profiles of human ATP-binding cassette and solute carrier transporter superfamilies. *Drug metabolism and pharmacokinetics*, 20(6):452–77, 2005. doi: 10.2133/dmpk.20.452.
- [14] B. Prasad, R. Evers, A. Gupta, C. E. C. A. Hop, L. Salphati, S. Shukla, S. V. Ambudkar, and J. D. Unadkat. Interindividual variability in hepatic organic anion - transporting polypeptides and P-glycoprotein (ABCB1) protein expression: quantification by liquid chromatography tandem mass spectroscopy and influence of genotype, age, and sex. *Drug metabolism and disposition: the biological fate of chemicals*, 42(1):78–88, 2014. doi: 10.1124/dmd.113.053819.

- [15] N. Kolesnikov, E. Hastings, M. Keays, O. Melnichuk, Y. A. Tang, E. Williams, M. Dylag, N. Kurbatova, M. Brandizi, T. Burdett, K. Megy, E. Pilicheva, G. Rustici, A. Tikhonov, H. Parkinson, R. Petryszak, U. Sarkans, and A. Brazma. ArrayExpress update-simplifying data submissions. *Nucleic Acids Research*, 43(D1):D1113–D1116, 2015. doi: 10.1093/nar/gku1057.
- [16] L. Wang, B. Prasad, L. Salphati, X. Chu, A. Gupta, C. E. Hop, R. Evers, and J. D. Unadkat. Interspecies variability in expression of hepatobiliary transporters across human, dog, monkey, and rat as determined by quantitative proteomics. *Drug Metabolism and Disposition*, 43(3):367–74, 2015. doi: 10.1124/dmd.114.061580.
- [17] N. Hanke, S. Frechen, D. Moj, H. Britz, T. Eissing, T. Wendl, and T. Lehr. PBPK models for CYP3A4 and P-gp DDI prediction: A modeling network of rifampicin, itraconazole, clarithromycin, midazolam, alfentanil, and digoxin. *CPT: Pharmacometrics & Systems Pharmacology*, 7(10):647–59, 2018. doi: 10.1002/psp4.12343.
- [18] K. Rowland Yeo, R. L. Walsky, M. Jamei, A. Rostami-Hodjegan, and G. T. Tucker. Prediction of time-dependent CYP3A4 drug-drug interactions by physiologically based pharmacokinetic modelling: Impact of inactivation parameters and enzyme turnover. *European Journal of Pharmaceutical Sciences*, 43(3):160–73, 2011. doi: 10.1016/j.ejps.2011.04.008.
- [19] D. J. Greenblatt, L. L. von Moltke, J. S. Harmatz, G. Chen, J. L. Weemhoff, C. Jen, C. J. Kelley, B. W. LeDuc, and M. A. Zinny. Time course of recovery of cytochrome P450 3A function after single doses of grapefruit juice. *Clinical Pharmacology and Therapeutics*, 74(2):121–29, 2003. doi: 10.1016/S0009-9236(03)00118-8.
- [20] T. Kanacher, A. Lindauer, E. Mezzalana, I. Michon, C. Veau, J. D. G. Mantilla, V. Nock, and A. Fleury. A Physiologically-Based Pharmacokinetic (PBPK) Model Network for the Prediction of CYP1A2 and CYP2C19 Drug-Drug-Gene Interactions with Fluvoxamine, Omeprazole, S-mephenytoin, Moclobemide, Tizanidine, Mexiletine, Ethinylestradiol, and Caffeine. *Pharmaceutics*, 12(12):1–15, 2020. doi: 10.3390/pharmaceutics12121191.
- [21] ICRP Publication 89. Third National Health and Nutrition Examination Survey (NHANES III). *Annals of the ICRP*, 3–4(32):5–265, 2014.
- [22] D. Fremstad, O. G. Nilsen, L. Storstein, J. Amlie, and S. Jacobsen. Pharmacokinetics of quinidine related to plasma protein binding in man. *European journal of clinical pharmacology*, 15(3):187–92, 1979. doi: 10.1007/BF00563104.
- [23] National Center for Health Statistics Hyattsville, MS 20782. Basic anatomical and physiological data for use in radiological protection: reference values. A report of age- and gender-related differences in the anatomical and physiological characteristics of reference individuals. 1997.
- [24] D. Darbar, S. Dell'Orto, K. Mörike, G. R. Wilkinson, and D. M. Roden. Dietary salt increases first-pass elimination of oral quinidine. *Clinical pharmacology and therapeutics*, 61(3):292–300, 1997. doi: 10.1016/S0009-9236(97)90161-2.
- [25] T. W. Guentert, N. H. Holford, P. E. Coates, R. A. Upton, and S. Riegelman. Quinidine pharmacokinetics in man: choice of a disposition model and absolute bioavailability studies. *Journal of pharmacokinetics and biopharmaceutics*, 7(4):315–30, 1979. doi: 10.1007/BF01062532.
- [26] Tanaka, G and Kawamura, H. Anatomical and physiological characteristics for Asian reference man: Male and female of different ages: Tanaka model. *Division of Radioecology. National Institute of Radiological Sciences. Hitachinaka 311-12 Japan. Report Number NIRS-M-115.*, 1996.
- [27] J.-G. Shin, W.-K. Kang, J.-H. Shon, M. Arefayene, Y.-R. Yoon, K.-A. Kim, D.-I. Kim, D.-S. Kim, K.-H. Cho, R. L. Woosley, and D. A. Flockhart. Possible interethnic differences in quinidine-induced QT prolongation between healthy Caucasian and Korean subjects. *British journal of clinical pharmacology*, 63(2):206–15, 2007. doi: 10.1111/j.1365-2125.2006.02793.x.
- [28] H. R. Ochs, E. Grube, D. J. Greenblatt, E. Woo, and G. Bodem. Intravenous quinidine: pharmacokinetic properties and effects on left ventricular performance in humans. *American Heart Journal*, 99(4):468–475, 1980. doi: 10.1016/0002-8703(80)90381-6.
- [29] O. S. Pharmacology. Japanese Population Report, 2019. URL https://github.com/Open-Systems-Pharmacology/OSPSuite.Documentation/blob/master/Japanese_Population/Report.md.

- [30] K. Maeda, J. Takano, Y. Ikeda, T. Fujita, Y. Oyama, K. Nozawa, Y. Kumagai, and Y. Sugiyama. Nonlinear Pharmacokinetics of Oral Quinidine and Verapamil in Healthy Subjects: A Clinical Microdosing Study. *Clinical Pharmacology & Therapeutics*, 90(2):263–270, 2011. doi: 10.1038/clpt.2011.108.
- [31] K. M. Kaukonen, K. T. Olkkola, and P. J. Neuvonen. Itraconazole increases plasma concentrations of quinidine. *Clinical pharmacology and therapeutics*, 62(5):510–7, 1997. doi: 10.1016/S0009-9236(97)90046-1.
- [32] A.-H. Andreasen, K. Brøsen, and P. Damkier. A Comparative Pharmacokinetic Study in Healthy Volunteers of the Effect of Carbamazepine and Oxcarbazepine on Cyp3a4. *Epilepsia*, 48(3):490–496, 2007. doi: 10.1111/j.1528-1167.2007.00924.x.
- [33] P. Damkier, L. L. Hansen, and K. Brøsen. Effect of fluvoxamine on the pharmacokinetics of quinidine. *European Journal of Clinical Pharmacology*, 55(6):451–456, 1999. doi: 10.1007/s002280050655.
- [34] P. Damkier, L. L. Hansen, and K. Brøsen. Rifampicin treatment greatly increases the apparent oral clearance of quinidine. *Pharmacology and Toxicology*, 85(6):257–262, 1999. doi: 10.1111/j.1600-0773.1999.tb02019.x.
- [35] S. Laganière, R. F. Davies, G. Carignan, K. Foris, L. Goernert, K. Carrier, C. Pereira, and I. McGilveray. Pharmacokinetic and pharmacodynamic interactions between diltiazem and quinidine. *Clinical pharmacology and therapeutics*, 60(3):255–64, 1996. doi: 10.1016/S0009-9236(96)90052-1.
- [36] W. D. Mason, J. O. Covinsky, J. L. Valentine, K. L. Kelly, O. H. Weddle, and B. L. Martz. Comparative plasma concentrations of quinidine following administration of one intramuscular and three oral formulations to 13 human subjects. *Journal of pharmaceutical sciences*, 65(9):1325–9, 1976. doi: 10.1002/jps.2600650916.
- [37] B. R. Rao and D. Rambhau. Absence of a pharmacokinetic interaction between quinidine and diazepam. *Drug Metabolism and Drug Interactions*, 12(1):45–52, 1995. doi: 10.1515/DMDI.1995.12.1.45.
- [38] B. E. Bleske, P. L. Carver, T. M. Annesley, J. R. M. Bleske, and F. Morady. The Effect of Ciprofloxacin on the Pharmacokinetic and ECG Parameters of Quinidine. *The Journal of Clinical Pharmacology*, 30(10):911–915, 1990. doi: 10.1002/j.1552-4604.1990.tb03570.x.
- [39] M. S. Ching, S. L. Elliott, C. K. Stead, R. T. Murdoch, S. Devenish-Meares, D. J. Morgan, and R. A. Smallwood. Quinidine single dose pharmacokinetics and pharmacodynamics are unaltered by omeprazole. *Alimentary pharmacology & therapeutics*, 5(5):523–31, 1991. doi: 10.1111/j.1365-2036.1991.tb00521.x.
- [40] D. J. Edwards, R. Lavoie, H. Beckman, R. Blevins, and M. Rubenfire. The effect of coadministration of verapamil on the pharmacokinetics and metabolism of quinidine. *Clinical Pharmacology and Therapeutics*, 41(1):68–73, 1987. doi: 10.1038/clpt.1987.11.
- [41] B. G. Hardy and J. J. Schentag. Lack of effect of cimetidine on the metabolism of quinidine: effect on renal clearance. *International journal of clinical pharmacology, therapy, and toxicology*, 26(8):388–91, 1983.
- [42] K. W. Kolb, W. R. Garnett, R. E. Small, G. W. Vetrovec, B. J. Kline, and T. Fox. Effect of Cimetidine on Quinidine Clearance. *Therapeutic Drug Monitoring*, 6(3):306–312, 1984. doi: 10.1097/00007691-198409000-00009.
- [43] H. R. Ochs, D. J. Greenblatt, E. Woo, K. Franke, H. J. Pfeifer, and T. W. Smith. Single and multiple dose pharmacokinetics of oral quinidine sulfate and gluconate. *The American journal of cardiology*, 41(4):770–7, 1978. doi: 10.1016/0002-9149(78)90830-5.
- [44] J. D. Strum, J. L. Colaizzi, J. M. Jaffe, P. C. Martineau, and R. I. Poust. Comparative bioavailability of four commercial quinidine sulfate tablets. *Journal of pharmaceutical sciences*, 66(4):539–42, 1977. doi: 10.1002/jps.2600660420.
- [45] G. M. Frigo, E. Perucca, M. Teggia-Droghi, G. Gatti, A. Mussini, and J. Salerno. Comparison of quinidine plasma concentration curves following oral administration of some short- and long-acting formulations. *British journal of clinical pharmacology*, 4(4):449–54, 1977. doi: 10.1111/j.1365-2125.1977.tb00760.x.
- [46] P. Bolme and U. Otto. Dose-dependence of the pharmacokinetics of quinidine. *European journal of clinical pharmacology*, 12(1):73–6, 1977. doi: 10.1007/BF00561409.

- [47] D. S. Wishart, C. Knox, A. C. Guo, S. Shrivastava, M. Hassanali, P. Stothard, Z. Chang, and J. Woolsey. DrugBank: a comprehensive resource for in silico drug discovery and exploration. *Nucleic acids research*, 34(Database issue): D668–72, 2006. doi: 10.1093/nar/gkj067.
- [48] Drugbank-online. Quinidine - Drugbank, 2022. URL <https://go.drugbank.com/drugs/DB00908>.
- [49] Drugbank-online. 3-Hydroxyquinidine - Drugbank, 2022. URL <https://go.drugbank.com/metabolites/DBMET00382>.
- [50] J. Takano, K. Maeda, M. B. Bolger, and Y. Sugiyama. The prediction of the relative importance of CYP3A/P-glycoprotein to the nonlinear intestinal absorption of drugs by advanced compartmental absorption and transit model. *Drug Metabolism and Disposition*, 44(11):1808–1818, 2016. doi: 10.1124/dmd.116.070011.
- [51] ChemAxon. Chemicalize, 2020. URL <https://chemicalize.com>.
- [52] S. Grube, P. Langguth, H. E. Junginger, S. Kopp, K. K. Midha, V. P. Shah, S. Stavchansky, J. B. Dressman, and D. M. Barends. Biowaiver monographs for immediate release solid oral dosage forms: quinidine sulfate. *Journal of pharmaceutical sciences*, 98(7):2238–51, 2009. doi: 10.1002/jps.21606.
- [53] R. Watanabe, T. Esaki, H. Kawashima, Y. Natsume-Kitatani, C. Nagao, R. Ohashi, and K. Mizuguchi. Predicting Fraction Unbound in Human Plasma from Chemical Structure: Improved Accuracy in the Low Value Ranges. *Molecular Pharmaceutics*, 15(11):5302–5311, 2018. doi: 10.1021/acs.molpharmaceut.8b00785.
- [54] T. Tachibana, S. Kitamura, M. Kato, T. Mitsui, Y. Shirasaka, S. Yamashita, and Y. Sugiyama. Model analysis of the concentration-dependent permeability of p-gp substrates. *Pharmaceutical Research*, 27(3):442–446, 2010. doi: 10.1007/s11095-009-0026-9.
- [55] T. L. Nielsen, B. B. Rasmussen, J. P. Flinois, P. Beaune, and K. Brosen. In vitro metabolism of quinidine: the (3S)-3-hydroxylation of quinidine is a specific marker reaction for cytochrome P-4503A4 activity in human liver microsomes. *The Journal of pharmacology and experimental therapeutics*, 289(1):31–7, 1999.
- [56] R. P. Austin, P. Barton, S. L. Cockroft, M. C. Wenlock, and R. J. Riley. The influence of nonspecific microsomal binding on apparent intrinsic clearance, and its prediction from physicochemical properties. *Drug Metabolism and Disposition*, 30(12):1497–1503, 2002. doi: 10.1124/dmd.30.12.1497.
- [57] A. A. Lumen, P. Acharya, J. W. Polli, A. Ayrton, H. Ellens, and J. Bentz. If the IC 50 Is Defined by the Free Energy of Binding to P-Glycoprotein, Which Kinetic Parameters Define the IC 50 for the Madin-Darby Canine Kidney II Cell Line Overexpressing Human Multidrug Resistance 1 Confluent Cell Monolayer? *Drug Metabolism and Disposition*, 38(2):260–269, 2010. doi: 10.1124/dmd.109.029843.
- [58] A. A. Moghadamnia, A. Rostami-Hodjegan, R. Abdul-Manap, C. E. Wright, A. H. Morice, and G. T. Tucker. Physiologically based modelling of inhibition of metabolism and assessment of the relative potency of drug and metabolite: dextromethorphan vs . dextrorphan using quinidine inhibition. *British Journal of Clinical Pharmacology*, 56(1):57–67, 2003. doi: 10.1046/j.1365-2125.2003.01853.x.
- [59] M. S. Ching, C. L. Blake, H. Ghabrial, S. W. Ellis, M. S. Lennard, G. T. Tucker, and R. A. Smallwood. Potent inhibition of yeast-expressed CYP2D6 by dihydroquinidine, quinidine, and its metabolites. *Biochemical pharmacology*, 50(6): 833–7, 1995. doi: 10.1016/0006-2952(95)00207-g.
- [60] L. M. Berezhkovskiy. Volume of distribution at steady state for a linear pharmacokinetic system with peripheral elimination. *Journal of Pharmaceutical Sciences*, 93(6):1628–1640, 2004. doi: 10.1002/jps.20073.
- [61] Open Systems Pharmacology Suite Community. Open Systems Pharmacology Documentation., 2018. URL <https://docs.open-systems-pharmacology.org/working-with-pk-sim/pk-sim-documentation>.
- [62] C. A. Nguyen, Y. N. Konan-Kouakou, E. Allémann, E. Doelker, D. Quintanar-Guerrero, H. Fessi, and R. Gurny. Preparation of surfactant-free nanoparticles of methacrylic acid copolymers used for film coating. *AAPS PharmSciTech*, 7 (3):1–7, 2006. doi: 10.1208/pt070363.
- [63] Y. Zhang, M. Huo, J. Zhou, A. Zou, W. Li, C. Yao, and S. Xie. DDSolver: An add-in program for modeling and comparison of drug dissolution profiles. *AAPS Journal*, 12(3):263–271, 2010. doi: 10.1208/s12248-010-9185-1.

- [64] F. Langenbucher. Linearization of dissolution rate curves by the Weibull distribution. *The Journal of pharmacy and pharmacology*, 24(12):979–81, 1972. doi: 10.1111/j.2042-7158.1972.tb08930.x.
- [65] L. M. Fuhr, F. Z. Marok, N. Hanke, D. Selzer, and T. Lehr. Pharmacokinetics of the CYP3A4 and CYP2B6 Inducer Carbamazepine and Its Drug-Drug Interaction Potential: A Physiologically Based Pharmacokinetic Modeling Approach. *Pharmaceutics*, 13(2), 2021. doi: 10.3390/pharmaceutics13020270.
- [66] N. Hanke, D. Türk, D. Selzer, N. Ishiguro, T. Ebner, S. Wiebe, F. Müller, P. Stopfer, V. Nock, and T. Lehr. A Comprehensive Whole-Body Physiologically Based Pharmacokinetic Drug-Drug-Gene Interaction Model of Metformin and Cimetidine in Healthy Adults and Renally Impaired Individuals. *Clinical pharmacokinetics*, 59(11):1419–1431, 2020. doi: 10.1007/s40262-020-00896-w.
- [67] H. Britz, N. Hanke, A.-K. Volz, O. Spigset, M. Schwab, T. Eissing, T. Wendl, S. Frechen, and T. Lehr. Physiologically-Based Pharmacokinetic Models for CYP1A2 Drug-Drug Interaction Prediction: A Modeling Network of Fluvoxamine, Theophylline, Caffeine, Rifampicin, and Midazolam. *CPT: pharmacometrics & systems pharmacology*, 8(5):296–307, 2019. doi: 10.1002/psp4.12397.
- [68] X. Q. Li, T. B. Andersson, M. Ahlström, and L. Weidolf. Comparison of inhibitory effects of the proton pump-inhibiting drugs omeprazole, esomeprazole, lansoprazole, pantoprazole, and rabeprazole on human cytochrome P450 activities. *Drug Metabolism and Disposition*, 32(8):821–827, 2004. doi: 10.1124/dmd.32.8.821.
- [69] N. Hanke, D. Türk, D. Selzer, S. Wiebe, É. Fernandez, P. Stopfer, V. Nock, and T. Lehr. A Mechanistic, Enantios-selective, Physiologically Based Pharmacokinetic Model of Verapamil and Norverapamil, Built and Evaluated for Drug-Drug Interaction Studies. *Pharmaceutics*, 12(6), 2020. doi: 10.3390/pharmaceutics12060556.
- [70] S. Rüdesheim, D. Selzer, U. Fuhr, M. Schwab, and T. Lehr. Physiologically-based pharmacokinetic modeling of dextromethorphan to investigate interindividual variability within CYP2D6 activity score groups. *CPT: pharmacometrics & systems pharmacology*, 11(4):494–511, 2022. doi: 10.1002/psp4.12776.
- [71] S. Rüdesheim, J.-G. Wojtyniak, D. Selzer, N. Hanke, F. Mahfoud, M. Schwab, and T. Lehr. Physiologically Based Pharmacokinetic Modeling of Metoprolol Enantiomers and α -Hydroxymetoprolol to Describe CYP2D6 Drug-Gene Interactions. *Pharmaceutics*, 12(12), 2020. doi: 10.3390/pharmaceutics12121200.
- [72] S. Rüdesheim, D. Selzer, T. Mürdter, S. Igel, R. Kerb, M. Schwab, and T. Lehr. Physiologically Based Pharmacokinetic Modeling to Describe the CYP2D6 Activity Score-Dependent Metabolism of Paroxetine, Atomoxetine and Risperidone. *Pharmaceutics*, 14(8), 2022. doi: 10.3390/pharmaceutics14081734.
- [73] D. A. Capon, F. Bochner, N. Kerry, G. Mikus, C. Danz, and A. A. Somogyi. The influence of CYP2D6 polymorphism and quinidine on the disposition and antitussive effect of dextromethorphan in humans. *Clinical Pharmacology and Therapeutics*, 60(3):295–307, 1996. doi: 10.1016/S0009-9236(96)90056-9.
- [74] M. Schadel, D. Wu, S. V. Otton, W. Kalow, and E. M. Sellers. Pharmacokinetics of Dextromethorphan and Metabolites in Humans. *Journal of Clinical Psychopharmacology*, 15(4):263–269, 1995. doi: 10.1097/00004714-199508000-00005.
- [75] K. A. Schoedel, L. E. Pope, and E. M. Sellers. Randomized Open-Label Drug-Drug Interaction Trial of Dextromethorphan/Quinidine and Paroxetine in Healthy Volunteers. *Clinical Drug Investigation*, 32(3):157–169, 2012. doi: 10.2165/11599870-000000000-00000.
- [76] E. Steiness, S. Waldorff, P. B. Hansen, H. Egebald, J. Buch, and H. Egebald. Reduction of digoxin-induced inotropism during quinidine administration. *Clinical Pharmacology and Therapeutics*, 27(6):791–795, 1980. doi: 10.1038/clpt.1980.112.
- [77] H. R. Ochs, G. Bodem, and D. J. Greenblatt. Impairment of digoxin clearance by coadministration of quinidine. *Journal of clinical pharmacology*, 21(10):396–400, 1981. doi: 10.1002/j.1552-4604.1981.tb01739.x.
- [78] T. D. Leemann, K. P. Devi, and P. Dayer. Similar effect of oxidation deficiency (debrisoquine polymorphism) and quinidine on the apparent volume of distribution of (+/-)-metoprolol. *European journal of clinical pharmacology*, 45(1):65–71, 1993. doi: 10.1007/BF00315352.

- [79] J. A. Johnson and B. S. Burlew. Metoprolol metabolism via cytochrome P4502D6 in ethnic populations. *Drug metabolism and disposition: the biological fate of chemicals*, 24(3):350–5, 1996.
- [80] Z. Abolfathi, C. Fiset, M. Gilbert, K. Moerike, P. M. Belanger, and J. Turgeon. Role of polymorphic debrisoquin 4-hydroxylase activity in the stereoselective disposition of mexiletine in humans. *Journal of Pharmacology and Experimental Therapeutics*, 266(3):1196–1201, 1993.
- [81] E. J. Guest, L. Aarons, J. B. Houston, A. Rostami-Hodjegan, and A. Galetin. Critique of the two-fold measure of prediction success for ratios: application for the assessment of drug-drug interactions. *Drug metabolism and disposition: the biological fate of chemicals*, 39(2):170–3, 2011. doi: 10.1124/dmd.110.036103.